



저작자표시-비영리-변경금지 2.0 대한민국

이용자는 아래의 조건을 따르는 경우에 한하여 자유롭게

- 이 저작물을 복제, 배포, 전송, 전시, 공연 및 방송할 수 있습니다.

다음과 같은 조건을 따라야 합니다:



저작자표시. 귀하는 원저작자를 표시하여야 합니다.



비영리. 귀하는 이 저작물을 영리 목적으로 이용할 수 없습니다.



변경금지. 귀하는 이 저작물을 개작, 변형 또는 가공할 수 없습니다.

- 귀하는, 이 저작물의 재이용이나 배포의 경우, 이 저작물에 적용된 이용허락조건을 명확하게 나타내어야 합니다.
- 저작권자로부터 별도의 허가를 받으면 이러한 조건들은 적용되지 않습니다.

저작권법에 따른 이용자의 권리는 위의 내용에 의하여 영향을 받지 않습니다.

이것은 [이용허락규약\(Legal Code\)](#)을 이해하기 쉽게 요약한 것입니다.

[Disclaimer](#)

A THESIS  
FOR THE DEGREE OF DOCTOR OF PHILOSOPHY

The effect of marine algal natural product,  
Diphlorethohydroxycarmalol on  
TNF- $\alpha$  or H<sub>2</sub>O<sub>2</sub>-induced inflammatory myopathy  
in *in vitro* and *in vivo* zebrafish model

SEO-YOUNG KIM

Department of Marine Life Sciences

GRADUATE SCHOOL

JEJU NATIONAL UNIVERSITY

AUGUST, 2018

**The effect of marine algal natural product,  
Diphlorethohydroxycarmalol on TNF- $\alpha$  or H<sub>2</sub>O<sub>2</sub>-induced  
inflammatory myopathy in *in vitro* and *in vivo* zebrafish model**


**Seo-Young Kim  
(Supervised by Professor You-Jin Jeon)**

A thesis submitted in partial fulfillment of the requirement  
for the degree of DOCTOR OF PHILOSOPHY

2018. 08.

This thesis has been examined and approved by

Thesis director, Coon Bok Song, Prof. of Marine Life Sciences  
Jeju National University



Seungheon Lee, Prof. of Marine Life Sciences  
Jeju National University



Gi-Young Kim, Prof. Marine Life Sciences  
Jeju National University



Jung-Rae Rho, Prof. of Department of Oceanography  
Kunsan National University



You-Jin Jeon, Prof. of Marine Life Sciences  
Jeju National University



2018.08.  
Date

**Department of Marine Life Science  
GRADUATE SCHOOL  
JEJU NATIONAL UNIVERSITY**

## CONTENTS

국문초록.....	v
LIST OF FIGURES .....	x
LIST OF TABLES .....	xxii

### Part I. Screening of protective effects of marine brown algae on inflammatory myopathy in *in vitro*

ABSTRACT.....	2
INTRODUCTION.....	4
MATERIALS AND METHODS .....	7
Chemicals and reagents.....	7
Preparation of crude extract from marine brown algae .....	7
Macrophage cell culture .....	10
Cell toxicity.....	10
Determination of Nitric oxide (NO) production.....	10
Myoblast cell culture and differentiation .....	11
Cytotoxic assessment on C2C12 cells .....	11
Skeletal muscle cell proliferation activity .....	11

<i>In silico</i> docking of new inhibitor candidates to TNF- $\alpha$ .....	12
Molecular docking analysis of candidate compounds on TNF- $\alpha$ .....	12
Statistical analysis .....	13
<b>RESULTS AND DISCUSSIONS</b> .....	<b>15</b>
<b>CONCLUSION</b> .....	<b>23</b>

**Part II. Effect of marine algal bioactive compound on inflammatory myopathy in  
C2C12 skeletal muscle cells**

<b>ABSTRACT</b> .....	<b>37</b>
<b>INTRODUCTION</b> .....	<b>38</b>
<b>MATERIALS AND METHODS</b> .....	<b>41</b>
<b>Chemicals and reagents</b> .....	<b>41</b>
<b>Experimental design of TNF-<math>\alpha</math> or H<sub>2</sub>O<sub>2</sub>-induced myopathy</b> .....	<b>41</b>
<b>Cytotoxic assessment</b> .....	<b>41</b>
<b>Myotubes analysis</b> .....	<b>42</b>
<b>Determination of NO production and ROS production</b> .....	<b>42</b>
<b>Determination of antioxidant enzymes activity</b> .....	<b>42</b>
<b>Measurement of pro-inflammatory cytokines expression</b> .....	<b>43</b>
<b>Western blot analysis</b> .....	<b>43</b>

Statistical analysis .....	44
<b>RESULTS AND DISCUSSIONS</b> .....	<b>45</b>
<b>CONCLUSION</b> .....	<b>55</b>

**Part III. Effect of Dipflorothohydroxycarmalol (DPHC) on inflammatory myopathy  
in zebrafish model**

<b>ABSTRACT</b> .....	<b>72</b>
<b>INTRODUCTION</b> .....	<b>73</b>
<b>MATERIALS AND METHODS</b> .....	<b>75</b>
<b>Chemicals and reagents</b> .....	<b>75</b>
<b>The origin and maintenance of zebrafish</b> .....	<b>75</b>
<b>Experimental design of TNF-<math>\alpha</math> or H<sub>2</sub>O<sub>2</sub>-induced myopathy</b> .....	<b>75</b>
<b>Measurement of survival rates and body weights</b> .....	<b>76</b>
<b>Endurance test</b> .....	<b>76</b>
<b>Western blot analysis</b> .....	<b>78</b>
<b>Histological analysis</b> .....	<b>78</b>
<b>Statistical analysis</b> .....	<b>79</b>
<b>RESULTS AND DISCUSSIONS</b> .....	<b>80</b>

**CONCLUSION** .....93

**REFERENCES** .....96

**ACKNOWLEDGEMENT** ..... 110

## 국문초록

염증성 근육병증(inflammatory myopathy)은 주로 근육 조직에 염증세포가 침윤되어 근육의 만성 염증을 일으키며, 근육 조직 외에 폐, 심장, 관절 및 혈관 등에도 만성 염증을 일으키는 염증 질환이다(Baek et al., 2008). 급성 또는 만성 염증상태가 다른 병리학을 보이지만 골격근의 양과 생리물질이 분해되는 공통적인 특징을 보인다. 사이토카인은 면역세포 및 염증세포의 염증 반응을 유발하고 매개하는 주요한 분자(molecules)로 염증성 질환의 병인에 주요한 역할을 한다. 외부 환경 물질들에 반응하여, 골격근은 근육을 리모델링하기 위한 다양한 신호 경로를 활성화시키며 근육 성능을 유지한다. 신호 경로 중 어떤 경로들은 골격근의 발달에 긍정적인 영향을 미치는 반면, 다른 경로들을 골격근의 발달을 저해한다. 근육 위축이 발생하는 동안 이들의 신호 전달 경로가 활성화되고, 이는 근육의 발달을 돕는 단백질 합성의 저하를 촉매한다. 골격근 발달을 저해하는 신호 경로 중 대표적인 것은 E3 ubiquitin ligase 유전자인 muscle RING-finger protein-1(MuRF-1)과 muscle atrophy F-box(MAFbx/Atrogin-1)로 이들이 극도로 발현되게 된다. 따라서, 이들의 발현을 조절하는 세포 내 메커니즘을 찾는 것이 중요하다. 이 외 nuclear factor kappa B (NF- $\kappa$ B) 신호 경로 또한 골격근 위축에 관여한다. C2C12 골격근 세포에서 NF- $\kappa$ B가 염증성 사이토카인 tumor necrosis factor alpha(TNF- $\alpha$ )에 조절된다는 것이 밝혀졌다(Cai et al., 2004; Mourkioti et al., 2006; Guttridge et al., 2000; Li et al., 2005). TNF- $\alpha$ 는 종양괴사인자로 급성 염증 반응 사이토카인이다. TNF- $\alpha$ 는 체내 발



열원으로써 열이 나게 유도하거나, 세포 자살을 유도하거나, interleukin-1(IL-1)과 IL-6 사이토카인의 생산을 통해 패혈증을 유발하거나, 악액질을 유도하거나, 감염을 유발하며 종양 생성과 바이러스 복제를 억제하는 능력을 갖는다. TNF- $\alpha$ 의 비정상적인 조절은 알츠하이머 병, 암, 우울증, 그리고 염증성질환 등의 질병에서 나타난다(Swardfager et al., 2010; Locksley et al., 2001; Dowlati et al., 2010). 이 때문에 항염증 치료제로 TNF- $\alpha$  억제제가 개발되고 사용된다. 이들은 비스테로이드성 소염진통제(Non-steroidal anti-inflammatory drugs, NSAIDs) 및 스테로이드 대체제로 사용되고 있으며, 류마티스 관절염, 건성성 관절염 및 척추염 치료제에 특화되어 있다. TNF- $\alpha$  억제제 치료제는 주사제로 사용되고 있는데, 이 때문에 주사 부위의 발열, 홍반, 두드러기, 경화, 통증, 가려움, 자극 및 지각(감각) 이상을 나타내며 간혹적으로 (결핵)바이러스 감염, 간기능부전, 백반증, 림프종이 보고되면서 부작용의 문제점이 발생하고 있다. 따라서, 본 연구에서는 해양생물 중 다양한 이차대사산물을 함유하고 있으며, 항산화, 항염, 항암, 항당뇨, 항고혈압, 및 항비만 등의 여러 가지 생리활성이 보고된(Kim et al., 2016; Sanjeeva et al., 2017; Lee et al., 2015; Kim et al., 2016; Wijesinghe et al., 2011; Kang et al., 2016) 갈조류로부터 얻을 수 있는 유용성분으로부터 천연 TNF- $\alpha$  억제제를 찾고자 하였다. 마우스 유래 C2C12 골격근세포와 Zebrafish (*Danio rerio*) 동물 모델을 이용하여 염증성 근육손상 모델을 정립하고, 6가지의 갈조류로부터 TNF- $\alpha$  저해제 역할을 하는 유용성분을 확인하였다.

본 연구에서 사용된 6가지의 갈조류는 패(*Ishige okamurae*, IO), 넓패(*Ishige foliacea*, IF), 감태(*Ecklonia cava*, EC), 툃(*Hizikia fusiforme*, HF), 바위수염(*Myelophycus*

*caespitosus*, MC), 갯쟁이모자반(*Sagarssum horneri*, SH)으로 에탄올 주정 추출물로 마우스 유래 대식세포인 RAW 264.7 세포에서 항염증 효능과 마우스 유래 골격근 세포인 C2C12 세포에서 근세포증식 효능을 탐색하였다. 6가지의 갈조류 추출물은 모두 LPS로 염증 자극된 RAW 264.7 세포에서 분비되는 nitric oxide(NO)의 양을 현저히 감소시켰으며, 패(IO)와 넓패(IF) 추출물이 C2C12 근세포 증식에 효능이 있는 것을 확인하였다. 또한, 6가지의 갈조류 추출물로부터 얻을 수 있는 유용성분이 근육 염증을 일으키는 TNF- $\alpha$ 의 억제제 역할을 할 수 있는지 확인하기 위하여 *in silico* molecular docking 분석을 통하여 TNF- $\alpha$ 와의 결합능력을 확인하였다. 그 결과, 패(IO) 유래 Diphlorethohydroxycarmalol(DPHC), 감태(EC) 유래 Dieckol(DK), 톳(HF) 유래 Saringosterol A(SA), 바위수염(MC) 유래 Gadoleic acid (GA), 갯쟁이모자반(SH) 유래 Sargachromanol E(SC-E)의 총 5가지 유용성분이 TNF- $\alpha$ 와 안정적으로 결합하는 것을 확인하였다. 그러나, 이 중 DPHC가 다른 4가지의 유용성분보다 가장 높은 결합력(-53.73 kcal/mol of Binding energy)으로 TNF- $\alpha$ 와 결합하는 것을 확인하였다. 이를 통하여, 항염증 및 근세포증식 효능을 나타내며 TNF- $\alpha$  저해제 역할이 가능할 것으로 예상되는 DPHC를 염증성 근육손상의 잠재적 보호 물질로 예상되어 C2C12 근세포와 zebrafish 동물모델의 근육에 염증을 유도하여 DPHC의 보호능력을 확인하였다.

근육 염증을 유도하는 물질로는 직접적인 영향을 미치는 TNF- $\alpha$ 와 염증성 사이토카인을 분비하게 하는 산화적 스트레스 유발물질은 H<sub>2</sub>O<sub>2</sub> 두 가지를 이용하였다. TNF- $\alpha$ 와 H<sub>2</sub>O<sub>2</sub>는 C2C12 근세포에 처리되면서 근육 다발로의 형성이 무너지며

손상된 근육 세포 내 대표적인 인자인 MuRF-1과 MAFbx/Atrogin-1의 발현이 강하게 발현하는 것을 확인하였다. 반면, 후보물질인 DPHC를 근육 다발로의 분화 과정 중에 처리하였을 때 TNF- $\alpha$ 와 H<sub>2</sub>O<sub>2</sub>에 의한 근육 손상이 보호되는 것을 근육 세포의 생존율, 크기, 세포에서 분비되는 NO 분비와 TNF- $\alpha$ , IL-1 $\beta$ , 및 IL-6 염증성 사이토카인의 발현이 감소되며 항산화 효소가 활성화하는 것을 확인하였다. 또한, TNF- $\alpha$ 가 TNF- $\alpha$  receptor에 결합하여 근육 손상을 유발하는 하위기전인 세포질 내 MAPKs(p-JNK 및 p-p38)과 p-I $\kappa$ B- $\alpha$  및 p-NF- $\kappa$ B의 단백질 발현과 이 신호전달에 의한 핵 내 MuRF-1과 MAFbx/Atrogin-1의 발현이 DPHC에 의해 크게 감소하는 것을 확인하였다. C2C12 골격근 세포에서 TNF- $\alpha$ 와 H<sub>2</sub>O<sub>2</sub>에 의한 근육 손상이 DPHC가 보호함에 따라 DPHC가 염증성 근육 손상의 천연 보호제 및 TNF- $\alpha$  억제제로 사용될 수 있을 것을 기대하여 유전자정보 및 조직기관이 인간과 유사한 척추동물로 분자생물학적 연구 동물 모델로 최근 각광받고 있는 제브라피쉬(Zebrafish)를 이용하여 염증성 근육 손상 모델을 만들고 이에 DPHC의 보호 효능을 확인하였다. 제브라피쉬 근육에 TNF- $\alpha$ 와 H<sub>2</sub>O<sub>2</sub>를 주입하여 근육 손상을 유도하였다. 그 결과, TNF- $\alpha$ 와 H<sub>2</sub>O<sub>2</sub>가 제브라피쉬 근육 조직을 분해하는 것을 확인하였고, 단백질 발현 분석을 통해 MuRF-1과 MAFbx/Atrogin-1의 발현이 강하게 발현하는 것을 확인하였다. 반면, DPHC를 TNF- $\alpha$ 와 H<sub>2</sub>O<sub>2</sub>의 주입 전과 동시에 근육에 주입한 후 근육 조직을 얻어 조직 세포 내 MAPKs(p-JNK 및 p-p38)과 p-I $\kappa$ B- $\alpha$  및 p-NF- $\kappa$ B의 단백질 발현과 MAFbx/Atrogin-1의 발현을 확인하였을 때, TNF- $\alpha$ 와 H<sub>2</sub>O<sub>2</sub>만을 주입한 제브라피쉬의 근육 조직에서 강하게 발현한 위의 단백질이 크게 감소하는 것을 확인하였다. 또한, 조직 염색을 통하여 근육의 모양을 확인한 결과, TNF- $\alpha$ 와 H<sub>2</sub>O<sub>2</sub>

에 의해 근육의 모양이 무너지거나 세포가 깨진 모습이 DPHC를 주입한 제브라피쉬의 근육의 모양이 정상 제브라피쉬와 유사한 것을 확인하였다. 이와 더불어 근육의 양과 지구력이 상관관계를 지니는 점을 활용하여 물의 흐름과 경사도에 일정 시간 동안 놓였을 때의 지구력을 확인하였을 때, 아무것도 처리하지 않은 정상 제브라피쉬에 비해 TNF- $\alpha$ 와 H<sub>2</sub>O<sub>2</sub>를 주입한 제브라피쉬가 물의 흐름과 경사도에 버티지 못하고 쉽게 낙하하는 것을 확인하였으며, 반면, DPHC의 고농도를 주입한 제브라피쉬의 경우 TNF- $\alpha$ 와 H<sub>2</sub>O<sub>2</sub>를 주입한 제브라피쉬보다 물의 흐름과 경사도에 유의성 있게 버티는 것을 확인하였다.

위의 결과들을 종합하여 볼 때, 갈조류 중 패(IO)로부터 얻을 수 있는 유용성분인 DPHC가 TNF- $\alpha$ 와 H<sub>2</sub>O<sub>2</sub>에 의한 염증성 근육 손상을 MAPKs과 NF- $\kappa$ B 신호 전달 경로를 억제하며 보호하는 것을 C2C12 근세포와 제브라피쉬 근육 조직에서 확인하였다. 이를 통해 DPHC가 TNF- $\alpha$  저해제로 사용되는 주사제 대신에 근육의 염증을 감소시킬 수 있는 기능성식품으로 사용될 수 있을 것으로 기대된다.

## LIST OF FIGURES

**Fig. 1-1** The photography of six marine brown algae.

**Fig. 1-2** Crystal structure of TNF- $\alpha$  obtained from protein data bank (PDB, PDB ID: 2AZ5).

**Fig. 1-3** Screening of cell toxicity of brown marine algae extracts on RAW 264.7 macrophage cells by a MTT assay. Experiments were performed in triplicate and the data are expressed as mean  $\pm$  SE; <sup>#</sup>  $P < 0.05$ , and <sup>##</sup>  $P < 0.01$  as compared to the untreated group. \*  $P < 0.05$ , and \*\*  $P < 0.01$  as compared to the LPS-treated group.

**Fig. 1-4** Screening of anti-inflammatory effects of brown marine algae extracts on RAW 264.7 macrophage cells by a Griess assay. Experiments were performed in triplicate and the data are expressed as mean  $\pm$  SE; <sup>#</sup>  $P < 0.05$ , and <sup>##</sup>  $P < 0.01$  as compared to the untreated group. \*  $P < 0.05$ , and \*\*  $P < 0.01$  as compared to the LPS-treated group.

**Fig. 1-5** Screening of anti-inflammatory effects of brown marine algae extracts by a MTT assay on RAW 264.7 macrophage cells. Experiments were performed in triplicate and the data are expressed as mean  $\pm$  SE; <sup>#</sup>  $P < 0.05$ , and <sup>##</sup>  $P < 0.01$  as compared to the untreated

group. \*  $P < 0.05$ , and \*\*  $P < 0.01$  as compared to the LPS-treated group.

**Fig. 1-6 Screening of cell toxicity of brown marine algae extracts on C2C12 skeletal myoblast cells by a MTT assay.** Experiments were performed in triplicate and the data are expressed as mean  $\pm$  SE; \*  $P < 0.05$ , and \*\*  $P < 0.01$  as compared to the untreated group.

**Fig. 1-7 Screening of skeletal muscle cell proliferation effects of brown marine algae extracts on C2C12 skeletal muscle cells by a BrdU assay. OCT, Octacosanol (25  $\mu$ g/mL) treated group.** Experiments were performed in triplicate and the data are expressed as mean  $\pm$  SE; \*  $P < 0.05$ , and \*\*  $P < 0.01$  as compared to the untreated group.

**Fig. 1-8 The structures of marine brown algae-derived natural compounds.**

**Fig. 1-9 Computational prediction of the 3D structure for TNF- $\alpha$  (PDB ID: 2AZ5) and docking simulation with DPHC.**

**Fig. 1-10 Computational prediction of the 3D structure for TNF- $\alpha$  (PDB ID: 2AZ5) and docking simulation with HDP.**

**Fig. 1-11 Computational prediction of the 3D structure for TNF- $\alpha$  (PDB ID: 2AZ5) and docking simulation with DK.**

**Fig. 1-12 Computational prediction of the 3D structure for TNF- $\alpha$  (PDB ID: 2AZ5) and docking simulation with PHB.**

**Fig. 1-13 Computational prediction of the 3D structure for TNF- $\alpha$  (PDB ID: 2AZ5) and docking simulation with SA.**

**Fig. 1-14 Computational prediction of the 3D structure for TNF- $\alpha$  (PDB ID: 2AZ5) and docking simulation with GA.**

**Fig. 1-15 Computational prediction of the 3D structure for TNF- $\alpha$  (PDB ID: 2AZ5) and docking simulation with SC-E.**

**Fig. 1-16 Computational prediction of the 3D structure for TNF- $\alpha$  (PDB ID: 2AZ5) and docking simulation with AF.**

**Fig. 1-17 Computational prediction of the 3D structure for TNF- $\alpha$  (PDB ID: 2AZ5) and**

**docking simulation with OCT.**

**Fig. 2-1 Evaluation of cell toxicity of TNF- $\alpha$  on C2C12 skeletal myoblast cells by a MTT assay.** Experiments were performed in triplicate and the data are expressed as mean  $\pm$  SE; \*  $P < 0.05$ , and \*\*  $P < 0.01$  as compared to the untreated group.

**Fig. 2-2 Evaluation of cell toxicity of H<sub>2</sub>O<sub>2</sub> on C2C12 skeletal myoblast cells by a MTT assay.** Experiments were performed in triplicate and the data are expressed as mean  $\pm$  SE; \*  $P < 0.05$ , and \*\*  $P < 0.01$  as compared to the untreated group.

**Fig. 2-3 Analysis of TNF- $\alpha$ -induced inflammatory myotubes on length of myotubes.** Experiments were performed in duplicate and the data are expressed as mean  $\pm$  SE; \*  $P < 0.05$ , and \*\*  $P < 0.01$  as compared to the untreated group.

**Fig. 2-4 Analysis of H<sub>2</sub>O<sub>2</sub>-induced inflammatory myotubes on length of myotubes.** Experiments were performed in duplicate and the data are expressed as mean  $\pm$  SE; \*  $P < 0.05$ , and \*\*  $P < 0.01$  as compared to the untreated group.

**Fig. 2-5 Analysis of TNF- $\alpha$ -induced inflammatory myotubes on MuRF-1 (A), and MAFbx (B) protein expression.** Experiments were performed in triplicate and the data are



expressed as mean  $\pm$  SE; \*  $P < 0.05$ , and \*\*  $P < 0.01$  as compared to the untreated group.

**Fig. 2-6 Analysis of H<sub>2</sub>O<sub>2</sub>-induced inflammatory myotubes on MuRF-1 (A), and MAFbx (B) protein expression.** Experiments were performed in triplicate and the data are expressed as mean  $\pm$  SE; \*  $P < 0.05$ , and \*\*  $P < 0.01$  as compared to the untreated group.

**Fig. 2-7 Evaluation of cell toxicity of diphlorethohydroxycarmalol (DPHC) by a MTT assay on C2C12 skeletal myoblast cells.** Experiments were performed in triplicate and the data are expressed as mean  $\pm$  SE; \*  $P < 0.05$ , and \*\*  $P < 0.01$  as compared to the untreated group.

**Fig. 2-8 Evaluation of cell protective effects of DPHC by a MTT assay on TNF- $\alpha$ -induced myopathy C2C12 skeletal muscle cells.** Experiments were performed in triplicate and the data are expressed as mean  $\pm$  SE; #  $P < 0.05$ , and ##  $P < 0.01$  as compared to the untreated group. \*  $P < 0.05$ , and \*\*  $P < 0.01$  as compared to the TNF- $\alpha$ -treated group.

**Fig. 2-9 Evaluation of cell protective effects of DPHC by a MTT assay on H<sub>2</sub>O<sub>2</sub>-induced myopathy C2C12 skeletal muscle cells.** Experiments were performed in triplicate and the data are expressed as mean  $\pm$  SE; #  $P < 0.05$ , and ##  $P < 0.01$  as compared to the untreated group. \*  $P < 0.05$ , and \*\*  $P < 0.01$  as compared to the H<sub>2</sub>O<sub>2</sub>-treated group.

**Fig. 2-10 Evaluation of DPHC-treated length of myotubes by a MTT assay on TNF- $\alpha$ -induced myopathy C2C12 skeletal muscle cells.** Experiments were performed in triplicate and the data are expressed as mean  $\pm$  SE; #  $P < 0.05$ , and ##  $P < 0.01$  as compared to the untreated group. \*  $P < 0.05$ , and \*\*  $P < 0.01$  as compared to the TNF- $\alpha$ -treated group.

**Fig. 2-11 Evaluation of DPHC-treated length of myotubes by a MTT assay on H<sub>2</sub>O<sub>2</sub>-induced myopathy C2C12 skeletal muscle cells.** Experiments were performed in triplicate and the data are expressed as mean  $\pm$  SE; #  $P < 0.05$ , and ##  $P < 0.01$  as compared to the untreated group. \*  $P < 0.05$ , and \*\*  $P < 0.01$  as compared to the H<sub>2</sub>O<sub>2</sub>-treated group.

**Fig. 2-12 Evaluation of NO and ROS production in DPHC-treated myotubes on TNF- $\alpha$ -induced myopathy C2C12 skeletal muscle cells.** Experiments were performed in triplicate and the data are expressed as mean  $\pm$  SE; #  $P < 0.05$ , and ##  $P < 0.01$  as compared to the untreated group. \*  $P < 0.05$ , and \*\*  $P < 0.01$  as compared to the TNF- $\alpha$ -treated group.

**Fig. 2-13 Evaluation of NO and ROS production in DPHC-treated myotubes on H<sub>2</sub>O<sub>2</sub>-induced myopathy C2C12 skeletal muscle cells.** Experiments were performed in triplicate and the data are expressed as mean  $\pm$  SE; #  $P < 0.05$ , and ##  $P < 0.01$  as compared to the untreated group. \*  $P < 0.05$ , and \*\*  $P < 0.01$  as compared to the H<sub>2</sub>O<sub>2</sub>-treated group.

**Fig. 2-14 Evaluation of SOD and CAT activity in DPHC-treated myotubes on TNF- $\alpha$ -induced myopathy C2C12 skeletal muscle cells.** Experiments were performed in triplicate and the data are expressed as mean  $\pm$  SE; #  $P < 0.05$ , and ##  $P < 0.01$  as compared to the untreated group. \*  $P < 0.05$ , and \*\*  $P < 0.01$  as compared to the TNF- $\alpha$ -treated group.

**Fig. 2-15 Evaluation of SOD and CAT activity in DPHC-treated myotubes on H<sub>2</sub>O<sub>2</sub>-induced myopathy C2C12 skeletal muscle cells.** Experiments were performed in triplicate and the data are expressed as mean  $\pm$  SE; #  $P < 0.05$ , and ##  $P < 0.01$  as compared to the untreated group. \*  $P < 0.05$ , and \*\*  $P < 0.01$  as compared to the H<sub>2</sub>O<sub>2</sub>-treated group.

**Fig. 2-16 Evaluation of TNF- $\alpha$ , IL-1 $\beta$ , and IL-6 cytokines mRNA expression in DPHC-treated myotubes on TNF- $\alpha$ -induced myopathy C2C12 skeletal muscle cells.** Experiments were performed in triplicate and the data are expressed as mean  $\pm$  SE; #  $P < 0.05$ , and ##  $P < 0.01$  as compared to the untreated group. \*  $P < 0.05$ , and \*\*  $P < 0.01$  as compared to the TNF- $\alpha$ -treated group.

**Fig. 2-17 Evaluation of TNF- $\alpha$ , IL-1 $\beta$ , and IL-6 cytokines mRNA expression on H<sub>2</sub>O<sub>2</sub>-induced myopathy C2C12 skeletal muscle cells.** Experiments were performed in triplicate and the data are expressed as mean  $\pm$  SE; #  $P < 0.05$ , and ##  $P < 0.01$  as compared to the untreated group. \*  $P < 0.05$ , and \*\*  $P < 0.01$  as compared to the H<sub>2</sub>O<sub>2</sub>-treated group.

**Fig. 2-18 Evaluation of p-I $\kappa$ B- $\alpha$ , p-NF- $\kappa$ B, p-JNK, and p-p38 protein expression in DPHC-treated myotubes on TNF- $\alpha$ -induced myopathy C2C12 skeletal muscle cells.** Experiments were performed in triplicate and the data are expressed as mean  $\pm$  SE; <sup>#</sup>  $P < 0.05$ , and <sup>##</sup>  $P < 0.01$  as compared to the untreated group. \*  $P < 0.05$ , and \*\*  $P < 0.01$  as compared to the TNF- $\alpha$ -treated group.

**Fig. 2-19 Evaluation of p-I $\kappa$ B- $\alpha$ , p-NF- $\kappa$ B, p-JNK, and p-p38 protein expression in DPHC-treated myotubes on H<sub>2</sub>O<sub>2</sub>-induced myopathy C2C12 skeletal muscle cells.** Experiments were performed in triplicate and the data are expressed as mean  $\pm$  SE; <sup>#</sup>  $P < 0.05$ , and <sup>##</sup>  $P < 0.01$  as compared to the untreated group. \*  $P < 0.05$ , and \*\*  $P < 0.01$  as compared to the H<sub>2</sub>O<sub>2</sub>-treated group.

**Fig. 2-20 Evaluation of MuRF-1, and MAFbx/Atrogin-1 protein expression in DPHC-treated myotubes on TNF- $\alpha$ -induced myopathy C2C12 skeletal muscle cells.** Experiments were performed in triplicate and the data are expressed as mean  $\pm$  SE; <sup>#</sup>  $P < 0.05$ , and <sup>##</sup>  $P < 0.01$  as compared to the untreated group. \*  $P < 0.05$ , and \*\*  $P < 0.01$  as compared to the TNF- $\alpha$ -treated group.

**Fig. 2-21 Evaluation MuRF-1, and MAFbx/Atrogin-1 protein expression in DPHC-treated myotubes on H<sub>2</sub>O<sub>2</sub>-induced myopathy C2C12 skeletal muscle cells.** Experiments were performed in triplicate and the data are expressed as mean  $\pm$  SE; <sup>#</sup>  $P < 0.05$ , and <sup>##</sup>  $P < 0.01$  as compared to the untreated group.

0.01 as compared to the untreated group. \*  $P < 0.05$ , and \*\*  $P < 0.01$  as compared to the H<sub>2</sub>O<sub>2</sub>-treated group.

**Fig. 3-1 The schematic diagram of zebrafish behavior tank for endurance test against water flow and gradient.** The behavioral test Section A has a length of 55 cm and a width of 40 cm, which are divided to 4 rails (1 rail has 10 cm of width), and Section B 1 has a length of 25 cm and a width of 40 cm. A constant water flow (0.3 cm/sec) at an angle of 16° was maintained. The figure represents the tank view (A) from above and (B) the front view.

**Fig. 3-2 Effects of DPHC on survival rates (A) and body weights (B) in TNF- $\alpha$ -induced myopathy zebrafish.** Experiments were performed in duplicate and the data are expressed as mean  $\pm$  SE; #  $P < 0.05$ , and ##  $P < 0.01$  as compared to the untreated group. \*  $P < 0.05$ , and \*\*  $P < 0.01$  as compared to the TNF- $\alpha$ -treated group.

**Fig. 3-3 Effects of DPHC on survival rates and body weights in H<sub>2</sub>O<sub>2</sub>-induced myopathy zebrafish.** Experiments were performed in duplicate and the data are expressed as mean  $\pm$  SE; #  $P < 0.05$ , and ##  $P < 0.01$  as compared to the untreated group. \*  $P < 0.05$ , and \*\*  $P < 0.01$  as compared to the H<sub>2</sub>O<sub>2</sub>-treated group.

**Fig. 3-4 Effects of DPHC on endurance training in TNF- $\alpha$  -induced myopathy zebrafish.** Experiments were performed in duplicate and the data are expressed as mean  $\pm$  SE; #  $P < 0.05$ ,

and <sup>##</sup>  $P < 0.01$  as compared to the untreated group. \*  $P < 0.05$ , and \*\*  $P < 0.01$  as compared to the TNF- $\alpha$ -treated group.

**Fig. 3-5 Effects of DPHC on endurance training in H<sub>2</sub>O<sub>2</sub>-induced myopathy zebrafish.**

Experiments were performed in duplicate and the data are expressed as mean  $\pm$  SE; #  $P < 0.05$ , and <sup>##</sup>  $P < 0.01$  as compared to the untreated group. \*  $P < 0.05$ , and \*\*  $P < 0.01$  as compared to the H<sub>2</sub>O<sub>2</sub>-treated group.

**Fig. 3-6 Effects of DPHC on endurance training in TNF- $\alpha$  -induced myopathy zebrafish.**

Experiments were performed in duplicate and the data are expressed as mean  $\pm$  SE; #  $P < 0.05$ , and <sup>##</sup>  $P < 0.01$  as compared to the untreated group. \*  $P < 0.05$ , and \*\*  $P < 0.01$  as compared to the TNF- $\alpha$ -treated group.

**Fig. 3-7 Effects of DPHC on endurance training in H<sub>2</sub>O<sub>2</sub>-induced myopathy zebrafish.**

Experiments were performed in duplicate and the data are expressed as mean  $\pm$  SE; #  $P < 0.05$ , and <sup>##</sup>  $P < 0.01$  as compared to the untreated group. \*  $P < 0.05$ , and \*\*  $P < 0.01$  as compared to the H<sub>2</sub>O<sub>2</sub>-treated group.

**Fig. 3-8 Effects of DPHC on NF- $\kappa$ B and MAPKs signaling pathways in TNF- $\alpha$ -induced myopathy zebrafish.**

Experiments were performed in duplicate and the data are expressed as mean  $\pm$  SE; #  $P < 0.05$ , and <sup>##</sup>  $P < 0.01$  as compared to the untreated group. \*  $P < 0.05$ , and \*\*

$P < 0.01$  as compared to the TNF- $\alpha$ -treated group.

**Fig. 3-9 Effects of DPHC on MuRF-1, and MAFbx/Atrogin-1, which are key genes in muscle atrophy in TNF- $\alpha$ -induced myopathy zebrafish.** Experiments were performed in duplicate and the data are expressed as mean  $\pm$  SE; #  $P < 0.05$ , and ##  $P < 0.01$  as compared to the untreated group. \*  $P < 0.05$ , and \*\*  $P < 0.01$  as compared to the TNF- $\alpha$  -treated group.

**Fig. 3-10 Effects of DPHC on NF- $\kappa$ B and MAPKs signaling pathways in H<sub>2</sub>O<sub>2</sub>-induced myopathy zebrafish.** Experiments were performed in duplicate and the data are expressed as mean  $\pm$  SE; #  $P < 0.05$ , and ##  $P < 0.01$  as compared to the untreated group. \*  $P < 0.05$ , and \*\*  $P < 0.01$  as compared to the H<sub>2</sub>O<sub>2</sub>-treated group.

**Fig. 3-11 Effects of DPHC on MuRF-1, and MAFbx/Atrogin-1, which are key genes in muscle atrophy H<sub>2</sub>O<sub>2</sub>-induced myopathy zebrafish.** Experiments were performed in duplicate and the data are expressed as mean  $\pm$  SE; #  $P < 0.05$ , and ##  $P < 0.01$  as compared to the untreated group. \*  $P < 0.05$ , and \*\*  $P < 0.01$  as compared to the H<sub>2</sub>O<sub>2</sub>-treated group.

**Fig. 3-12 Effects of DPHC on Hematoxylin & Eosin (H&E) staining in muscle tissue of in TNF- $\alpha$ -induced myopathy zebrafish.**

**Fig. 3-13 Effects of DPHC on Hematoxylin & Eosin (H&E) staining in muscle tissue of in H<sub>2</sub>O<sub>2</sub>-induced myopathy zebrafish.**



## LIST OF TABLES

**Table 1-1. The list of marine brown algae.**

**Table 1-2. The effects of anti-inflammatory and cell proliferation of brown marine algae extracts in RAW 264.7 macrophage cells, and C2C12 skeletal muscle cells, respectively.** Experiments were performed in triplicate and the data are expressed as mean  $\pm$  SE; \*  $P < 0.05$ , and \*\*  $P < 0.01$  as compared to the untreated group.

**Table 1-3. The list of six marine brown algae extract-derived natural bioactive compounds for *in silico* molecular docking simulation with TNF- $\alpha$ , which is regulator of muscle degradation.**

**Table 1-4. Results of docking simulations of marine brown algae-derived natural compounds with TNF- $\alpha$  (PDB ID: 2AZ5).**

## **Part I.**

# **Screening of protective effects of marine brown algae on inflammatory myopathy in *in vitro***

## Part I.

### Screening of protective effects of marine brown algae on inflammatory myopathy in *in vitro*

#### ABSTRACT

In the study, protective effects of six species of marine brown algae [*Ishige okamurae* (IO), *Ishige foliacea* (IF), *Ecklonia cava* (EC), *Hizikia fusiforme* (HF), *Myelophycus caespitosus* (MC), *Sagarssum horneri* (SH)] were collected from Jeju Island to examine inflammatory myopathy. First, seaweed extracts were assessed for anti-inflammatory activity and cell proliferation activity in RAW 264.7 macrophage cells, and C2C12 skeletal myocytes, respectively. All separated from seaweeds extracts showed non-cytotoxic effect on RAW 264.7 cells and dramatically inhibited nitric oxide (NO) production in lipopolysaccharide (LPS)-induced RAW 264.7 cells at the tested concentrations. Especially, the extracts collected from IO and IF significantly increased cell proliferation of C2C12 myoblasts compared to the non-treated cells without showing toxicity. Moreover, a prospective TNF- $\alpha$  inhibitor, which control signaling pathway of muscle degradation are searched from these six marine brown algae-derived natural bioactive compounds. Eight natural compounds isolated from seaweeds were subjected to *in silico* molecular docking analysis to identify potential TNF- $\alpha$  inhibitor. Among compounds, Diphlorethohydroxycarmalol (DPHC) isolated from IO, Dieckol (DK) isolated from EC, Saringosterol acetated (SA) isolated from HF, Gadoleic acid (GA) isolated from MC, and Sargachromanol E isolated from (SH) are favorably docked to the TNF- $\alpha$ . Especially, DPHC had the lowest binding energy value, despite the lowest

number of poses combined with TNF- $\alpha$ . It was expected that DPHC isolated from IO would be efficiently developed into agent for inflammatory myopathy which acts as a TNF- $\alpha$  inhibitor. Therefore, DPHC used in further experiments.

## 1. INTRODUCTION

Inflammation is an important host defense system response to external physical or chemical infection and injury, and it plays a role in maintain health state against variety stimuli. The inflammatory process is regulated by inflammatory cells including macrophages, neutrophils, eosinophils, and mononuclear phagocytes (Kim et al., 2014). Normal inflammatory responses are mediated by a correlation between down-regulation of pro-inflammatory proteins and up-regulation of anti-inflammatory proteins (Lawrence et al., 2002). Inflammation can be classified into two phase as acute and chronic. The acute phase is associated with accumulation of fluids, elevated blood flow, the increase of the number of leukocytes and inflammatory mediators, whereas the chronic inflammation is associated with progression of specific humeral and cellular immune responses (Fernando et al., 2016). Inflammation affects various organs of the body, and also is associated with disruption of anabolic signals initiating muscle growth. Therefore, inflammation is an important contributor to the pathology diseases implicated in skeletal muscle dysfunction (Londhe et al., 2015). While acute or chronic inflammation disease states exhibit different pathologies, all have in common the loss skeletal muscle mass and a deregulated skeletal muscle physiology. Cytokines are intracellular signaling molecules, potent mediators of a number of cell functions and are essential in coordinating inflammatory responses (Salomonsson et al., 2006). Pro-inflammatory cytokines are key contributors to acute/chronic inflammation found in many of pathologies (Londhe et al., 2015). In skeletal muscle, tumor necrosis factor (TNF)- $\alpha$ , one of the pro-inflammatory cytokines, influences satellite cell proliferation and accelerates the G1 to S phase transition (Li et al., 2003). Moreover, in dystrophic muscle, elevated levels of TNF- $\alpha$  inhibit the regenerative potential of satellite cells and are associated with loss of muscle (Acharyya et al.,

2010; Farber et al., 2000).

Muscle growth is regulated via a complex interaction of diverse biochemical signaling pathways during development (Elkina et al., 2011; Yoon et al., 2008; Glass et al., 2005). One of the main positive regulators of muscle growth is IGF-1 that induces an increase in muscle mass by stimulating the phosphatidylinositol 3-kinase (PI3K) and Akt pathways (Elkina et al., 2011; Yoon et al., 2008). Increased IGF-1 levels in muscle cells promote myotube hypertrophy, and the binding of IGF-1 to its receptors triggers the activation of several intracellular kinases (Glass et al., 2005; Bodine et al., 2001; Lai et al., 2004).

Excessive TNF- $\alpha$  release enhances protein degradation of insulin-like growth factor I (IGF-1) and induces an early activation of the atrogin-1 gene expression (Dehoux et al., 2007). The loss of muscle by inflammation is called inflammatory myopathy, muscle wasting, and muscle atrophy. Myopathy is a combination of ‘myo’, meaning muscle, and ‘patheia’, which means suffering, in the Greek. Another term used to describe inflammatory myopathies is myositis – ‘myo’ meaning muscle and ‘itis’ meaning inflammation (Londhe et al., 2015). TNF- $\alpha$  inhibitors are developed and used as anti-inflammatory and therapeutic agents. They are NSAIDs and steroids, however, this is specific to the treatment of rheumatism, dry arthritis, and spondylitis. Moreover, it has the characteristics of injection, and injection site is known to have side effects such as fever, pain, itching, and virus infection. Therefore, in this study, a prospective TNF- $\alpha$  inhibitor among diverse natural compounds from marine algae was searched.

Marine organisms are rich sources of structurally diverse bioactive compounds with various biological activities. Especially, various marine brown algae are widely distributed in Jeju

Island. Marine brown algae contain a variety of bioactive compounds including phlorotannins, polysaccharide, and pigments and exhibit different biological activities and potential health benefits such as antioxidant activity (Kim et al., 2016b), anti-inflammatory activity (Sanjeeva et al., 2017), anti-cancer activity (Lee et al., 2015), anti-diabetic activity (Kim et al., 2016a), anti-hypertensive effects (Wijesinghe et al., 2011), and anti-obesity activity (Kang et al., 2016). However, studies on its effect of muscle growth and myopathy are scarce. In this study, therefore, I looked for a prospective TNF- $\alpha$  inhibitor among diverse marine brown algae-derived biological substances. To select candidate affecting the TNF- $\alpha$  signaling pathway from a various natural compounds, first anti-inflammatory and skeletal muscle cell proliferation activities was assessed in RAW 264.7 macrophages and C2C12 myoblasts, respectively. Moreover, an *in silico* analysis was performed using the crystal structure of the TNF- $\alpha$  [Protein Data Bank (PDB) ID: 2AZ5] in Accelrys Discovery Studio (DS) 3.5 program.

## **2. MATERILAS AND METHODS**

### **2.1. Chemicals and reagents**

Dulbecco's Modified Eagle's Medium (DMEM), fetal bovine serum (FBS), horse serum (HS), penicillin-streptomycin, trypsin-EDTA, and Dulbecco's Phosphate Buffered Saline (DPBS) were purchased from Gibco-BRL (Burlington, Ont, Canada).

### **2.2. Preparation of crude extract from marine brown algae**

Six species of marine brown algae [*Ishige okamurae* (IO), *Ishige foliacea* (IF), *Ecklonia cava* (EC), *Hizikia fusiforme* (HF), *Myelophycus caespitosus* (MC), *Sagarssum horneri* (SH)] collected on the coast of Jeju Island (Table 1-1, and Fig. 1-1). The dried algae (10 g) were extracted with 70% ethanol (EtOH) for 24 h at room temperature. The solutions were filtered and the filtrates were concentrated in a rotary vacuum evaporator.



Table 1-1. The list of marine brown algae.

No.	Korean name	Scientific name	Abbreviation
1	패	<i>Ishige okamurae</i>	IO
2	넓패	<i>Ishige foliacea</i>	IF
3	감태	<i>Ecklonia cava</i>	EC
4	툃	<i>Hizikia fusiforme</i>	HF
5	바위수염	<i>Myelophcus caespitosus</i>	MC
6	괭생이모자반	<i>Sargassum horneri</i>	SH



Fig. 1-1. The photography of six marine brown algae.

### **2.3. Macrophage cell culture**

The murine macrophage cell line RAW 264.7 was purchased from the Korean Cell Line Bank (KCLB, Seoul, Korea). RAW 264.7 cells were cultured in DMEM supplemented with 10% heat-inactivated FBS, streptomycin (100 µg/mL), and penicillin (100 unit/mL) at 37°C under 5% CO<sub>2</sub> humidified incubator. Exponential phase cells were used throughout the experiments.

### **2.4. Cell toxicity**

RAW 264.7 cells ( $1.5 \times 10^4$  cells/mL) plated in 24-well plates were pre-incubated for 16 h and then treated with lipopolysaccharide (LPS; 1 µg/mL) plus aliquots of the six marine brown algae ethanol extracts. The cells were then incubated for an additional 24 h at 37°C. The medium was carefully removed from each well, and the MTT stock solution (50 µL; 2 mg/mL in PBS) was added to each well. After 3 h of incubation, the formazan crystals were dissolved in dimethyl sulfoxide (DMSO), and the absorbance was measured using an ELISA plate reader at 540 nm (BioTek Instruments, Inc., Winooski, USA). The optical density of the formazan generated in non-treated control cells was considered to represent 100% viability.

### **2.5. Determination of Nitric oxide (NO) production**

RAW 264.7 cells ( $1.5 \times 10^4$  cells/mL) were seeded in 24-well plates and incubated for 16 h and then treated with six marine brown algae ethanol extracts for 1 h and stimulated LPS (1 µg/mL) for 24 h. After, the quantity of nitrite accumulated in the culture medium was measured as an indicator of NO production. Briefly, equal amounts of the culture medium

and Griess reagent [1% sulfanilamide and 0.1% naphthylethylenediamine dihydrochloride in 2.5% phosphoric acid] were reacted in a 96-well plate for 10 min at room temperature and the absorbance was measured at 540 nm using an ELISA plate reader (BioTek Instruments, Inc., Winooski, USA).

## **2.6. Myoblast cell culture and differentiation**

The murine C2C12 skeletal myoblasts were obtained from American Type Culture Collection (ATCC, Manassas, VA, USA) were cultured in DMEM supplemented with 10% heat-inactivated FBS, streptomycin (100 mg/mL), and penicillin (100 unit/mL) at 37°C under 5% CO<sub>2</sub> humidified incubator. To induce differentiation, 80% confluent cultures were switched to DMEM containing 2% HS for 4 days with medium changes every other day.

## **2.7. Cytotoxic assessment on C2C12 cells**

C2C12 myoblasts were seeded in 48-well plates at a concentration  $5.0 \times 10^4$  cells/mL. After 16 h, the cells were treated with six marine brown algae ethanol extracts and then incubated for an additional 24 h at 37°C under 5% CO<sub>2</sub> humidified incubator. After incubation, cytotoxic assessment was performed using MTT assay.

## **2.8. Skeletal muscle cell proliferation activity**

The skeletal muscle cell proliferation effects of six marine brown algae on C2C12 cells were

determined using the 5-bromo-2'-deoxyuridine (BrdU) assay (Millipore, Billerica, MA, USA). C2C12 cells ( $5.0 \times 10^4$  cells/mL) plated in 48-well plates were pre-incubated for 48 h and then converted into a differentiation medium (DMEM containing 2% HS) and treated with sixmarine brown algae ethanol extracts every other day. Cell proliferation was calculated by comparison with the absorbance at 450 nm of standard solutions of BrdU in the non-treated cells.

### **2.9. *In silico* docking of new inhibitor candidates to TNF- $\alpha$**

For molecular docking studies, the crystal structure of protein was allocated from PDB (<http://www.pdb.org>) and the docking of the protein-ligand complex, the possibility of binding, and value of binding energy were performed using flexible docking in Accelrys Discovery Studio (DS) 3.5 (BIOVIA, CA, USA). To prepare of the docking procedure, we performed the following steps: (1) conversion of the 2D structure into 3D structure; (2) preparing protein and defining the binding site; (3) preparing ligands (bioactive natural compounds obtained from six marine brown algae)

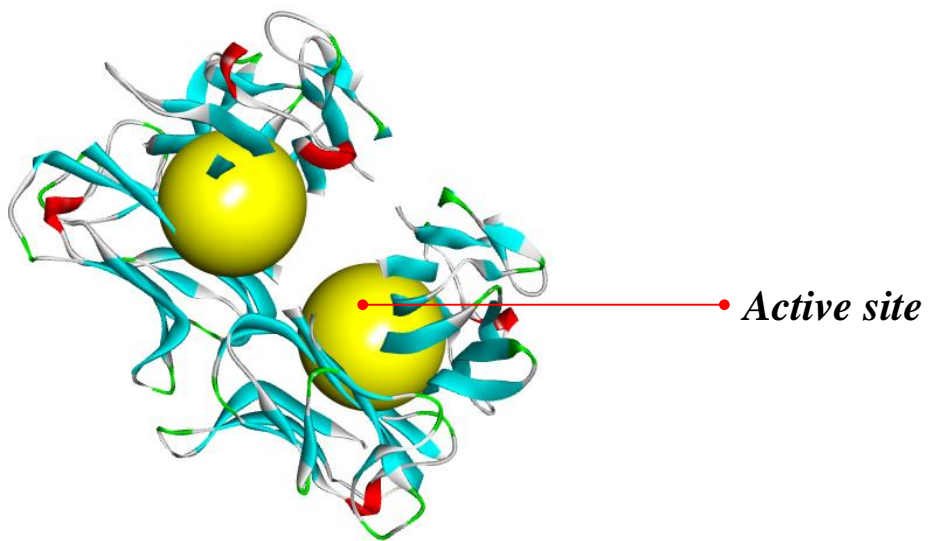
### **2.10. Molecular docking analysis of candidate compounds on TNF- $\alpha$**

Docking of the selected bioactive natural compounds from six marine brown algae were predicted by simulating the interaction between the compounds and TNF- $\alpha$  by flexible docking tool in an *in silico* study. The structure of TNF- $\alpha$  was allocated from PDB (PDB ID: 2AZ5, Fig. 1-2). The structural information of candidate compounds was provided from our

previous studies and the structures were drawn by CDocker tool. To select the candidates of various marine-derived compounds, two kinds of energy value of relative complexes were compared as following: -CDocker interaction energy (kcal/mol) and binding energy (kcal/mol). Also, the docking poses of the selected compounds to TNF- $\alpha$  were expressed as 3D crystal structure.

### **2.11. Statistical analysis**

All experiments were conducted in triplicate (n=3) and an one-way analysis of variance (ANOVA) test (using SPSS 12.0 statistical software) was to analyze the data. Significant differences between the means of parameters were determined by using Tukey test to analyze the difference. P-values of less than 0.05 ( $P < 0.05$ ) and 0.01 ( $P < 0.01$ ) was considered as significant.



***PDB ID: 2AZ5 (TNF- $\alpha$ )***

Fig. 1-2. Crystal structure of TNF- $\alpha$  obtained from protein data bank (PDB, PDB ID: 2AZ5).

### **3. RESULTS and DISCUSSION**

#### **3.1. Effect of ethanol extracts on macrophage cell viability**

Prior to evaluation of the NO inhibitory activity of marine brown algae ethanol extracts, their cytotoxic effects on the viability of RAW 264.7 cells were examined. Cytotoxicity of all the ethanol extracts was assessed using the MTT assay. All the ethanol extracts showed non-cytotoxic effect on RAW 264.7 cells at the tested concentrations (Fig. 1-3). Thus, those concentrations were used in subsequent experiments.

#### **3.2. Effect of marine brown algae ethanol extracts on NO production in LPS-stimulated RAW 264.7 cells**

To examine the potential anti-inflammatory properties of six marine brown algae ethanol extracts on LPS-induced NO production in RAW 264.7 cells, cells were treated with or without extracts (6.25, 12.5, 25, 50, 100, and 200  $\mu\text{g/mL}$ ) for 24 h. NO production in the culture supernatants were measured by the Griess assay. The level of NO production is significantly increased in the LPS-treated cells compared to the untreated cells. However, all the ethanol extracts significantly inhibited the LPS-induced NO production (Fig. 1-4). All ethanolic extracts did not affect the cytotoxic of RAW 264.7 cells at the used concentrations except MC extracts (Fig. 1-5).



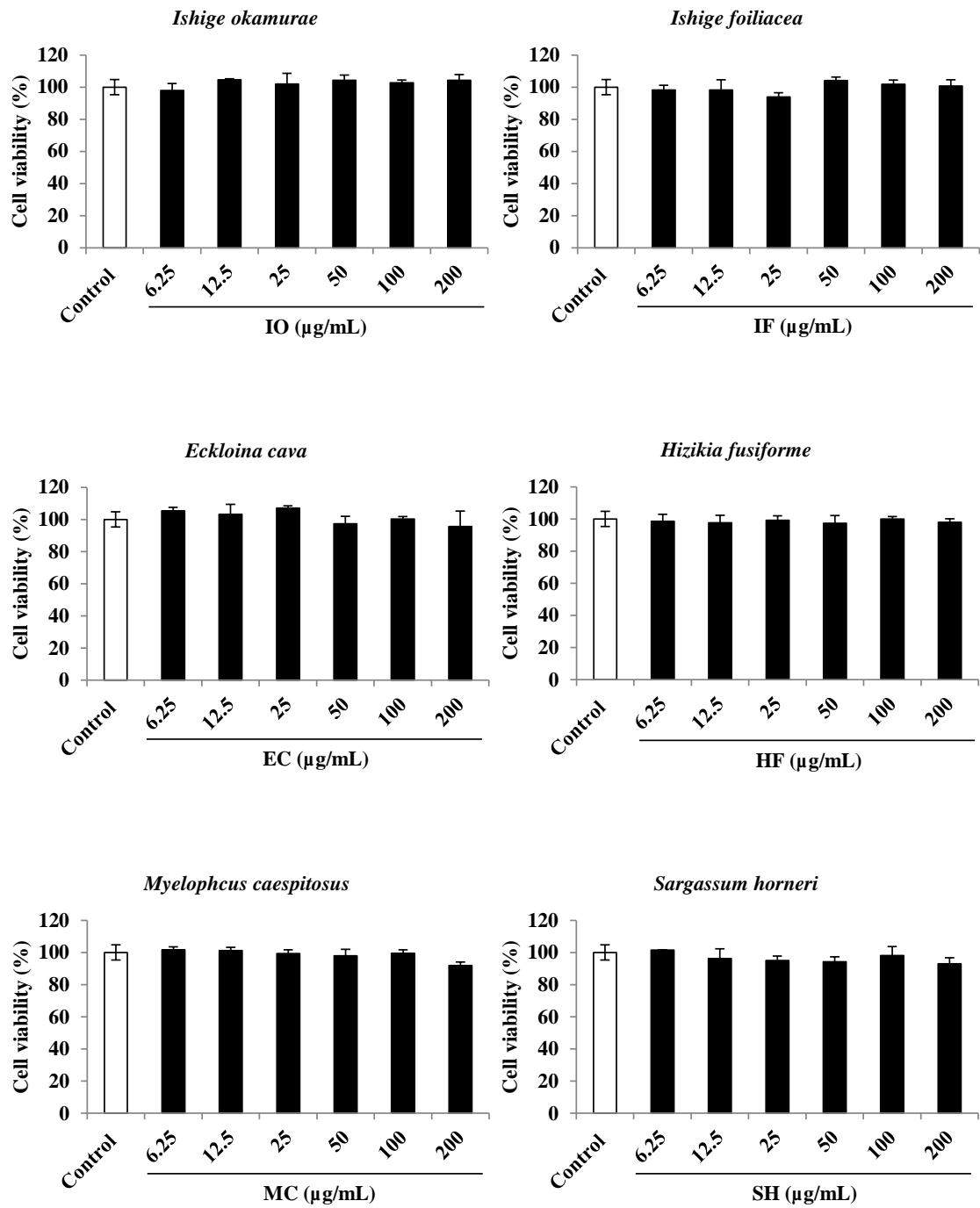


Fig. 1-3. Cell toxicity of marine brown algae extracts on RAW 264.7 macrophage cells by a MTT assay. Experiments were performed in triplicate and the data are expressed as mean  $\pm$  SE; #  $P < 0.05$ , and ##  $P < 0.01$  as compared to the untreated group.

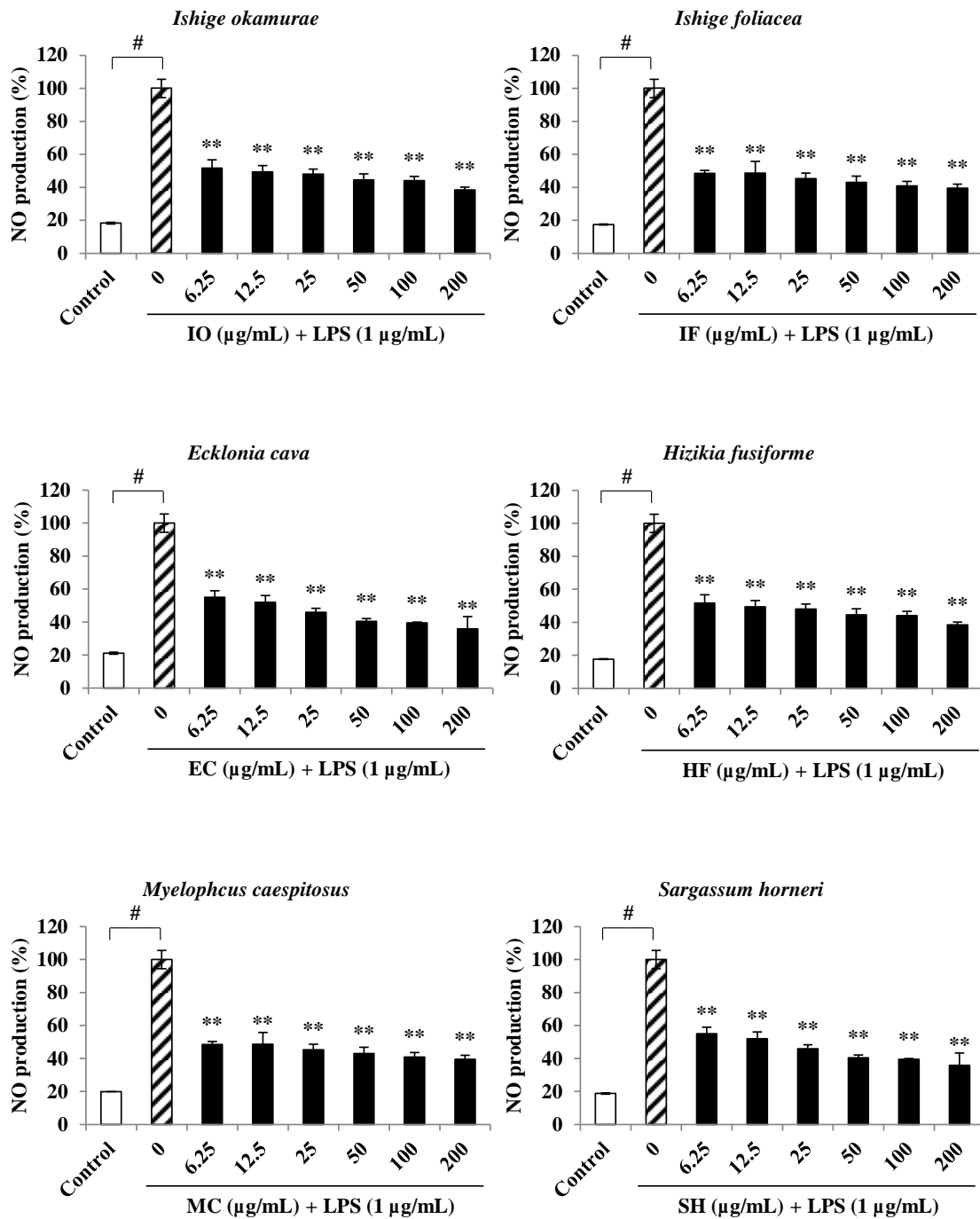


Fig. 1-4. Anti-inflammatory effect of marine brown algae extracts on RAW 264.7 macrophage cells by a Griess assay. Experiments were performed in triplicate and the data are expressed as mean  $\pm$  SE; <sup>#</sup>  $P < 0.05$ , and <sup>##</sup>  $P < 0.01$  as compared to the untreated group. \*  $P < 0.05$ , and <sup>\*\*</sup>  $P < 0.01$  as compared to the LPS-treated group.

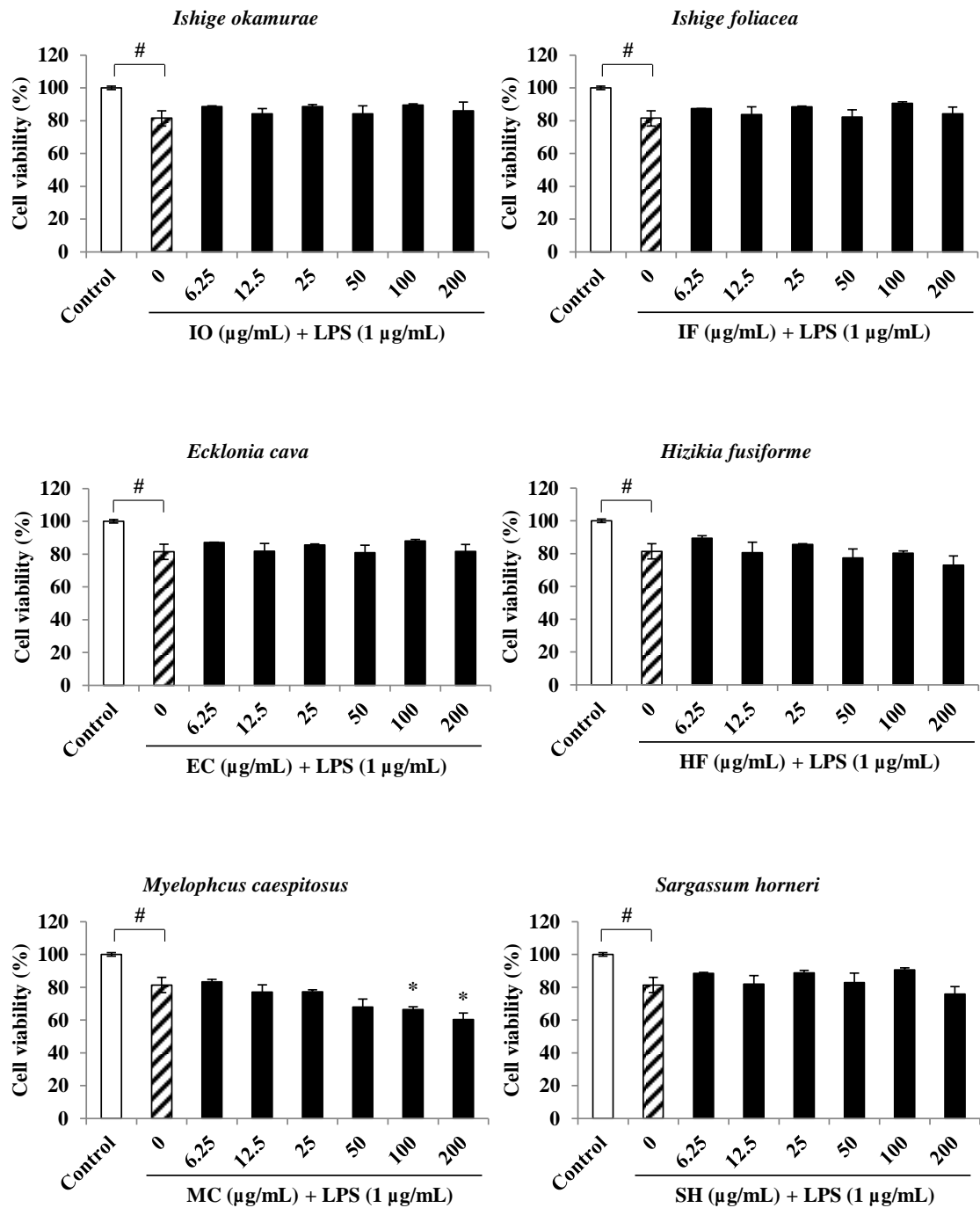


Fig. 1-5. Anti-inflammatory effect of marine brown algae extracts by a MTT assay on RAW 264.7 macrophage cells. Experiments were performed in triplicate and the data are expressed as mean  $\pm$  SE; #  $P < 0.05$ , and ##  $P < 0.01$  as compared to the untreated group. \*  $P < 0.05$ , and \*\*  $P < 0.01$  as compared to the LPS-treated group.

### **3.3. Cytotoxicity of marine brown algae ethanol extracts on C2C12 myoblasts**

Prior to evaluating the cell proliferation effect of marine brown algae ethanol extracts, their cytotoxic effects on the viability of C2C12 myoblasts were examined. Cytotoxicity of marine brown ethanol extracts was evaluated with MTT assay and all the extracts showed non-cytotoxic effect on C2C12 cells at the tested concentrations (Fig. 1-6). Thus, those concentrations were used in subsequent experiments.

### **3.4. Cell proliferation activity of marine brown algae ethanol extracts on C2C12 cells**

The skeletal muscle cell proliferation activity of the different marine brown algae ethanol extracts was measured using BrdU cell proliferation assay. BrdU cell proliferation assay is a non-isotopic assay for the in vitro quantitative detection of newly synthesized DNA of actively proliferating cells. Among extracts, IO and IF extracts significantly increased proliferation of myoblast compared to the non-treated cells. However, other four extracts (EC, HF, MC, and SH) did not affect cell proliferation on C2C12 cells (Fig. 1-7).

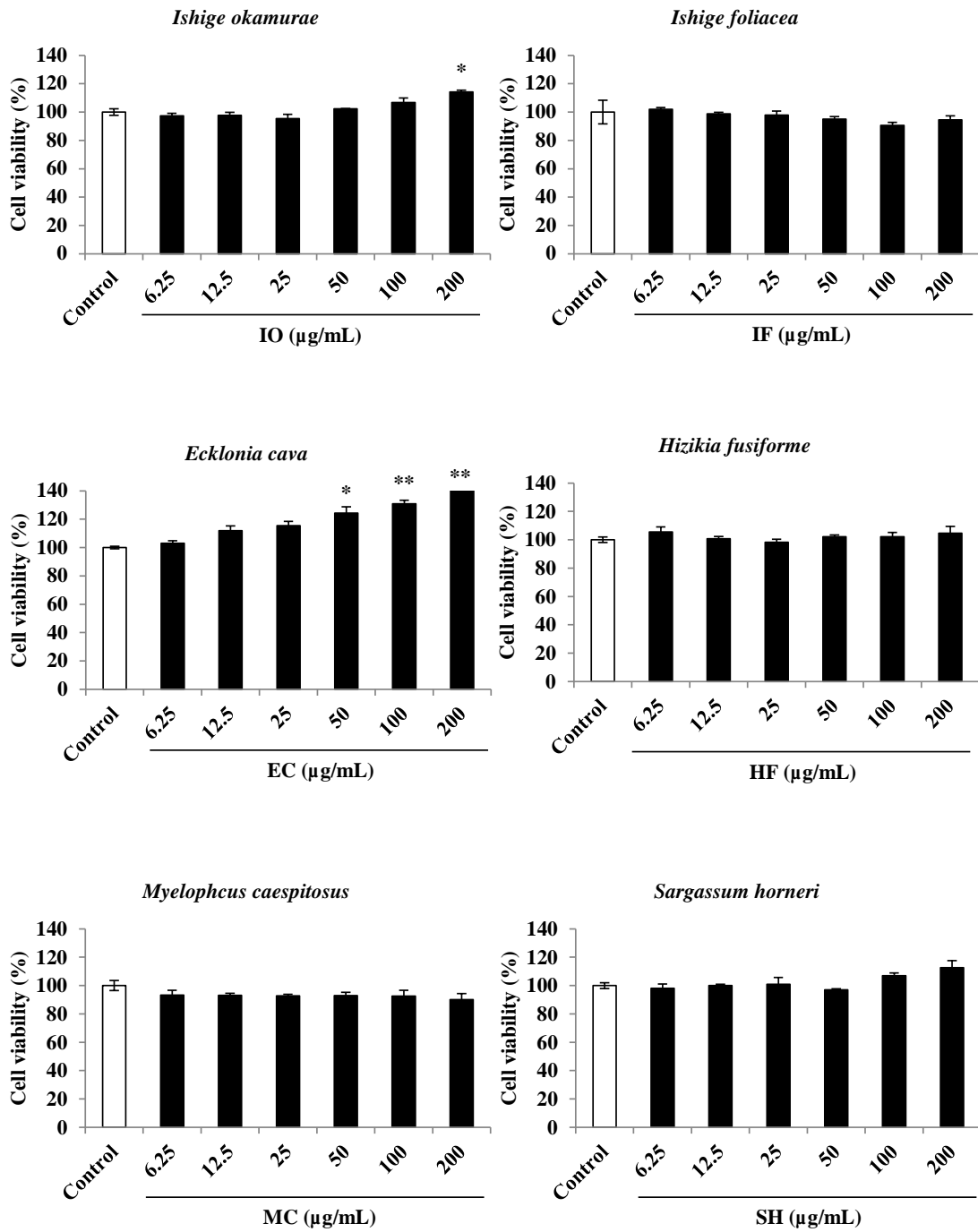


Fig. 1-6. Cell toxicity of marine brown algae extracts on C2C12 skeletal myoblast cells by a MTT assay. Experiments were performed in triplicate and the data are expressed as mean  $\pm$  SE; \*  $P < 0.05$ , and \*\*  $P < 0.01$  as compared to the untreated group.

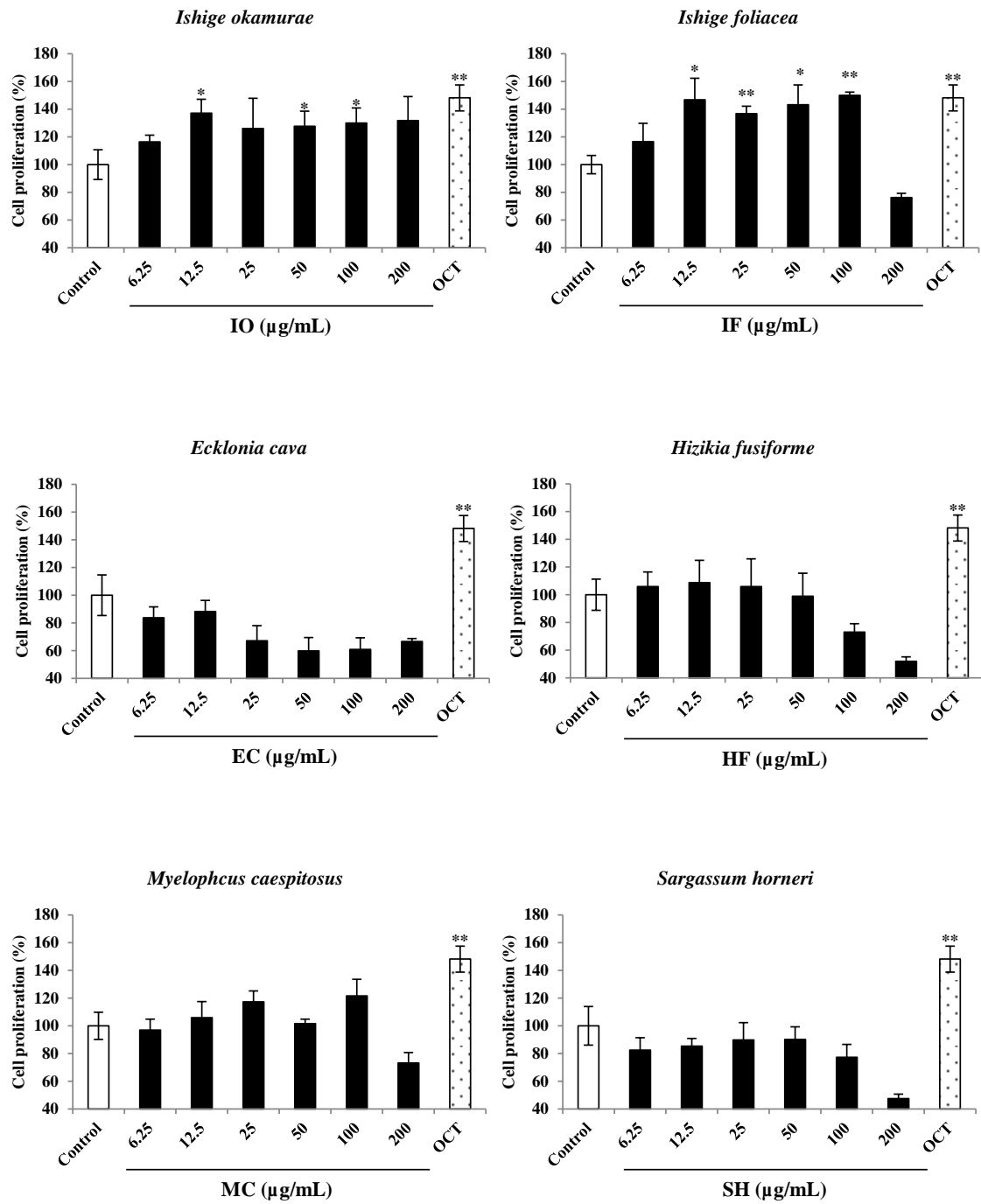


Fig. 1-7. Skeletal muscle cell proliferation effect of marine brown algae extracts on C2C12 skeletal muscle cells by a BrdU assay. OCT, Octacosanol (25 µg/mL) treated group. Experiments were performed in triplicate and the data are expressed as mean ±SE; \*  $P < 0.05$ , and \*\*  $P < 0.01$  as compared to the untreated group.

Table 1-2. The effect of anti-inflammatory and cell proliferation of marine brown algae extracts in RAW 264.7 macrophage cells, and C2C12 skeletal muscle cells, respectively. Experiments were performed in triplicate and the data are expressed as mean  $\pm$ SE; \*  $P < 0.05$ , and \*\*  $P < 0.01$  as compared to the untreated group.

Sample	RAW 264.7 cells	C2C12 cells
	NO inhibition (IC <sub>50</sub> , $\mu$ g/mL)	Muscle cell proliferation (% of control at 100 $\mu$ g/mL)
IO	0.33 $\pm$ 0.13	27.90 $\pm$ 10.93*
IF	1.51 $\pm$ 0.04	50.00 $\pm$ 2.28**
EC	0.33 $\pm$ 0.06	-39.14 $\pm$ 8.54
HF	0.42 $\pm$ 0.56	-26.94 $\pm$ 6.07
MC	0.13 $\pm$ 0.13	21.57 $\pm$ 12.02
SH	0.83 $\pm$ 0.32	-22.57 $\pm$ 9.12
OCT	0	48.14 $\pm$ 9.39**

### 3.5. *In silico* docking simulation of marine-derived bioactive compounds to TNF- $\alpha$

Bioactive compounds possess multi-functional activities based on their structural characteristics such as hydrophobicity, charge, microelement binding activity. To explore a TNF- $\alpha$  inhibitor from marine-derived products, the biological network dynamic between TNF- $\alpha$  and these marine-derived natural compounds were simulated in computational space. Crystal structure of TNF- $\alpha$  was allocated from PDB (PDB ID: 2AZ5). Eight kinds of natural compounds derived from brown algae (IO, IF, EC, HF, MC, and SH) with biological activities were selected as TNF- $\alpha$  inhibitor candidates (Table 1-3). The structural information of these compounds was provided from previous studies and the structures were drawn by ChemDraw Ultra 12.0 (Chemistry.Com.Pk, Fig. 1-8). All docking poses of the TNF- $\alpha$  inhibitor candidates to TNF- $\alpha$  were expressed as 2 dimensional chart using -CDOCKER interaction energy (kcal/mol) (Fig. 1-9 ~ 1-17) and binding energy (kcal/mol) (Table 1-4). Among the TNF- $\alpha$  inhibitor candidates, five compound candidates (Diphlorethohydroxycarmalol; DPHC, Dieckol; DK, Saringosterol acetate; SA, Gadoleic acid; GA, Sargachromanol E; SC-E) stably bind to TNF- $\alpha$ . Specially, DPHC showed the lowest binding energy value, despite the lowest number of poses combined with TNF- $\alpha$ .

## 4. Conclusion

DPHC is isolable from IO, which has anti-inflammatory effects in macrophage RAW 264.7 cells and exhibit cell proliferation activity of C2C12 myoblasts. It was expected that DPHC isolated from IO would be efficiently developed into inflammatory myopathy which acts as a TNF- $\alpha$  inhibitor agent. Therefore, DPHC are used in further experiments.



Table 1-3. The list of six marine brown algae extract-derived natural bioactive compounds for *in silico* molecular docking simulation with TNF- $\alpha$ , which is regulator of myopathy.

No.	Marine brown algae	Natural compounds (Ligands)	Abbreviation	Molecular weight (g/mol)
1	IO	Diphlorethohydroxycarmalol	DPHC	513.05
2	IF	Hexakaidecaphlorethol	HDP	1986.2630
3	EC	Dieckol	DK	742.554
4	EC	2,7''-phloroglucinol-6,6-'bieckol	PHB	973
5	HF	Saringosterol acetate	SA	469.58
6	MC	Gadoleic acid	GA	310.522
7	SH	Sargachromanol E	SC-E	428.613
8	SH	Apo-9'-fucoxanthinone	AF	266.333
9	Positive control	Octacosanol	OCT	410.76

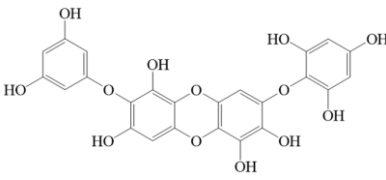
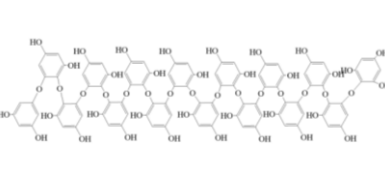
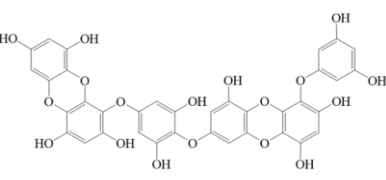
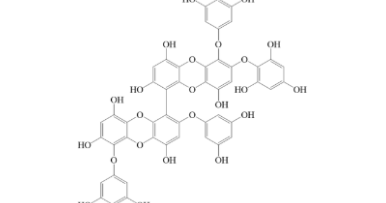
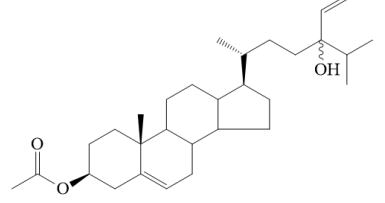
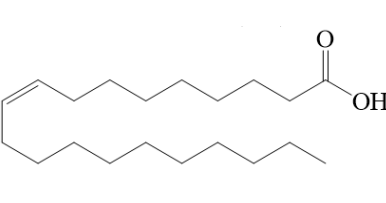
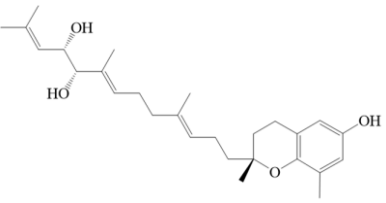
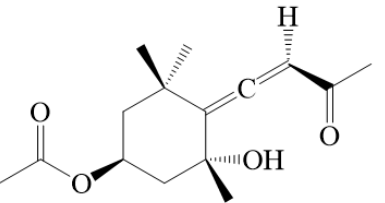
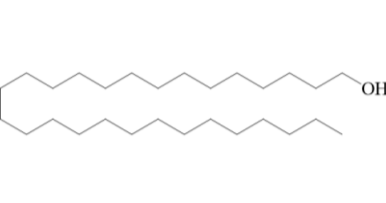
DPHC	HDP	DK
		
PHB	SA	GA
		
SC-E	AF	OCT
		

Fig. 1-8. The chemical structures of marine brown algae-derived natural compounds.

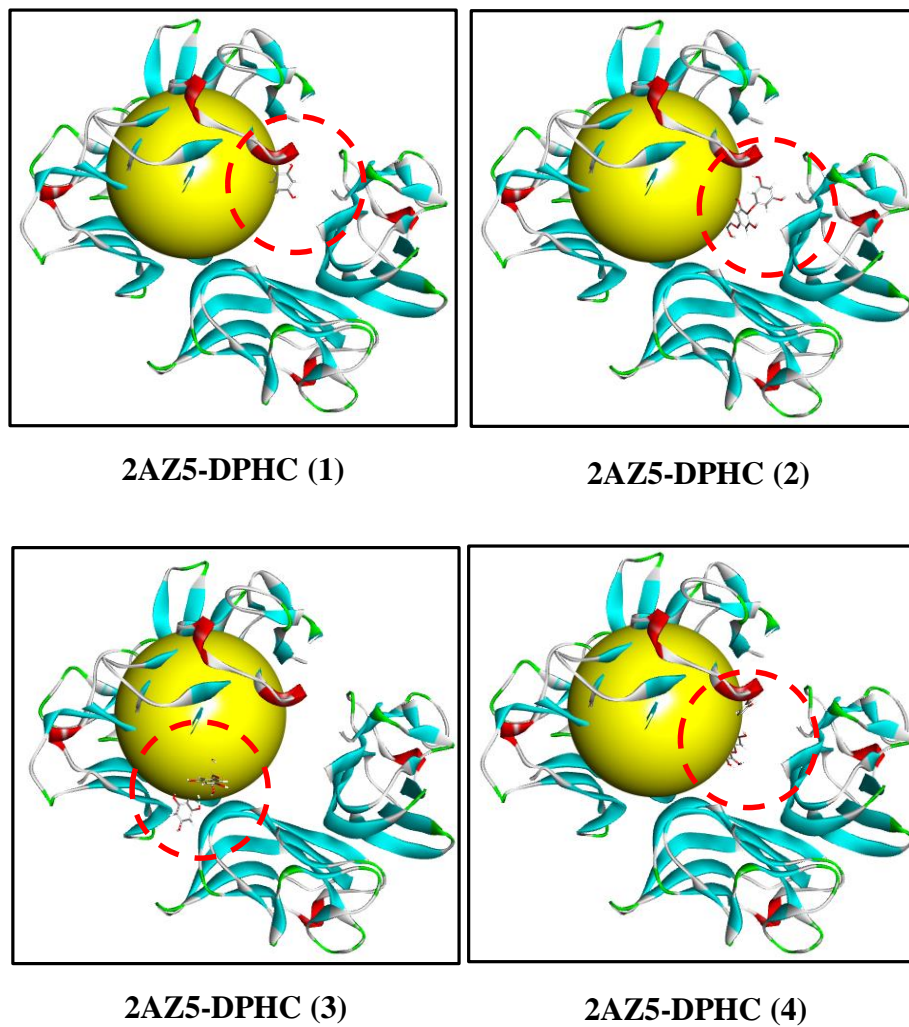


Fig. 1-9. Computational prediction of the 3D structure for TNF- $\alpha$  (PDB ID: 2AZ5) and docking simulation with DPHC.

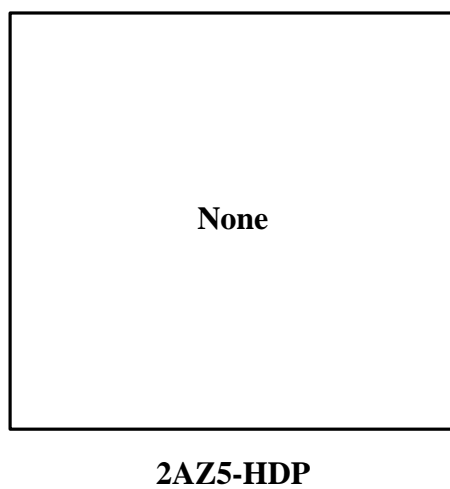


Fig. 1-10. Computational prediction of the 3D structure for TNF- $\alpha$  (PDB ID: 2AZ5) and docking simulation with HDP.

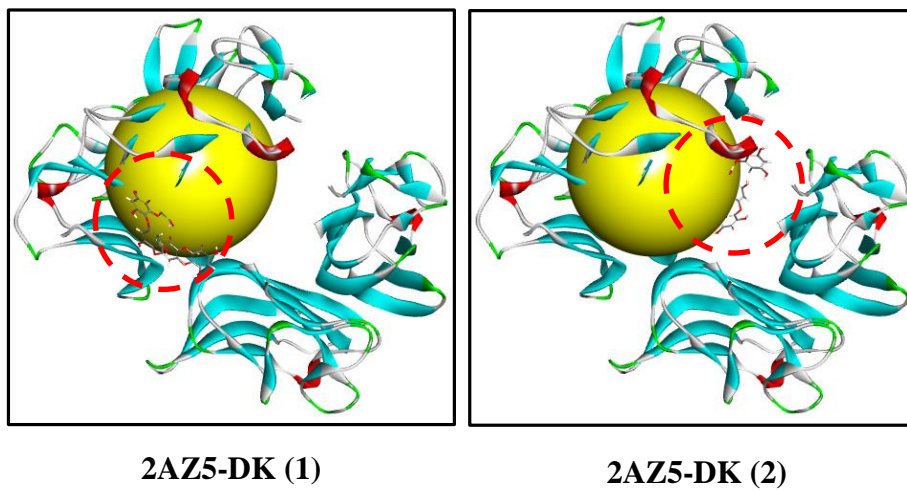


Fig. 1-11. Computational prediction of the 3D structure for TNF- $\alpha$  (PDB ID: 2AZ5) and docking simulation with DK.

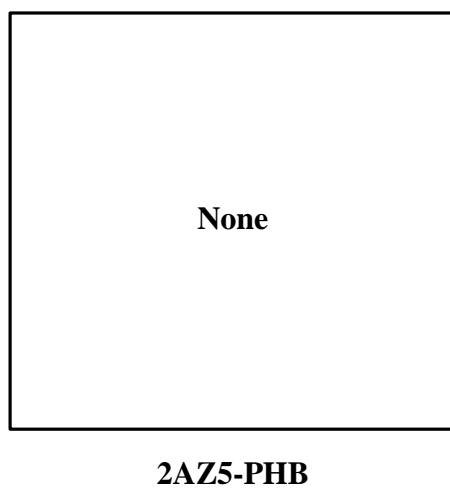


Fig. 1-12. Computational prediction of the 3D structure for TNF- $\alpha$  (PDB ID: 2AZ5) and docking simulation with PHB.

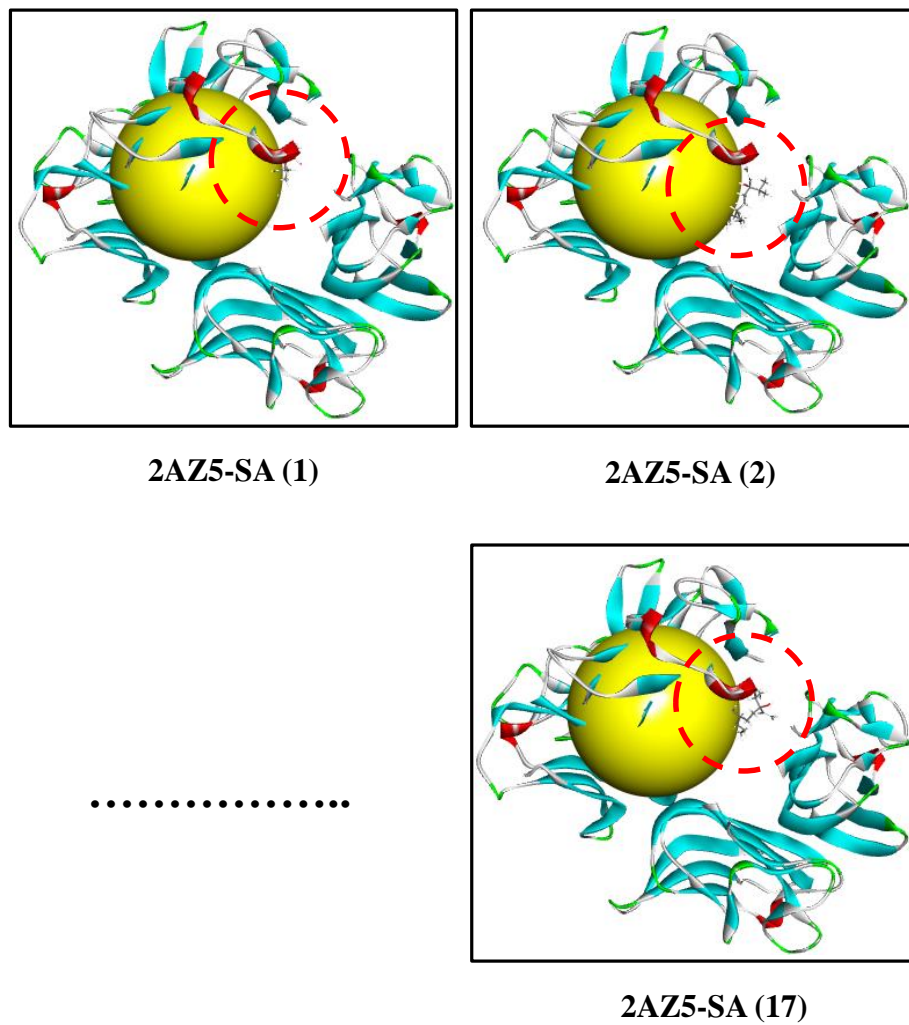


Fig. 1-13. Computational prediction of the 3D structure for TNF- $\alpha$  (PDB ID: 2AZ5) and docking simulation with SA.

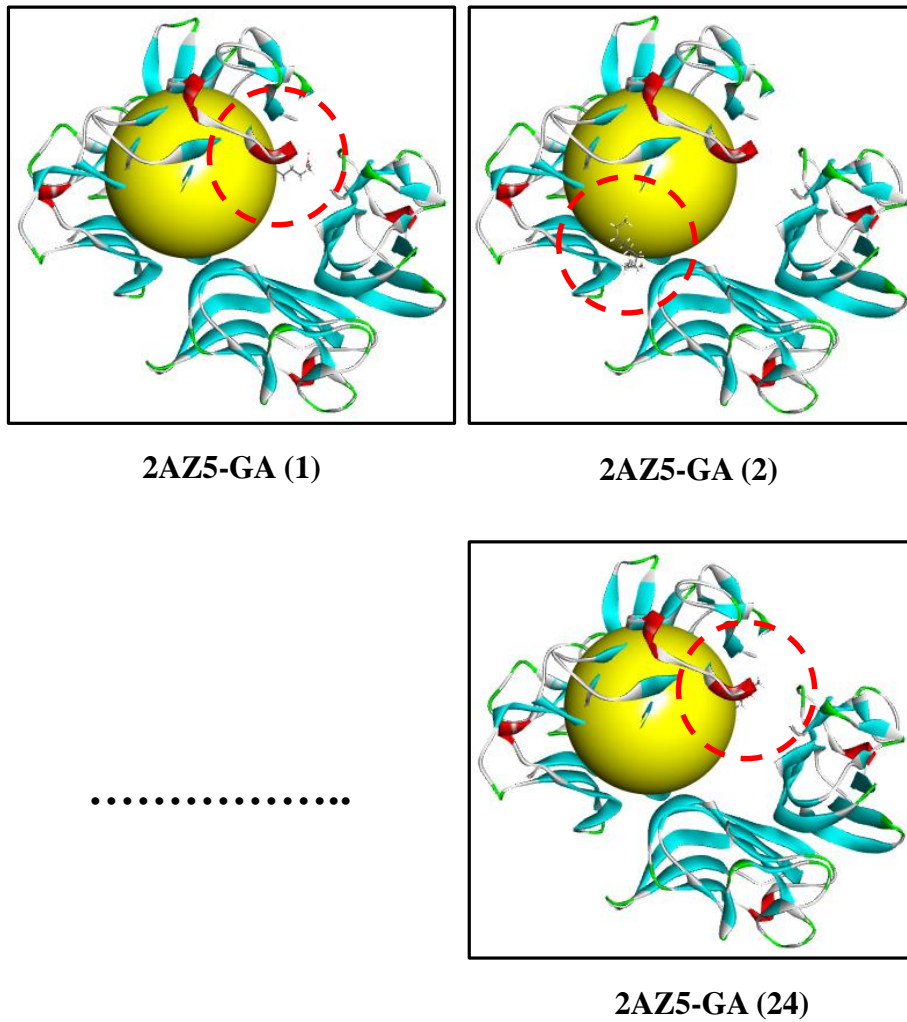


Fig. 1-14. Computational prediction of the 3D structure for TNF- $\alpha$  (PDB ID: 2AZ5) and docking simulation with GA.



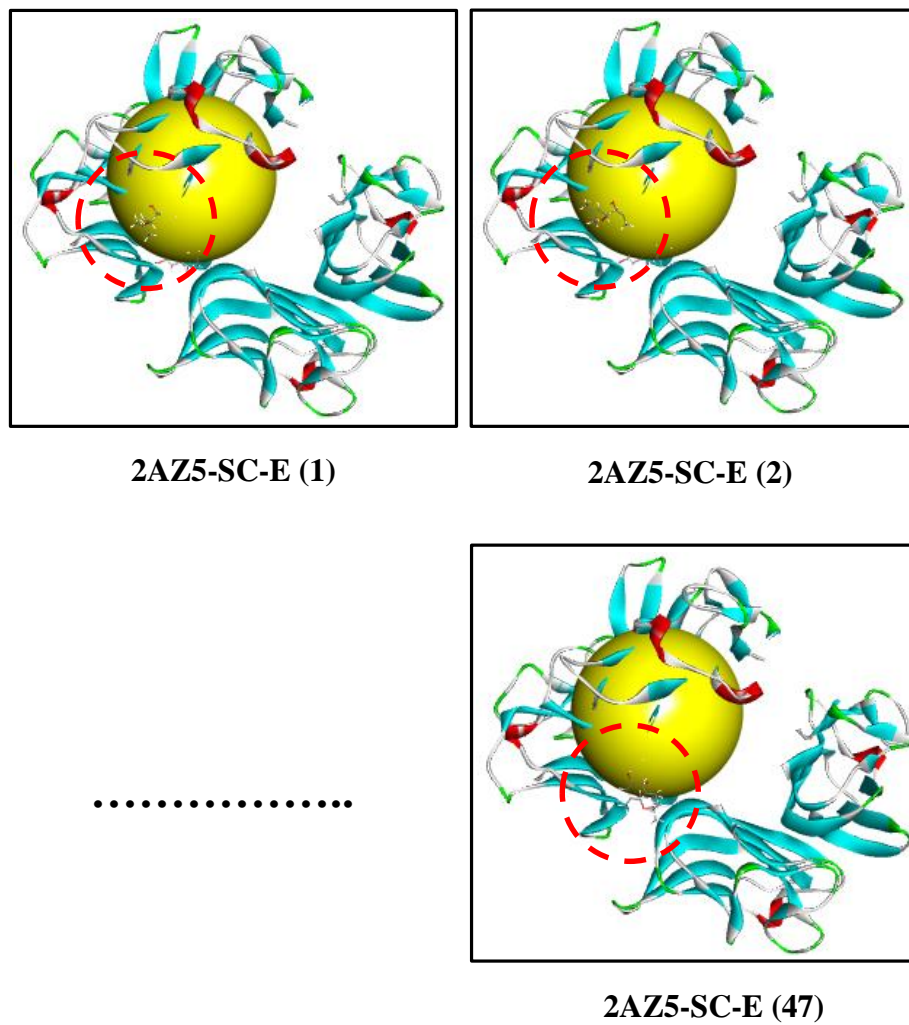


Fig. 1-15. Computational prediction of the 3D structure for TNF- $\alpha$  (PDB ID: 2AZ5) and docking simulation with SC-E.

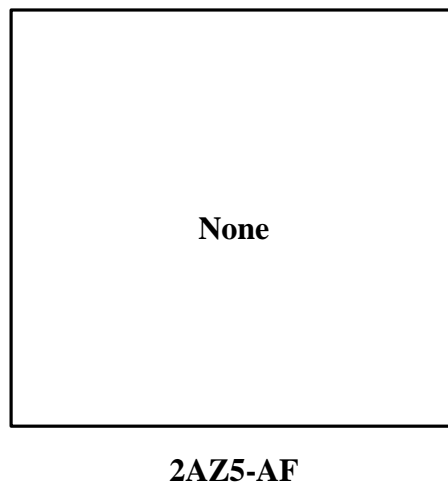


Fig. 1-16. Computational prediction of the 3D structure for TNF- $\alpha$  (PDB ID: 2AZ5) and docking simulation with AF.

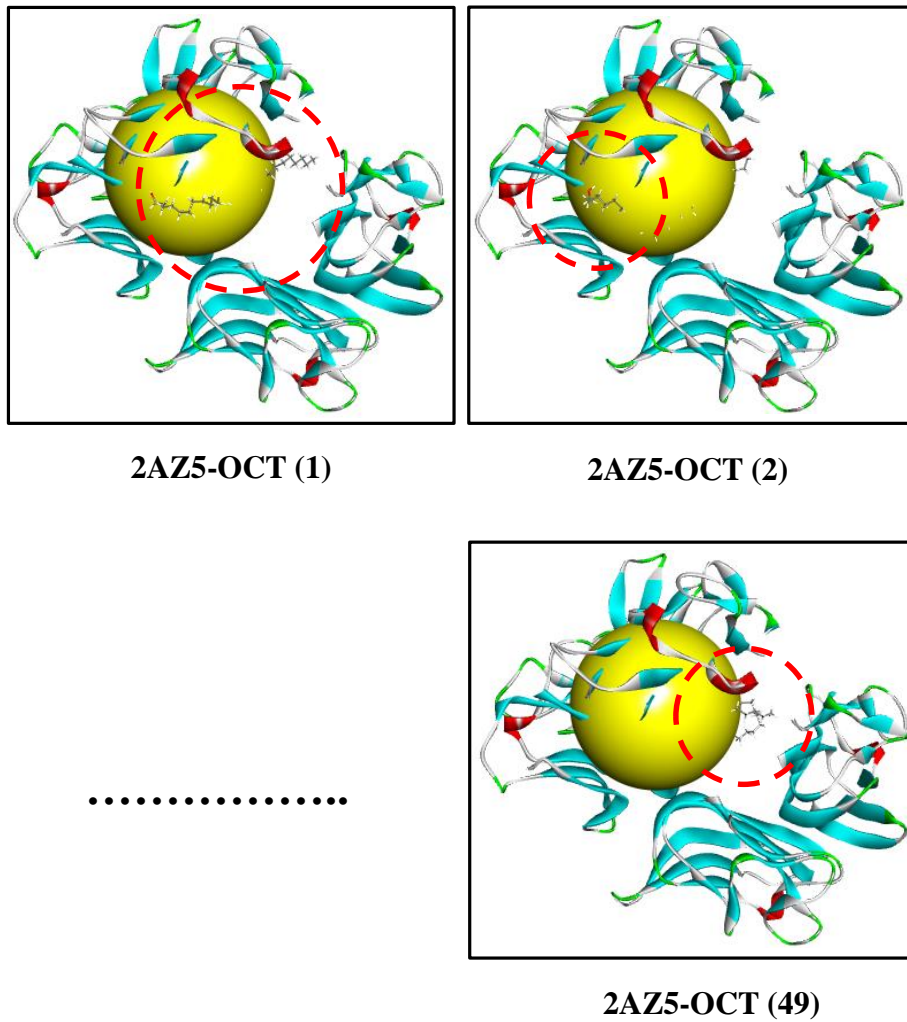


Fig. 1-17. Computational prediction of the 3D structure for TNF- $\alpha$  (PDB ID: 2AZ5) and docking simulation with OCT.

Table 1-4. Results of docking simulations of marine brown algae-derived natural compounds with TNF- $\alpha$  (PDB ID: 2AZ5).

Ligands	Pose	Binding energy (kcal/mol)	CDOCK interaction energy (kcal/mol)
DPHC	4	-53.73	-40.33
HDP	0		
DK	2	-36.09	-47.49
PHB	0		
SA	17	-39.33	-36.49
GA	24	-43.01	-31.26
SC-E	47	-33.47	-48.25
AF	0		
OCT	49	-44.01	-31.83

## **Part II.**

### **Effect of marine algal bioactive compound on inflammatory myopathy in C2C12 skeletal muscle cells**

## Part II.

### Effect of marine algal bioactive compound on inflammatory myopathy in C2C12 skeletal muscle cells

#### ABSTRACT

It is well known fact that pro-inflammatory mediators such as nitric oxide (NO), tumor necrosis factor-alpha (TNF- $\alpha$ ), interleukin (IL)-1 $\beta$ , and IL-6 contribute to the courses of many inflammatory disease including, Alzheimer's disease, cancer, major depression, psoriasis, and inflammatory bowel disease. Especially, TNF- $\alpha$  is a cell signaling protein (cytokine) involved in systemic inflammation and is one of the cytokines that make up the acute phase reaction. In the present study, I attempted to investigate the protective effect of diphlorethohydroxycarmalol (DPHC), a natural biologically active substance isolated from *Ishige okamurae* (IO) by examining its inhibitory effects on pro-inflammatory mediators, and anti-oxidant enzymes expression in TNF- $\alpha$  or H<sub>2</sub>O<sub>2</sub>-stimulated C2C12 myocytes. DPHC down-regulated the mRNA expression levels of pro-inflammatory cytokines (TNF- $\alpha$ , IL-1 $\beta$ , and IL-6) and up-regulated the antioxidant enzymes such as superoxide dismutase (SOD), and catalase (CAT) as well as inhibited nitric oxide (NO) production. In addition, DPHC down-regulated the NF- $\kappa$ B, and MAPKs signaling pathways related protein expressions in TNF- $\alpha$  or H<sub>2</sub>O<sub>2</sub>-stimulated myocytes. Furthermore, DPHC suppressed the MuRF-1 and MAFbx/Atrogin-1, which are the key protein of muscle atrophy. These results suggesting that DPHC, a marine-derived bioactive compound, has a potential to regulate inflammatory myopathy genes via monitoring the NF- $\kappa$ B, and MAPKs signaling pathways.

## 1. INTRODUCTION

Skeletal muscle is comprised of heterogeneous muscle fibers that enable the body to maintain posture and perform a wide range of movements and motions (Rhonda et al., 2006). In response to environmental demands, skeletal muscle remodels by activating signaling pathways to reprogram gene expression to sustain muscle performance (Rhonda et al., 2006). The skeletal muscle that are constantly stimulated by the environmental factors suffer a steady decline in mass and functional performance accompanied by a characteristic loss of muscle fiber (Musarò et al., 2001). Also, muscle suffers change intracellular signaling pathways by environmental change such as hormonal changes in the body, oxidative stresses, accumulation of reactive oxygen species (ROS), and secretion of inflammatory cytokines (Londhe et al., 2015; Duchesne et al., 2017; Li et al., 2005). Notably, both in animals and humans, muscle injury also activates an inflammatory response characterized by the coordinated recruitment of inflammatory cells to the site of injury (Smith et al., 2008). The onset, development, and resolution of the inflammatory process have a critical role on the guidance of satellite cell function and thus, on muscle regeneration (Tidball, 2005). In the acute inflammation, neutrophils and pro-inflammatory macrophages (M1) massively accumulated in the injured muscle and the M1 macrophages release a variety of pro-inflammatory agents including tumor necrosis factor-alpha (TNF- $\alpha$ ) (Arnold et al., 2007; Duchesne et al., 2017). In chronic inflammation, the persistence of neutrophils impairs macrophage conversion from M1 to M2 profile and these cells adopt a hybrid phenotype, which impairs muscle healing and triggers fibrosis by releasing an exaggerate amount TGF-beta (Duchesne et al., 2017; Mann et al., 2011; Lemos et al., 2015; Zhou et al., 2016). TNF- $\alpha$  is an inflammatory cytokine implicated in muscle atrophy conditions associated with various

diseases (Zhou et al., 2016). TNF- $\alpha$  signaling can be mediated by TNFR1 (p55) or TNFR2 (p75). TNFR1 is believed to mediate the muscle atrophy, whereas TNFR2 is protective (Zhou et al., 2016). In muscle tissue from patients with idiopathic inflammatory myopathies low expression of TNFR was detected in occasional T cells and macrophages, as well as in a proportion of endothelial cells surrounded by infiltrating inflammatory cells and on TNF- $\alpha$  expressing muscle fibres (Kuru et al., 2003). This observation further supports a role of TNF- $\alpha$  in the disease mechanism of inflammatory myopathies. TNFR1 and TNFR2 recruit separate downstream adaptor molecules to induce a cellular response, but converge on TNF receptor-associated factor 2 (TRAF2), to activate IKK and NF- $\kappa$ B (Wajant and Scheurich, 2011).

TNFR1-triggered nuclear factor-kappa B (NF- $\kappa$ B) activation leads to increased expression of muscle RING-finger protein 1 (MuRF1) and subsequent protein degradation through the ubiquitin proteasome pathway. NF- $\kappa$ B also inhibits satellite cell activation and differentiation by inhibiting MyoD expression (Zaho et al., 2015). Recent studies have identified NF- $\kappa$ B as an important transcription factor involved in skeletal muscle atrophy caused by TNF- $\alpha$  (Cai et al., 2004; Mourkioti et al., 2006; Li et al., 2005). In differentiating myoblasts, TNF- $\alpha$  induced activation of NF- $\kappa$ B led the reduced expression of the differentiation markers myogenin and myosin chain (Guttridge et al., 2000; Li et al., 2000). In addition, Li have demonstrated that an increase the expression of MuRF-1 and Muscle Atrophy F-Box (MAFbx)/Atrogin-1 proteins through NF- $\kappa$ B and MAPKs pathways in C2C12 cells exposed to TNF- $\alpha$ . Evidence suggests that MAFbx/Atrogin-1 plays a pivotal role in muscle atrophy (Bodine et al., 2001; Gomes et al., 2001). Overexpression of MAFbx/Atrogin-1 in cultured C2C12 myotubes produces cell atrophy and mice knocked out of the MAFbx/Atrogin-1 gene are more resistant to muscle wasting that results from muscular denervation than their wild-type littermates



(Bodine et al., 2001). As with TNF- $\alpha$ , Li have identified H<sub>2</sub>O<sub>2</sub> exposure up-regulates MAFbx/Atrogin-1 and MuRF-1 mRNA in C2C12 myotubes. Skeletal muscle myotubes continuously generate H<sub>2</sub>O<sub>2</sub> and other reactive oxygen species (ROS) that function as intracellular signaling molecules (Li et al., 2005). Production of ROS and ROS-mediated signaling are stimulated by TNF- $\alpha$  that increases general activity of the ubiquitin conjugating pathway (Li et al., 2005). In this study, therefore, I aimed to establish an inflammatory myopathy model in C2C12 cells by TNF- $\alpha$  and H<sub>2</sub>O<sub>2</sub> and identify marine brown algae-derived biological substance Diphlorethohydroxycarmalol (DPHC) that have protective effects inflammatory myopathy through NF- $\kappa$ B and MAPKs pathways.

## **2. MATERIALS AND METHODS**

### **2.1. Chemicals and reagents**

Dulbecco's Modified Eagle's Medium (DMEM), fetal bovine serum (FBS), horse serum (HS), penicillin-streptomycin, trypsin-EDTA, and Dulbecco's Phosphate Buffered Saline (DPBS) were purchased from Gibco-BRL (Burlington, Ont, Canada).

### **2.2. Experimental design of TNF- $\alpha$ or H<sub>2</sub>O<sub>2</sub>-induced myopathy**

The murine C2C12 skeletal myoblasts were obtained from American Type Culture Collection (ATCC, Manassas, VA, USA) were cultured in DMEM supplemented with 10% heat-inactivated FBS, streptomycin (100 mg/mL), and penicillin (100 unit/mL) at 37°C under 5% CO<sub>2</sub> humidified incubator. To induce differentiation, 80% confluent cultures were switched to DMEM containing 2% HS for 4 days with medium changes every other day. Differentiated myotubes were treated for 30 min with TNF- $\alpha$  (200 ng/mL) or H<sub>2</sub>O<sub>2</sub> (300  $\mu$ M) to induce inflammation.

### **2.3. Cytotoxic assessment**

C2C12 myoblasts were seeded in 48-well plates at a concentration  $5.0 \times 10^4$  cells/mL. Cells were pre-incubated for 48 h and then converted into a differentiation medium (DMEM containing 2% HS) and treated with DPHC every other day during differentiation period. After differentiation, cells were treated with TNF- $\alpha$  (200 ng/mL) or H<sub>2</sub>O<sub>2</sub> (300  $\mu$ M) and then incubated for an additional 30 min at 37°C under 5% CO<sub>2</sub> humidified incubator. After

incubation, cytotoxic assessment was performed using MTT assay.

#### **2.4. Myotubes analysis**

Myotube metrics were quantified using microscope equipped with a CoolSNAP-Pro color digital camera (Olympus, Japan) to determine myotube diameter. Briefly, C2C12 cells ( $5.0 \times 10^4$  cells/mL) were seeded in 12-well plates and incubated for 48 h and treated with DPHC during differentiation period. After that, cells were stimulated with TNF- $\alpha$  (200 ng/mL) or H<sub>2</sub>O<sub>2</sub> (300  $\mu$ M) for 30 min. Finally, average myotubes length was evaluated as the mean of ten approximately equidistant measurements taken along the length of the myotubes.

#### **2.5. Determination of NO production and ROS production**

To determine the effects of DPHC on NO production and intracellular ROS production in inflammatory C2C12 myotubes, C2C12 cells were differentiated with DPHC and then induced inflammation using TNF- $\alpha$  or H<sub>2</sub>O<sub>2</sub>. NO production was detected using Griess assay and ROS production was assessed using 2',7'-dichlorodihydrofluorescein diacetate (DCFH-DA, 5  $\mu$ g/mL). DCHF-DA was introduced to the cells, and fluorescence was detected at an excitation wavelength of 485 nm and an emission wave length of 535 nm.

#### **2.6. Determination of antioxidant enzymes activity**

Activities of superoxide dismutase (SOD) and catalase (CAT) were measured according to

the described method of BioVision Colorimetric/Fluorometric Assay kit.

## **2.7. Measurement of pro-inflammatory cytokines expression**

The inhibitory effects of DPHC on the pro-inflammatory cytokines (TNF- $\alpha$ , IL-1 $\beta$ , and IL-6) total RNA expression were analyzed. Total RNA of TNF- $\alpha$ , IL-1 $\beta$ , and IL-6 was isolated and determined the mRNA expression level using quantitative RT-PCR (qRT-PCR, Roche, Basel, Switzerland).

## **2.8. Western blot analysis**

To determine the effects of DPHC on the protein expression levels of I $\kappa$ B- $\alpha$ , NF- $\kappa$ B, MAPKs (JNK, and p38), MuRF-1, and MAFbx/Atrogin-1, which are key molecules involved in skeletal muscle atrophy, in TNF- $\alpha$  or H<sub>2</sub>O<sub>2</sub>-stimulated C2C12 cells, Western blot analysis was carried out. C2C12 cells were differentiated with DPHC and then induced inflammation by TNF- $\alpha$  or H<sub>2</sub>O<sub>2</sub>. Nucleic and cytoplasmic proteins were extracted from the cells, and p I $\kappa$ B- $\alpha$ , p-NF- $\kappa$ B, MAPK (p-JNK, and p-p38), MuRF-1, and MAFbx/Atrogin-1 protein expression were detected using specific primary rabbit/mouse polyclonal antibodies and goat anti-rabbit or –mouse IgG HRP conjugated secondary antibodies. Signals were developed using an enhanced chemiluminescence (ECL) Western blotting detection kit (Amersham, Arlington Heights, IL, USA) and exposed to FusionCapt Advance FX7 program (Vilber Lourmat, Australia). The basal levels of the each protein were normalized by analyzing the level of  $\beta$ -Actin or Lamin B protein by using Image J program.

## **2.9. Statistical analysis**

All experiments were conducted in triplicate (n=3) and an one-way analysis of variance (ANOVA) test (using SPSS 12.0 statistical software) was to analyze the data. Significant differences between the means of parameters were determined by using Tukey test to analyze the difference. P-values of less than 0.05 ( $P < 0.05$ ) and 0.01 ( $P < 0.01$ ) was considered as significant.

### 3. RESULTS and DISCUSSION

#### 3.1. Determination of TNF- $\alpha$ or H<sub>2</sub>O<sub>2</sub> concentrations

Prior to evaluation of the protective effects of DPHC on inflammatory myopathy in C2C12 cells, the nontoxic concentration range of TNF- $\alpha$  or H<sub>2</sub>O<sub>2</sub>, stimulators that lead to inflammation in C2C12 myotubes, was determined in various ways. First, cytotoxic effects on the viability of cells were examined using MTT assay. TNF- $\alpha$  showed non-cytotoxic effect on C2C12 cells at 25, 50, and 100 ng/mL, but 200 ng/mL TNF- $\alpha$  affect to cytotoxic effects (Fig. 2-1). For H<sub>2</sub>O<sub>2</sub>, 100 and 200  $\mu$ M showed no toxicity and 300 and 500  $\mu$ M showed toxicity in C2C12 cells (Fig. 2-2). And then myotube metrics were quantified using microscope with a CoolSNAP-Pro color digital camera (Olympus, Japan). Myotube diameters of 25, 50, and 100 ng/mL of TNF- $\alpha$ -treated cells were not change, but 200 ng/mL of TNF- $\alpha$ -treated cells significantly decreased myotube diameters (Fig. 2-3). The C2C12 cells were treated with 300 and 500  $\mu$ M of H<sub>2</sub>O<sub>2</sub> significantly decreased myotube diameters, and H<sub>2</sub>O<sub>2</sub> of 100 and 200  $\mu$ M did not affect myotube diameter (Fig. 2-4). Finally, protein expression of MuRF-1 and MAFbx/Atrogin-1, which are key molecules of skeletal muscle atrophy, was determined through Western blot analysis. MuRF-1 and MAFbx/Atrogin-1 proteins were strongly expressed in myotubes treated with 200 ng/ml TNF- $\alpha$  (Fig. 2-5), and 300 and 500  $\mu$ M H<sub>2</sub>O<sub>2</sub> (Fig. 2-6). Therefore, the concentration of TNF- $\alpha$  or H<sub>2</sub>O<sub>2</sub> stimulators that lead to inflammation in C2C12 myotubes, was used 200 ng/ml TNF- $\alpha$  and 300  $\mu$ M H<sub>2</sub>O<sub>2</sub> for further studies.

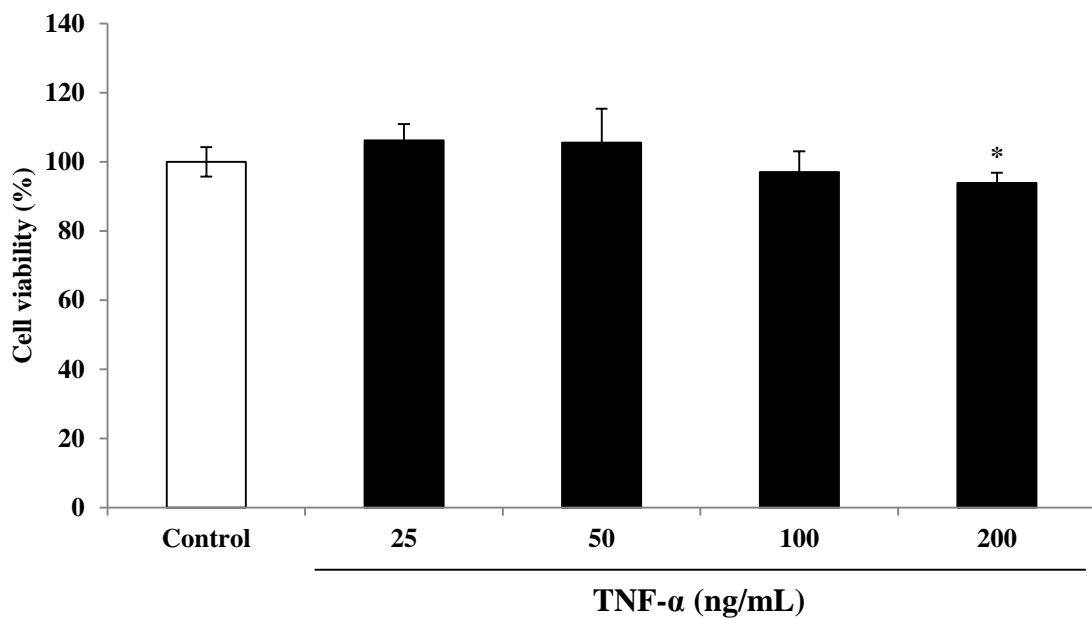


Fig. 2-1. Evaluation of cell toxicity of TNF- $\alpha$  on C2C12 skeletal myoblast cells by a MTT assay. Experiments were performed in triplicate and the data are expressed as mean  $\pm$  SE; \*  $P$  < 0.05, and \*\*  $P$  < 0.01 as compared to the untreated group.

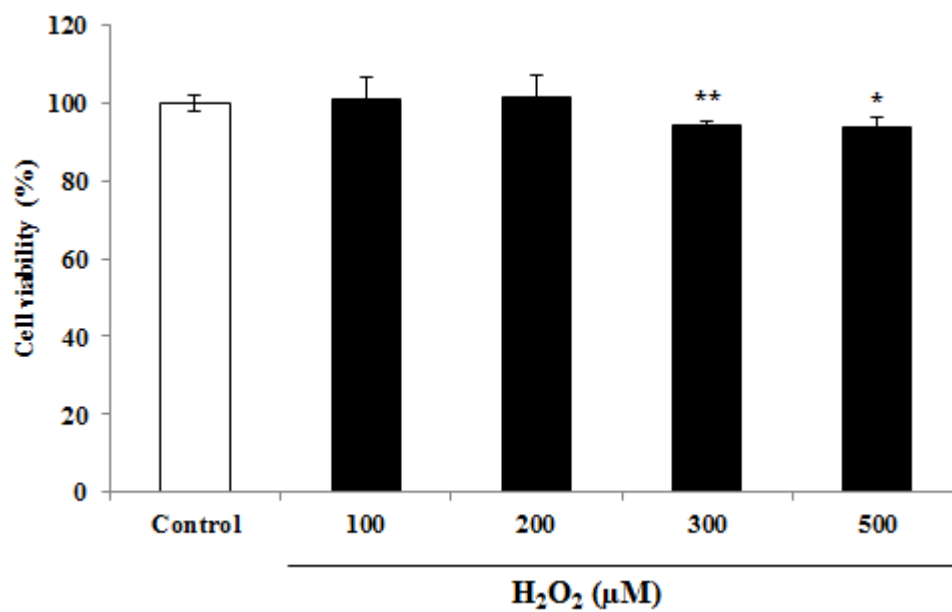


Fig. 2-2. Evaluation of cell toxicity of H<sub>2</sub>O<sub>2</sub> on C2C12 skeletal myoblast cells by a MTT assay. Experiments were performed in triplicate and the data are expressed as mean  $\pm$  SE; \*  $P < 0.05$ , and \*\*  $P < 0.01$  as compared to the untreated group.



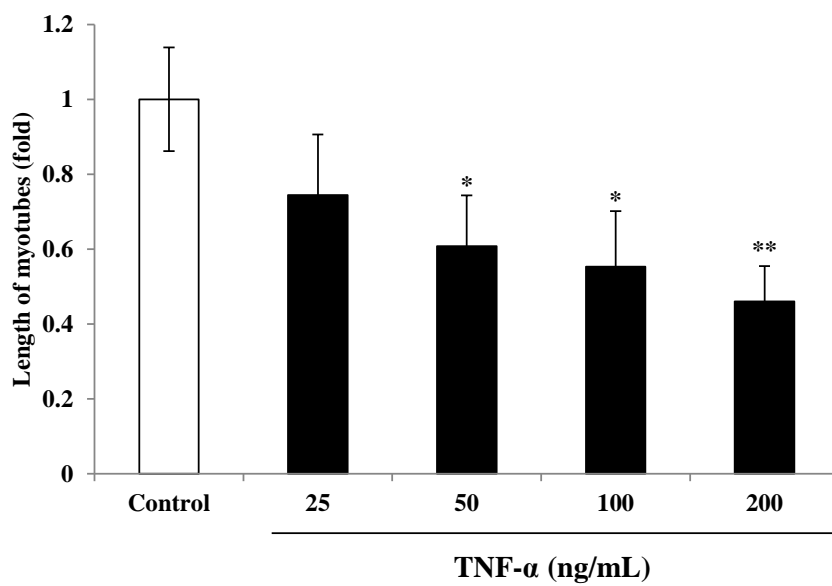
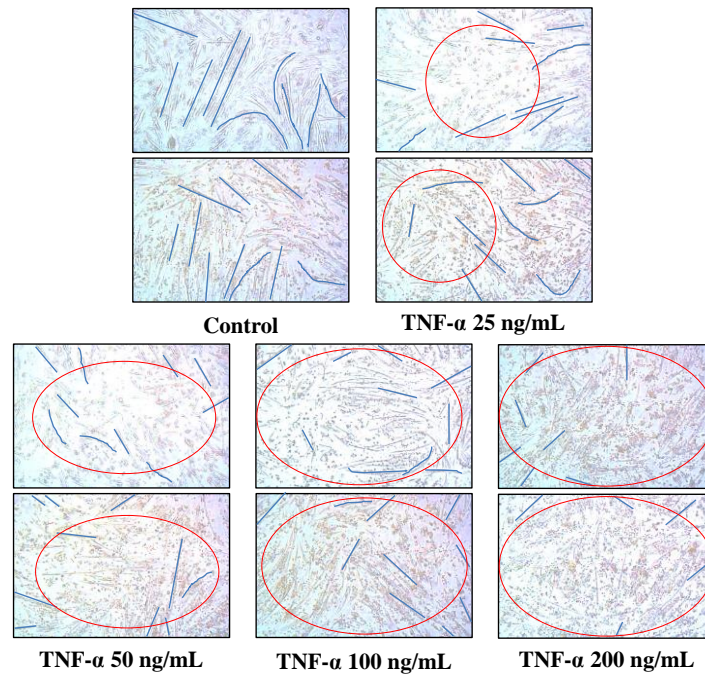


Fig. 2-3. Analysis of myotubes length on TNF- $\alpha$ -induced inflammatory cells. Experiments were performed in duplicate and the data are expressed as mean  $\pm$  SE; \*  $P < 0.05$ , and \*\*  $P < 0.01$  as compared to the untreated group.

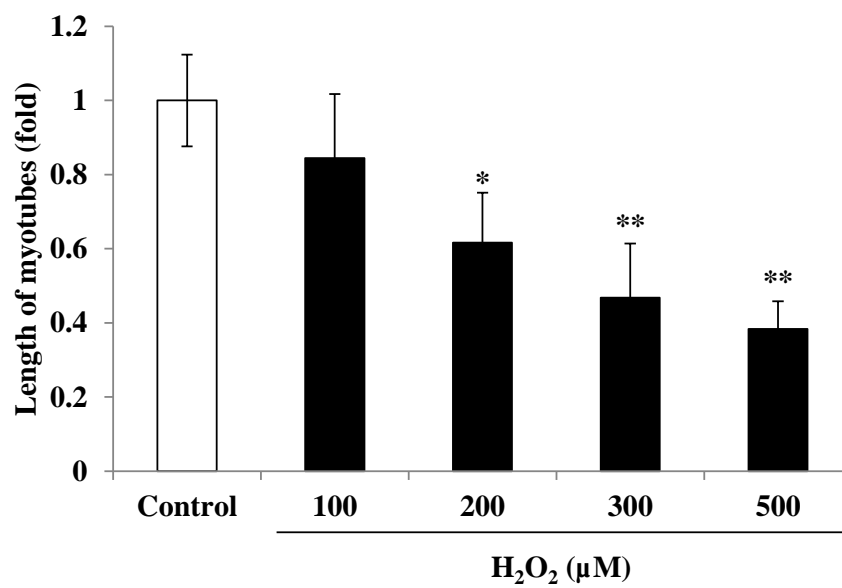
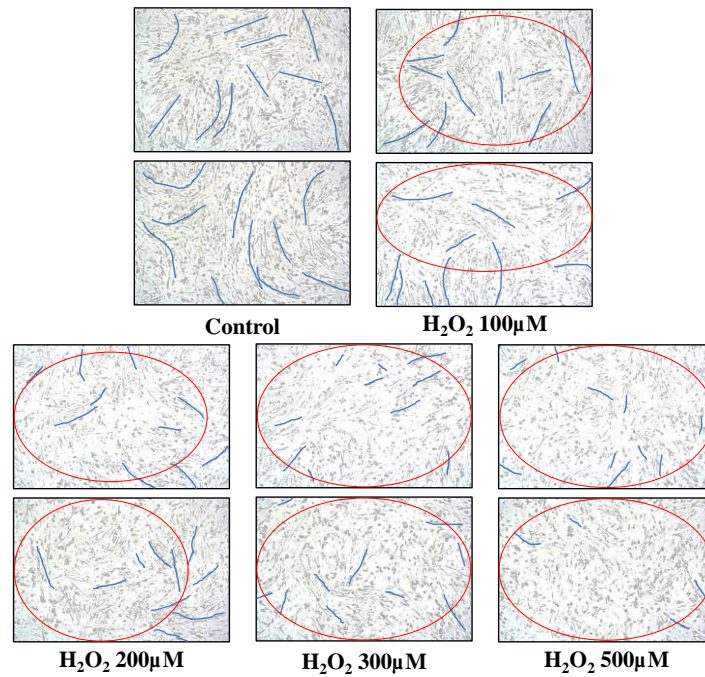


Fig. 2-4. Analysis of myotubes length on H<sub>2</sub>O<sub>2</sub>-induced inflammatory cells. Experiments were performed in duplicate and the data are expressed as mean  $\pm$  SE; \*  $P < 0.05$ , and \*\*  $P < 0.01$  as compared to the untreated group.

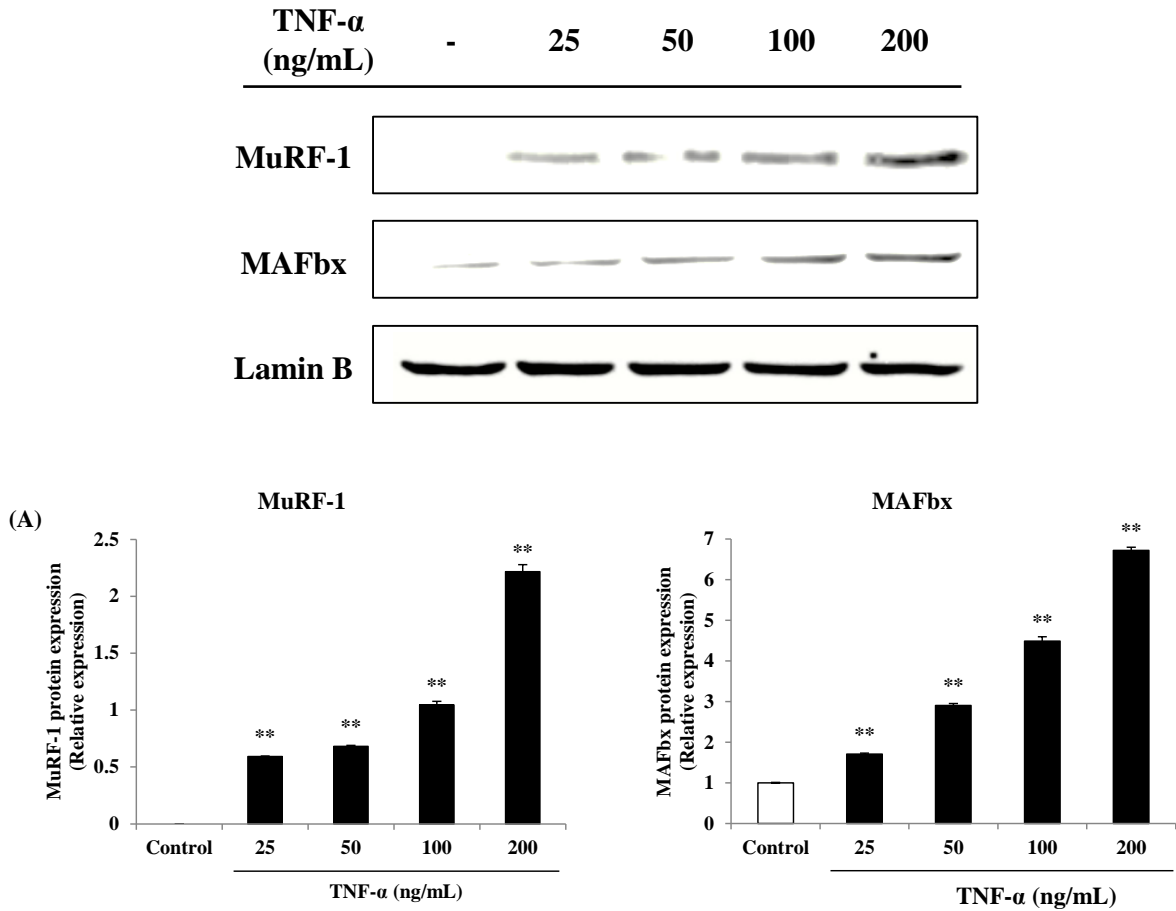


Fig. 2-5. The protein expressions of MuRF-1 (A), and MAFbx (B) on TNF- $\alpha$ -induced inflammatory cells. Experiments were performed in triplicate and the data are expressed as mean  $\pm$  SE; \*  $P < 0.05$ , and \*\*  $P < 0.01$  as compared to the untreated group.

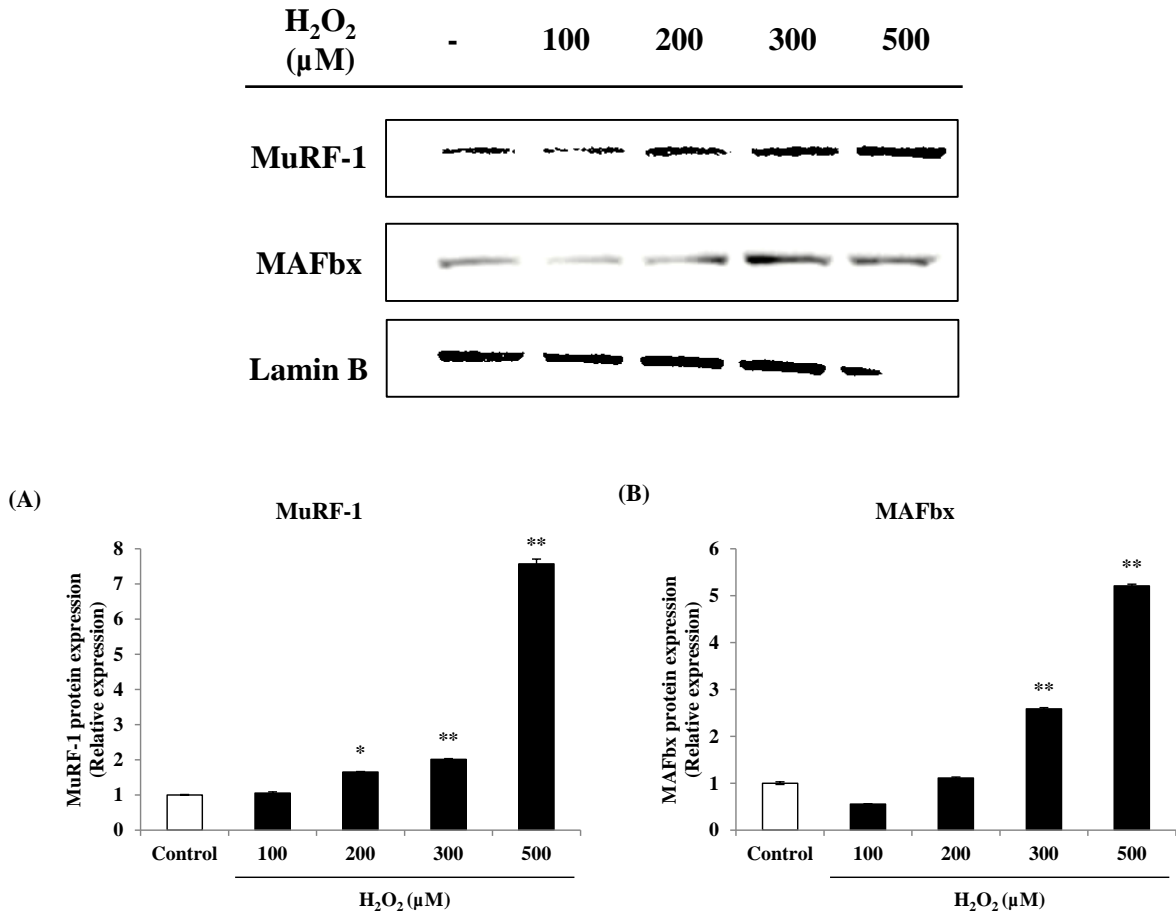


Fig. 2-6. The protein expressions of MuRF-1 (A), and MAFbx (B) on H<sub>2</sub>O<sub>2</sub>-induced inflammatory cells. Experiments were performed in triplicate and the data are expressed as mean  $\pm$  SE; \*  $P < 0.05$ , and \*\*  $P < 0.01$  as compared to the untreated group.

### **3.2. Effect of DPHC on cell viability and morphology**

Cytotoxicity of DPHC isolated from IO was assessed using the MTT assay. All the tested concentrations of DPHC showed non-cytotoxic effect on C2C12 cells, except for highest concentrations (50 and 100  $\mu\text{g/mL}$ ). Thus, non-cytotoxic concentrations (1.56, 3.125, 6.25, 12.5, and 25  $\mu\text{g/mL}$ ) were used in subsequent experiments (Fig. 2-7).

To examine the protective effects of DPHC on TNF- $\alpha$  or H<sub>2</sub>O<sub>2</sub>-induced inflammatory myopathy C2C12 cells, cells were treated with DPHC during differentiation period and induced inflammatory myopathy using TNF- $\alpha$  or H<sub>2</sub>O<sub>2</sub>. Cell viability was assessed using the MTT assay. As shown in Fig. 2-8, TNF- $\alpha$  reduced cell viability to 76.98%, whereas DPHC prevented TNF- $\alpha$ -induced cell damage and increased cell survival rates. And, H<sub>2</sub>O<sub>2</sub> significantly reduced cell viability, but DPHC increased H<sub>2</sub>O<sub>2</sub>-stimulated cell (Fig. 2-9). And also, to determine the protective effects of DPHC on TNF- $\alpha$  or H<sub>2</sub>O<sub>2</sub>-induced inflammatory myopathy C2C12 cells, myotube metrics were quantified using microscope with a CoolSNAP-Pro color digital camera (Olympus, Japan). DPHC recovers reduction of the length of myotubes by TNF- $\alpha$  (Fig. 2-10). H<sub>2</sub>O<sub>2</sub> significantly destroy cell morph, whereas DPHC restores cell morph and recovers the reduced length of myotbues (Fig. 2-11).

### **3.3. Determination of NO production and antioxidant enzymes**

NO is a representative indicator, one of various inflammatory factors, that is inflammatory responses against various inflammation stimuli such as pro-inflammatory cytokines and oxidative stress. Therefore, the protective effects of DPHC were assessed for the production of NO in skeletal muscle cells stimulated by TNF- $\alpha$  and H<sub>2</sub>O<sub>2</sub>. The level of NO generation is

significantly increased in the TNF- $\alpha$  and H<sub>2</sub>O<sub>2</sub>-stimulated cells compared to the untreated cells. However, DPHC significantly inhibited the TNF- $\alpha$  and H<sub>2</sub>O<sub>2</sub>-induced NO production in C2C12 cells (Fig. 2-12, and 2-13). Reactive oxygen species (ROS), unstable reactive molecules, are formed as byproducts of normal metabolism within mitochondria. Antioxidant enzymes such as glutathione peroxidase (GSH-px), catalase (CAT), and superoxide dismutase (SOD) contribute to the protection against pathogens including pollutants, drugs, and inflammation. Thus, diverse antioxidant enzymes from TNF- $\alpha$  and H<sub>2</sub>O<sub>2</sub>-induced inflammatory myopathy cells were detected using colorimetric assay kit. Antioxidant enzymes, including SOD, and CAT were significantly decreased in TNF- $\alpha$  and H<sub>2</sub>O<sub>2</sub>-stimulated C2C12 cells. However, DPHC-treated cells were significantly increased the levels of SOD, and CAT (Fig. 2-14, and 2-15).

#### **3.4. Effect of DPHC on expression of pro-inflammatory cytokines**

The inflammation process are activated by inflammatory stimulation secretes NO, prostaglandin, and cytokines such as interleukin (IL)-1 $\beta$ , IL-6, and TNF- $\alpha$ . These pro-inflammatory mediators are important role in various inflammatory diseases targets. To evaluate the protective effects of DPHC on TNF- $\alpha$  or H<sub>2</sub>O<sub>2</sub>-induced inflammatory myopathy C2C12 cells, the levels of inflammatory cytokines including TNF- $\alpha$ , IL-1 $\beta$ , and IL-6 mRNA were analyzed by qRT-PCR. The results clearly demonstrated that the expression of pro-inflammatory cytokines mRNA was sufficiently suppressed by DPHC treatment compared to the TNF- $\alpha$  or H<sub>2</sub>O<sub>2</sub>-stimulated cells (Fig. 2-16, and 2-17).

### **3.3. Protective effect of DPHC on inflammatory myopathy through NF- $\kappa$ B and MAPKs signaling pathway**

NF- $\kappa$ B is important transcriptional factors that may regulate a variety of inflammatory and immune responses (Jiang XH et al., 2001). Activation of NF- $\kappa$ B by external stimuli induces breakdown of heterodimer of the p65 and p50 subunits in the cytosol in a complex with the inhibitor protein I $\kappa$ B- $\alpha$ , and lead to the phosphorylation and degradation of I $\kappa$ B- $\alpha$ , and then NF- $\kappa$ B was translocated to nucleus (Ko and Cho et al., 2017).

It was previously reported that MAPKs (JNK and p38) play a role as upstream modulators in muscle atrophy in myocytes. In addition, Li et al. (2005) reported that the TNF- $\alpha$  and H<sub>2</sub>O<sub>2</sub> effectively promote JNK and p38 expression in simulated C2C12 cells, and the down-regulation of MAPK may contribute to the inhibition of MuRF-1 and MAFbx/atrogen-1 expression. Thus, TNF- $\alpha$  and H<sub>2</sub>O<sub>2</sub> can activate MuRF-1 and MAFbx/Atrogen-1 expression. To investigate whether the regulation of inflammatory response by DPHC mediated through a MAPK pathway, the effects of DPHC on TNF- $\alpha$  or H<sub>2</sub>O<sub>2</sub>-stimulated phosphorylation of JNK, and p38 MAPKs in C2C12 skeletal myocytes by Western blot analysis. TNF- $\alpha$  or H<sub>2</sub>O<sub>2</sub> significantly promoted the phosphorylations of MAPKs (JNK and p38) in C2C12 cells. However, DPHC dramatically decreased the phosphorylations MAPKs (JNK and p38) (Fig. 2-18, and 2-19).

The functional importance of MuRF-1 and MAFbx/Atrogen-1 in muscle atrophy was demonstrated by the generation of knockout mice for the two genes. Previous researcher reported that mRNA levels of MAFbx/Atrogen-1 are increased by exposing muscle cells to exogenous H<sub>2</sub>O<sub>2</sub>. Skeletal muscle cells continuously secret H<sub>2</sub>O<sub>2</sub> and ROS that function as

intracellular signaling molecules (Li et al., 2005). Also, he demonstrated that TNF- $\alpha$  up-regulate MAFbx/Atrogin-1 expression in skeletal muscle (Li et al., 2005). MAPK and NF- $\kappa$ B signaling pathways are clearly activated by TNF- $\alpha$  and H<sub>2</sub>O<sub>2</sub> in skeletal muscle cells. Therefore, to determine whether DPHC can inhibits TNF- $\alpha$  and H<sub>2</sub>O<sub>2</sub>-induced the MuRF-1 and MAFbx/Atrogin-1 expression in myocytes, MuRF-1 and MAFbx/Atrogin-1 protein expression were analyzed via Western blot analysis. TNF- $\alpha$  or H<sub>2</sub>O<sub>2</sub> significantly promoted the MuRF-1 and MAFbx/Atrogin-1 expression, but DPHC significantly inhibited the expression of MuRF-1 and MAFbx/Atrogin-1 (Fig. 2-20, and 2-21).

#### **4. Conclusion**

These results indicated that DPHC could be inhibit inflammatory myopathy by regulating NF- $\kappa$ B (p-I $\kappa$ B- $\alpha$ /p-NF- $\kappa$ B), and MAPKs (p-JNK/p-p38) signaling cascades and MuRF-1, and MAFbx/Atrogin-1 genes. Therefore, DPHC would be used as possible nutraceuticals or functional food to reduce inflammation in muscle.



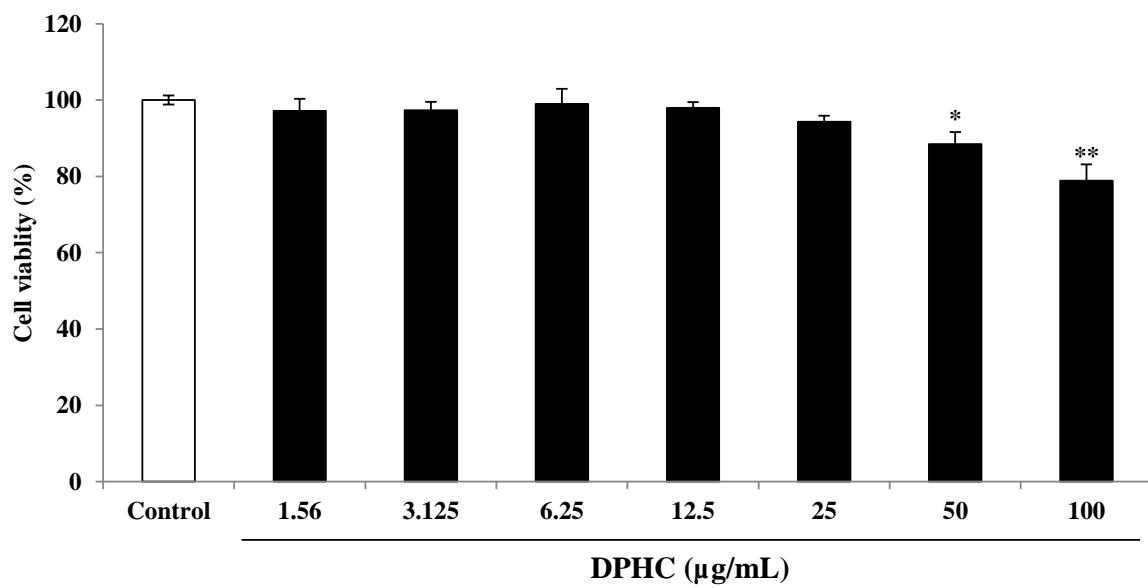


Fig. 2-7. Cell toxicity of Diphlorethohydroxycarmalol (DPHC) on C2C12 skeletal myoblasts by a MTT assay. Experiments were performed in triplicate and the data are expressed as mean  $\pm$  SE; \*  $P < 0.05$ , and \*\*  $P < 0.01$  as compared to the untreated group.

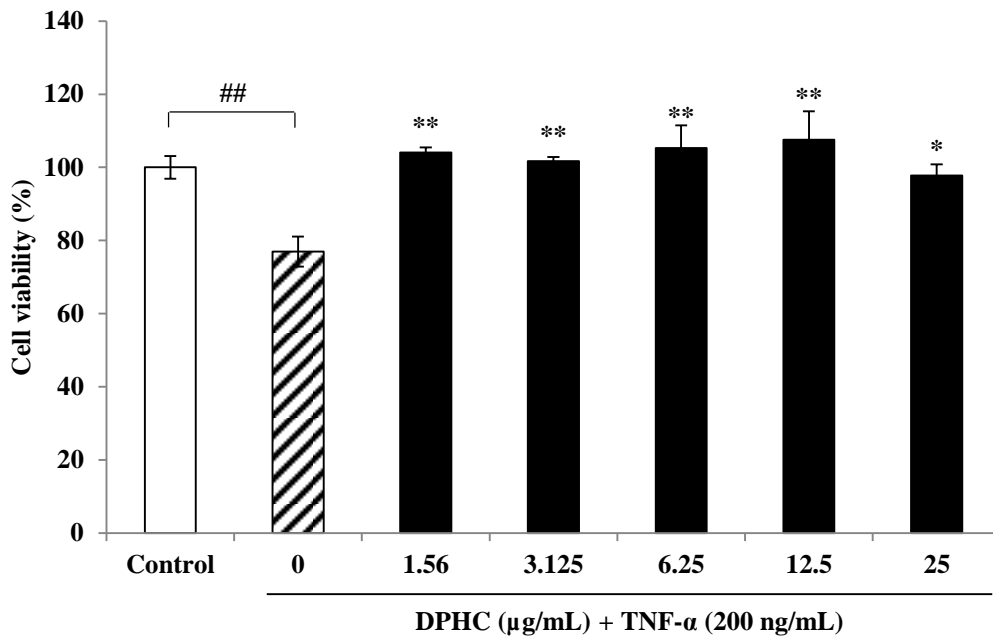


Fig. 2-8. Cell protective effect of DPHC on TNF- $\alpha$ -induced myopathy by a MTT assay. Experiments were performed in triplicate and the data are expressed as mean  $\pm$  SE; #  $P < 0.05$ , and ##  $P < 0.01$  as compared to the untreated group. \*  $P < 0.05$ , and \*\*  $P < 0.01$  as compared to the TNF- $\alpha$ -treated group.

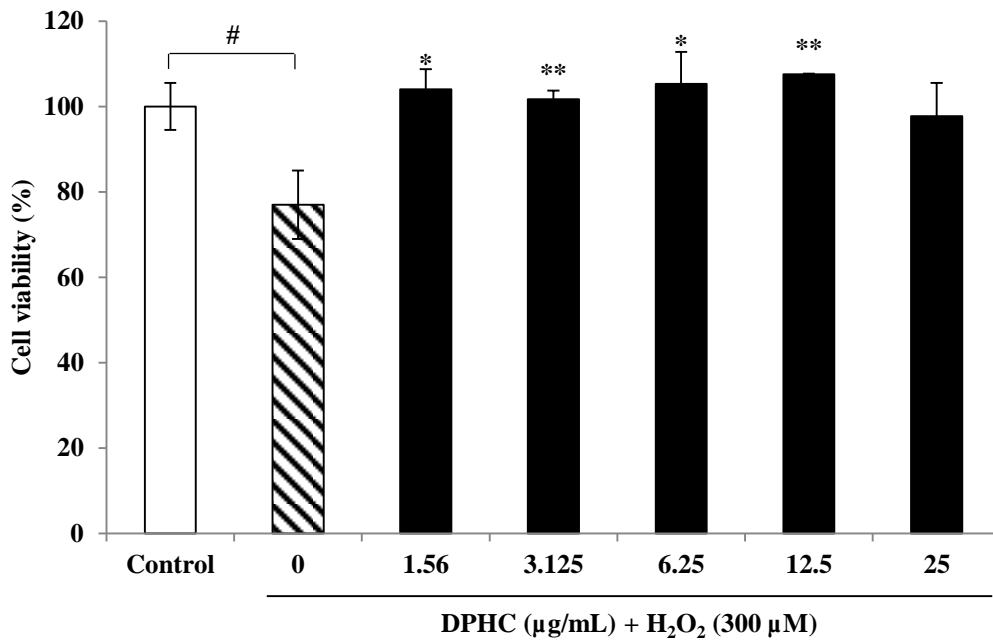


Fig. 2-9. Cell protective effect of DPHC on H<sub>2</sub>O<sub>2</sub>-induced myopathy by a MTT assay. Experiments were performed in triplicate and the data are expressed as mean ± SE; #  $P < 0.05$ , and ##  $P < 0.01$  as compared to the untreated group. \*  $P < 0.05$ , and \*\*  $P < 0.01$  as compared to the H<sub>2</sub>O<sub>2</sub>-treated group.

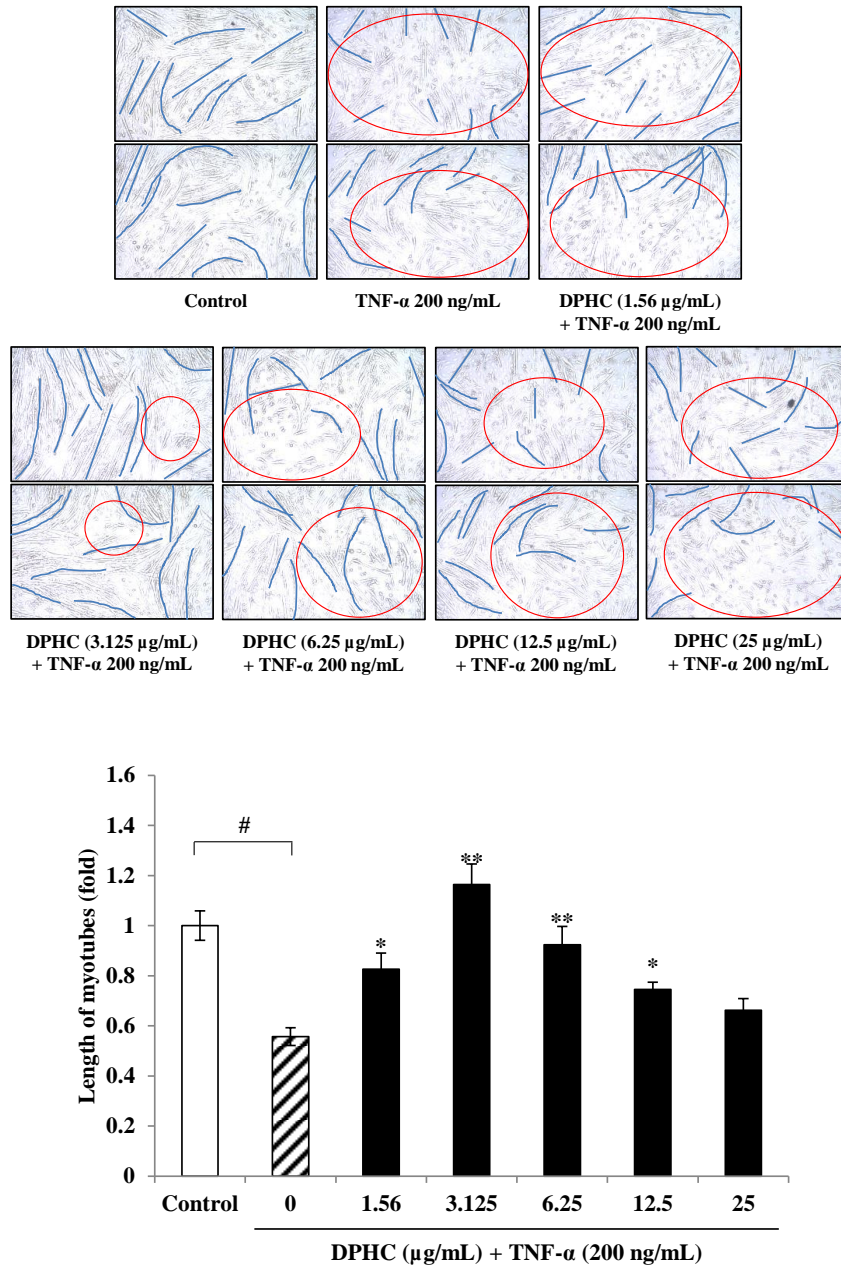


Fig. 2-10. Evaluation of myotubes length in DPHC-treated myotubes on TNF- $\alpha$ -induced myopathy. Experiments were performed in triplicate and the data are expressed as mean  $\pm$  SE; #  $P < 0.05$ , and ##  $P < 0.01$  as compared to the untreated group. \*  $P < 0.05$ , and \*\*  $P < 0.01$  as compared to the TNF- $\alpha$ -treated group.

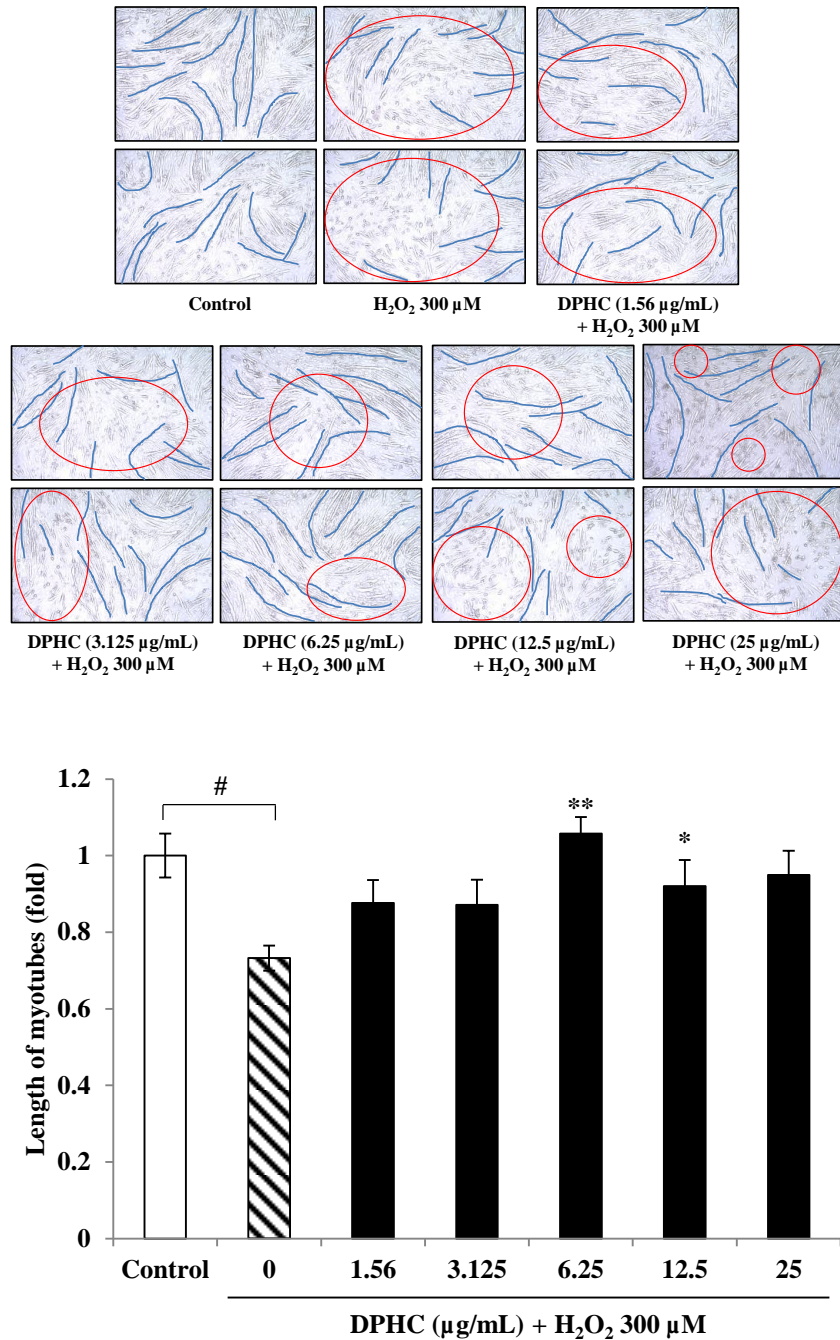


Fig. 2-11. Evaluation of myotubes length in DPHC-treated myotubes on H<sub>2</sub>O<sub>2</sub>-induced myopathy. Experiments were performed in triplicate and the data are expressed as mean ± SE; #  $P < 0.05$ , and ##  $P < 0.01$  as compared to the untreated group. \*  $P < 0.05$ , and \*\*  $P < 0.01$  as compared to the H<sub>2</sub>O<sub>2</sub>-treated group.

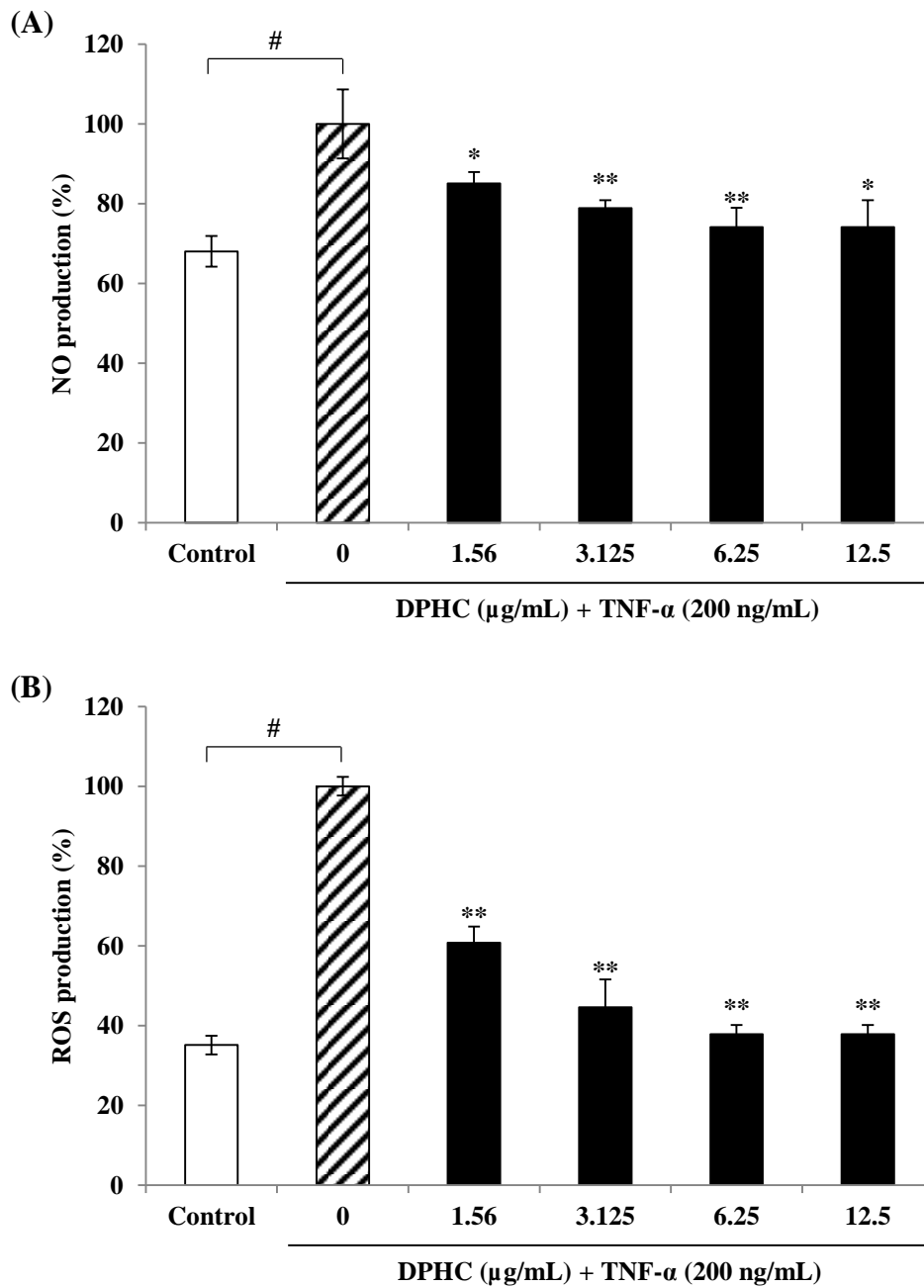


Fig. 2-12. NO and ROS production in DPHC-treated myotubes on TNF- $\alpha$ -induced myopathy. Experiments were performed in triplicate and the data are expressed as mean  $\pm$  SE; #  $P < 0.05$ , and ##  $P < 0.01$  as compared to the untreated group. \*  $P < 0.05$ , and \*\*  $P < 0.01$  as compared to the TNF- $\alpha$ -treated group.

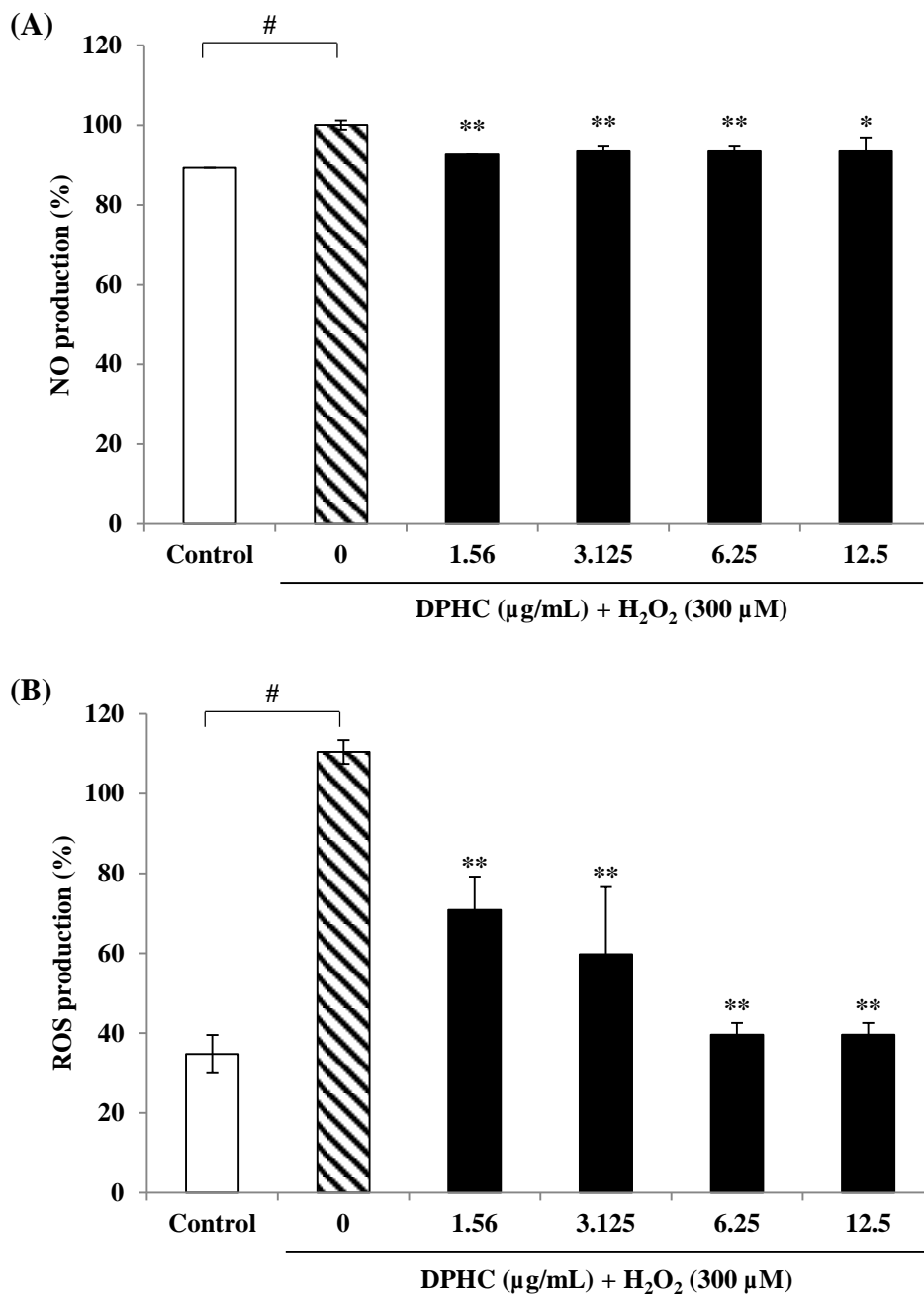


Fig. 2-13. NO and ROS production in DPHC-treated myotubes on H<sub>2</sub>O<sub>2</sub>-induced myopathy. Experiments were performed in triplicate and the data are expressed as mean ± SE; # *P* < 0.05, and ## *P* < 0.01 as compared to the untreated group. \* *P* < 0.05, and \*\* *P* < 0.01 as compared to the H<sub>2</sub>O<sub>2</sub>-treated group.

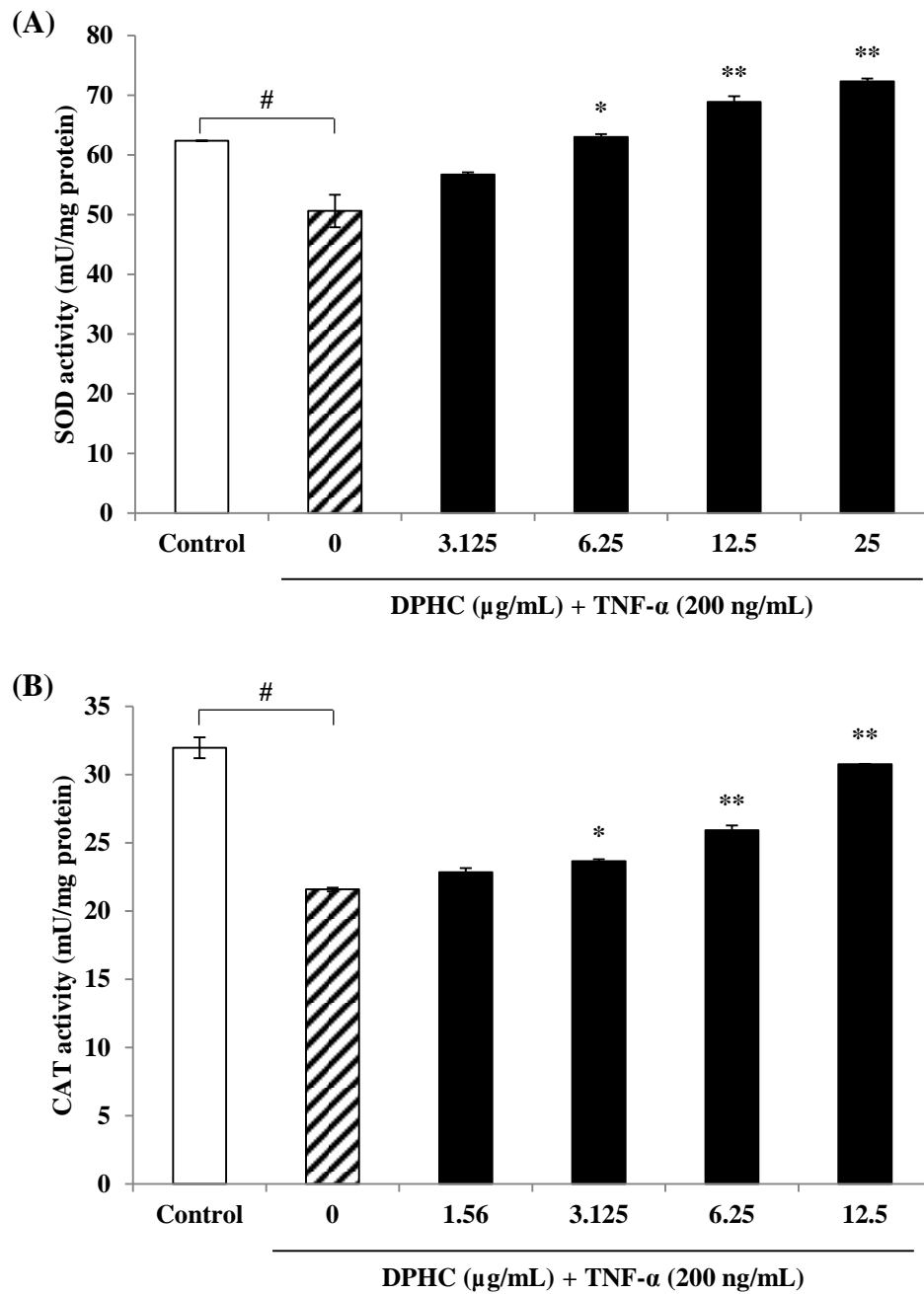


Fig. 2-14. SOD and CAT activities in DPHC-treated myotubes on TNF- $\alpha$ -induced myopathy. Experiments were performed in triplicate and the data are expressed as mean  $\pm$  SE; #  $P < 0.05$ , and  $^{##} P < 0.01$  as compared to the untreated group. \*  $P < 0.05$ , and \*\*  $P < 0.01$  as compared to the TNF- $\alpha$ -treated group.



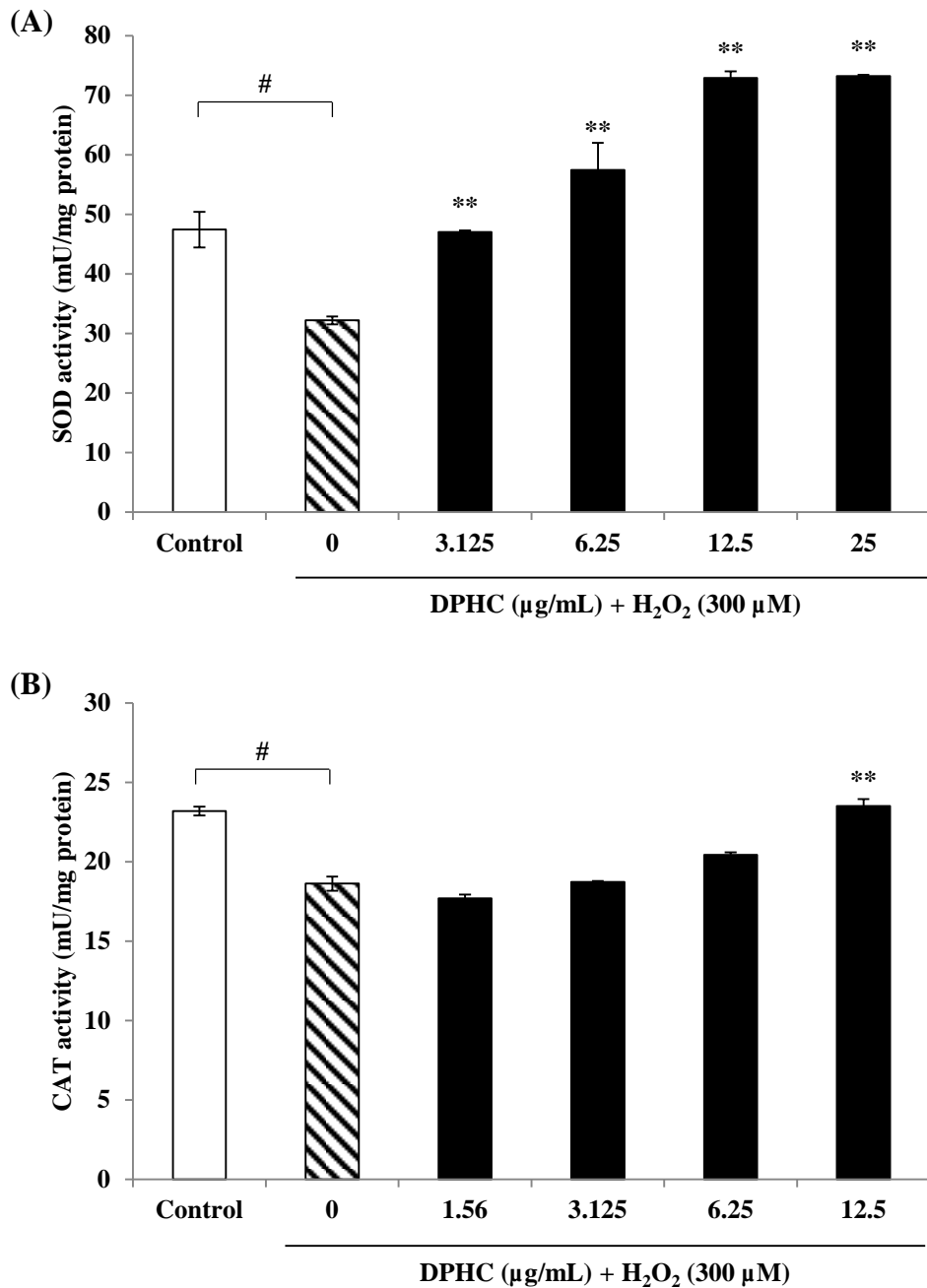


Fig. 2-15. SOD and CAT activities in DPHC-treated myotubes on H<sub>2</sub>O<sub>2</sub>-induced myopathy. Experiments were performed in triplicate and the data are expressed as mean  $\pm$  SE; #  $P < 0.05$ , and ###  $P < 0.01$  as compared to the untreated group. \*  $P < 0.05$ , and \*\*  $P < 0.01$  as compared to the H<sub>2</sub>O<sub>2</sub>-treated group.

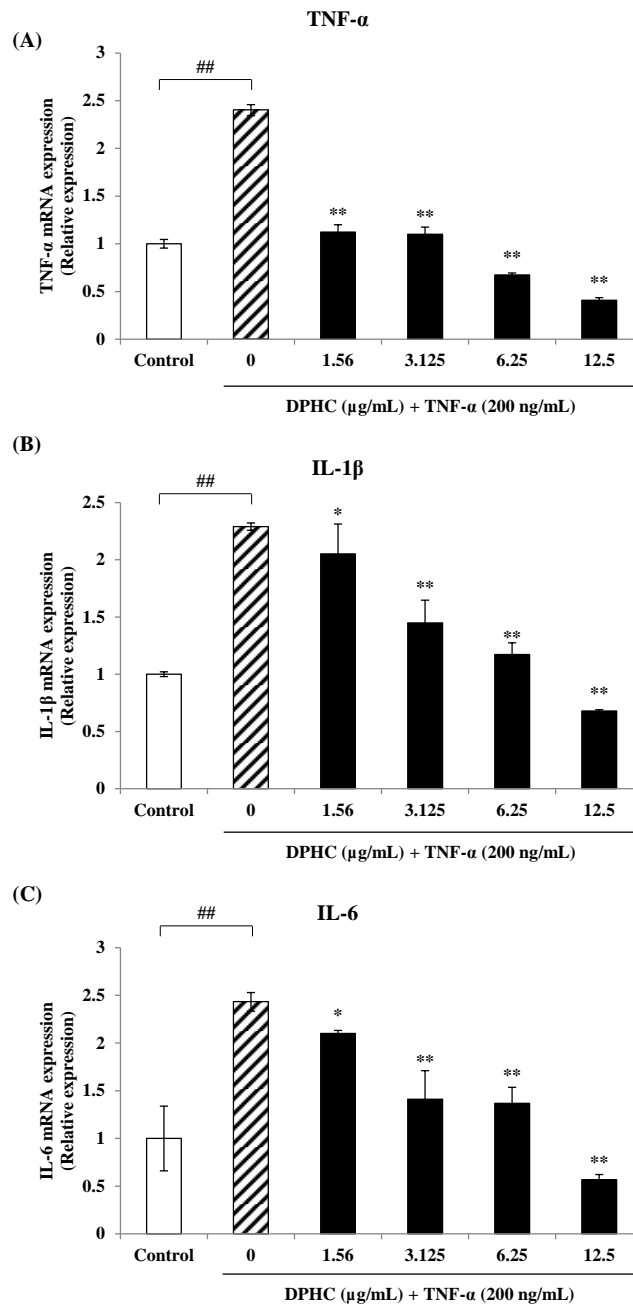


Fig. 2-16. The mRNA expressions of TNF- $\alpha$ , IL-1 $\beta$ , and IL-6 cytokines in DPHC-treated myotubes on TNF- $\alpha$ -induced myopathy. Experiments were performed in triplicate and the data are expressed as mean  $\pm$  SE; #  $P < 0.05$ , and ##  $P < 0.01$  as compared to the untreated group. \*  $P < 0.05$ , and \*\*  $P < 0.01$  as compared to the TNF- $\alpha$ -treated group.

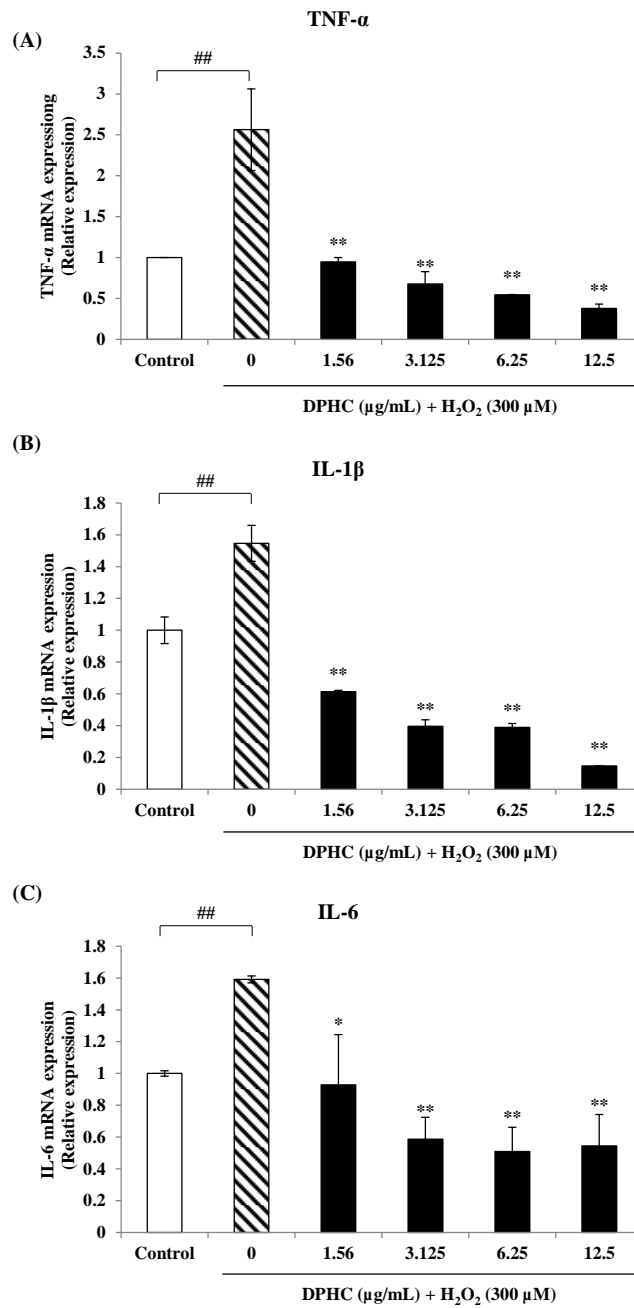


Fig. 2-17. The mRNA expressions of TNF- $\alpha$ , IL-1 $\beta$ , and IL-6 cytokines on  $\text{H}_2\text{O}_2$ -induced myopathy. Experiments were performed in triplicate and the data are expressed as mean  $\pm$  SE; #  $P < 0.05$ , and ##  $P < 0.01$  as compared to the untreated group. \*  $P < 0.05$ , and \*\*  $P < 0.01$  as compared to the  $\text{H}_2\text{O}_2$ -treated group.

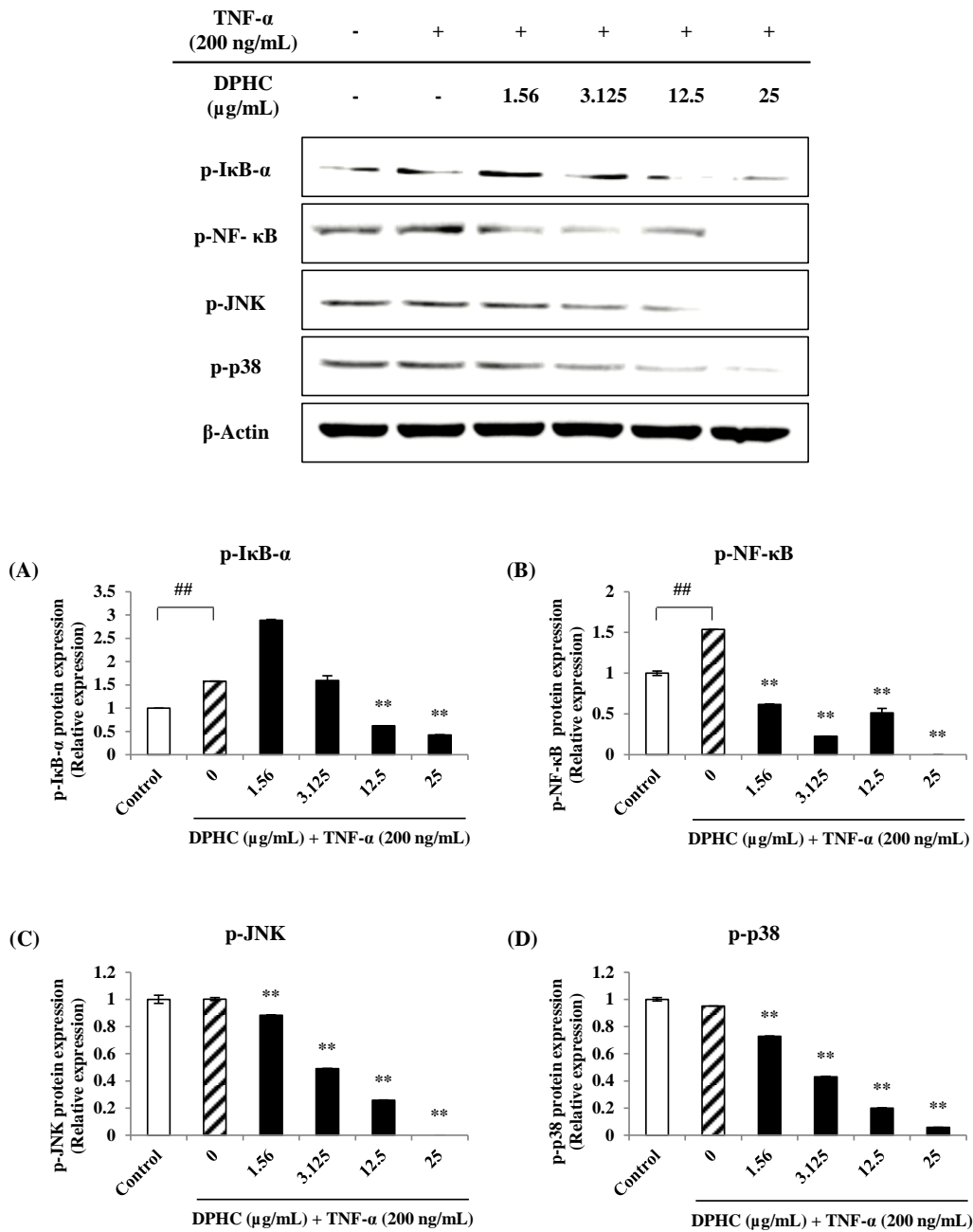


Fig. 2-18. The protein expressions of p-I $\kappa$ B- $\alpha$ , p-NF- $\kappa$ B, p-JNK, and p-p38 in DPHC-treated myotubes on TNF- $\alpha$ -induced myopathy. Experiments were performed in triplicate and the data are expressed as mean  $\pm$  SE; #  $P < 0.05$ , and ##  $P < 0.01$  as compared to the untreated group. \*  $P < 0.05$ , and \*\*  $P < 0.01$  as compared to the TNF- $\alpha$ -treated group.

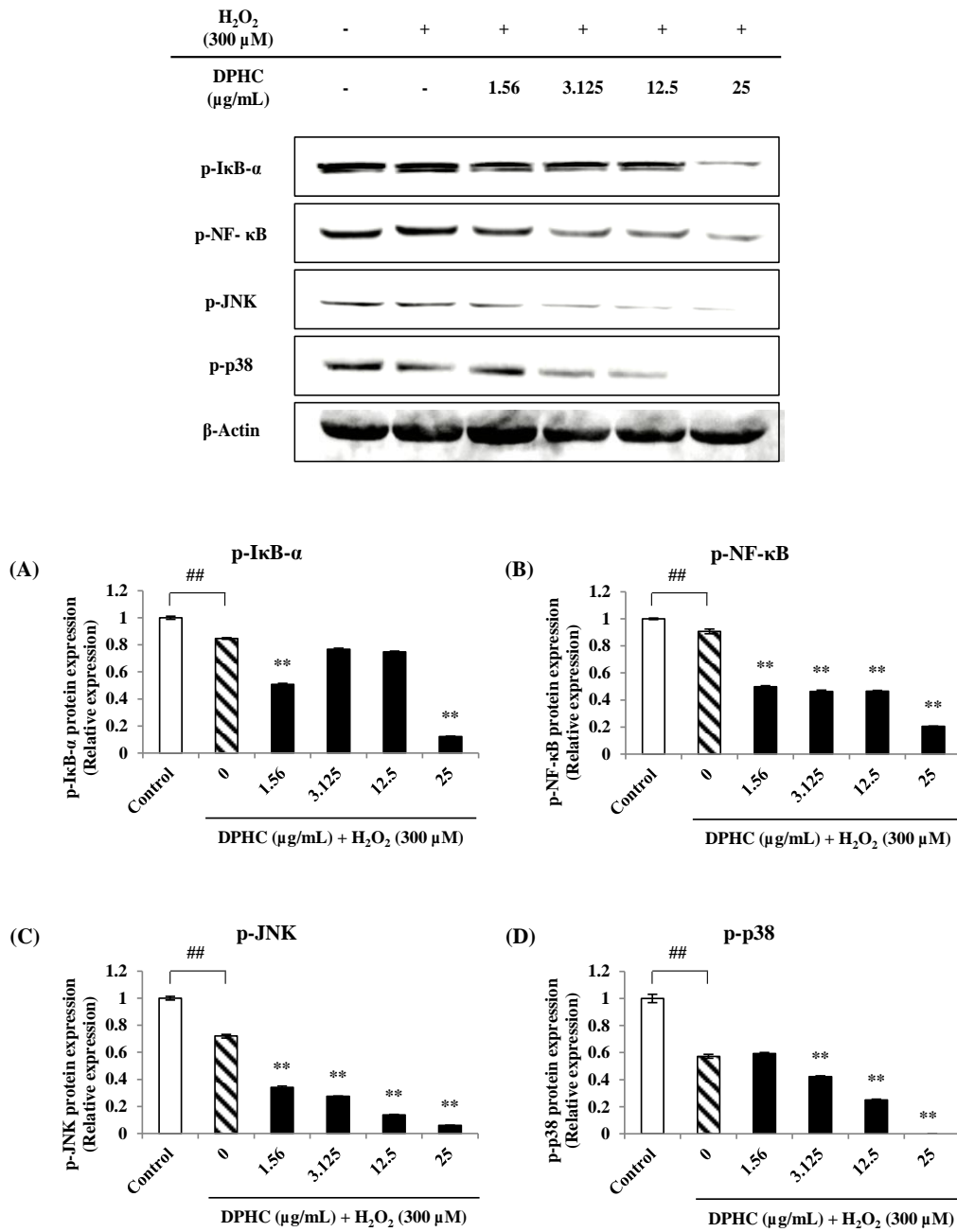


Fig. 2-19. The protein expressions of p-IκB-α, p-NF-κB, p-JNK, and p-p38 in DPHC-treated myotubes on H<sub>2</sub>O<sub>2</sub>-induced myopathy. Experiments were performed in triplicate and the data are expressed as mean ± SE; # *P* < 0.05, and ## *P* < 0.01 as compared to the untreated group. \* *P* < 0.05, and \*\* *P* < 0.01 as compared to the H<sub>2</sub>O<sub>2</sub>-treated group.

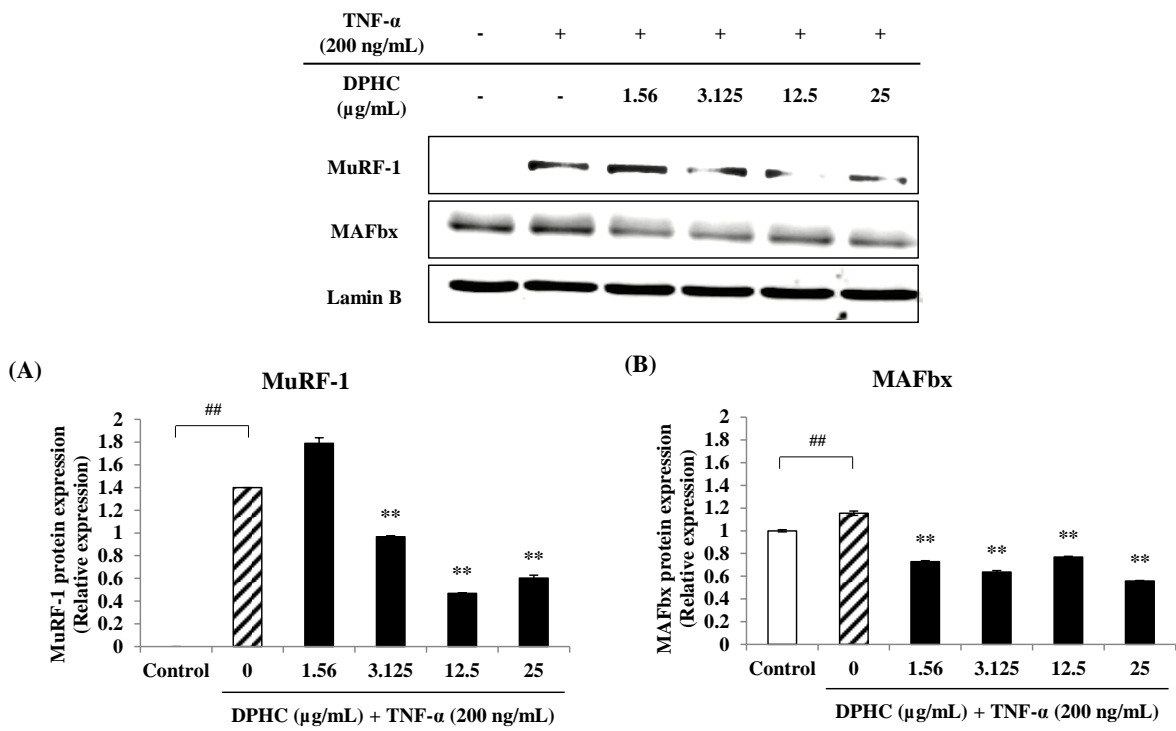


Fig. 2-20. The protein expressions of MuRF-1, and MAFbx/Atrogin-1 in DPHC-treated myotubes on TNF- $\alpha$ -induced myopathy. Experiments were performed in triplicate and the data are expressed as mean  $\pm$  SE; #  $P < 0.05$ , and ##  $P < 0.01$  as compared to the untreated group. \*  $P < 0.05$ , and \*\*  $P < 0.01$  as compared to the TNF- $\alpha$ -treated group.

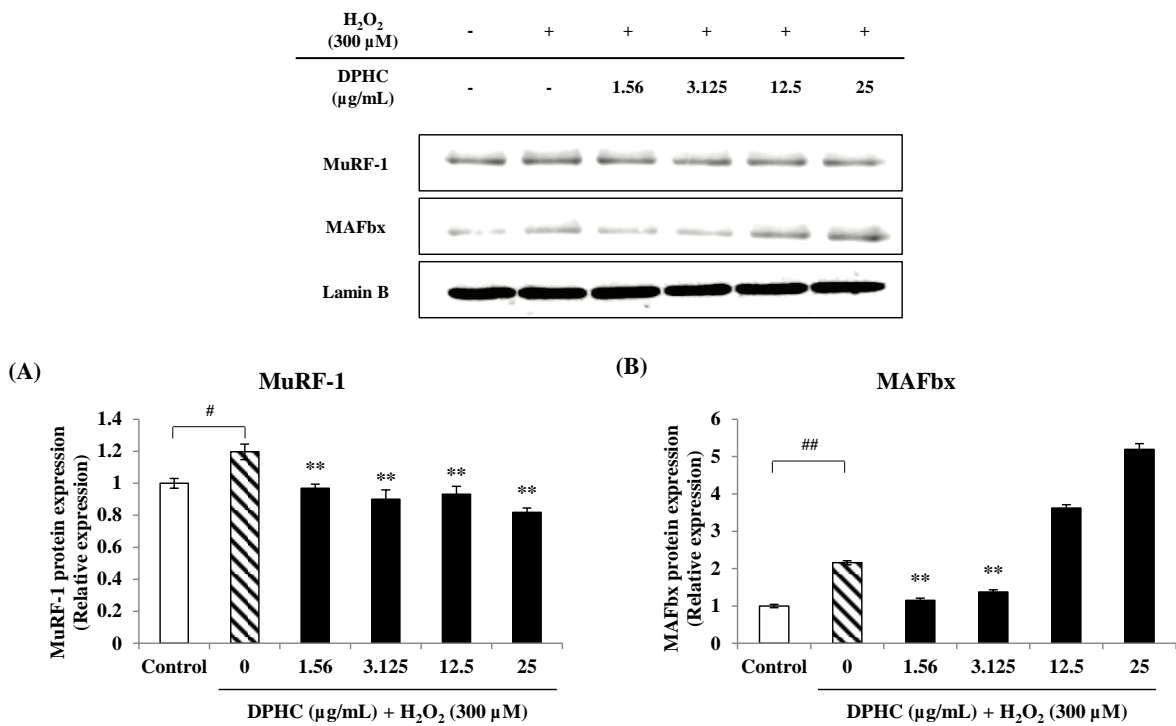


Fig. 2-21. The protein expressions of MuRF-1, and MAFbx/Atrogin-1 in DPHC-treated myotubes on H<sub>2</sub>O<sub>2</sub>-induced myopathy. Experiments were performed in triplicate and the data are expressed as mean ± SE; # *P* < 0.05, and ## *P* < 0.01 as compared to the untreated group. \* *P* < 0.05, and \*\* *P* < 0.01 as compared to the H<sub>2</sub>O<sub>2</sub>-treated group.

### **Part III.**

## **Effect of Diphlorethohydroxycarmalol (DPHC) on inflammatory myopathy in zebrafish model**



### Part III.

## Effect of Diphlorethohydroxycarmalol (DPHC) on inflammatory myopathy in zebrafish model

### ABSTRACT

The zebrafish (*Danio rerio*) model is one of the most widely used animal models. It has been developed into an important model organism for biomedical research over the last decades. Recently, the model has been used for molecular genetics, developmental biology, drug discovery and screening of human disease. Especially, the adult zebrafish has the potential to become an impact model for inflammation-related research. Therefore, in the present study I attempted to evaluate the protective effect of diphlorethohydroxycarmalol (DPHC), a natural biologically active substances isolated from *Ishige okamurae* (IO) in TNF- $\alpha$  or H<sub>2</sub>O<sub>2</sub>-stimulated inflammatory zebrafish model. According to the results, TNF- $\alpha$  and H<sub>2</sub>O<sub>2</sub> up-regulated the expressions of NF- $\kappa$ B, and MAPKs signaling in zebrafish muscle tissues. DPHC down-regulated the expressions of NF- $\kappa$ B, and MAPKs signaling pathways related protein expressions. Moreover, DPHC suppressed the MuRF-1, and MAFbx/Atrogin-1, which are key protein of muscle atrophy. In addition, DPHC enhanced the endurance of zebrafish reduced by TNF- $\alpha$  and H<sub>2</sub>O<sub>2</sub> without any training. These results indicate that TNF- $\alpha$  or H<sub>2</sub>O<sub>2</sub>-stimulated inflammatory zebrafish model can be used as an *in vivo* experiment to confirm the protective activities of inflammatory muscle atrophy. Furthermore, DPHC has a potential to regulate inflammatory myopathy genes via down-regulating the NF- $\kappa$ B, and MAPKs signaling pathway related protein expressions.

## 1. INTRODUCTION

The zebrafish (*Danio rerio*) is one of the most widely used animal models. It has been developed into an important model organism for biomedical research over the last decades because of it has diverse advantages. The characteristics features that make zebrafish a popular experimental animal to study the disease mechanisms includes: The embryos are optically transparent so all process of organogenesis may be visualized in vivo and investigated in real-time (Eisen et al., 1996). Not only that, the zebrafish acquire a large of eggs at a time, lower maintenance costs than other animals model, it has cardiovascular, nervous, and digestive systems that are similar to those of mammals, and its 84% genes are known to be related to human diseases (Howe et al., 2013; Ko et al., 2015; Kim et al., 2015). Therefore, the zebrafish has attracted the attention of scientists engaged in variety research owing to the similarities between zebrafish and mammalian biology (Stewart et al., 2014; Jing et al., 2011; Chico et al., 2008). Particularly, the evolutionary conserved genetic and molecular mechanisms that control muscle development and function in zebrafish and mammals, the zebrafish emanated as a vertebrate model system especially to study human striated muscle diseases including cardiomyopathies or muscular dystrophies (Vogel et al., 2009; Staudt et al., 2012; Kawahara et al., 2011). However, studies of muscle growth or muscle diseases using zebrafish animal model mostly involve gene modification, knock-out, or muscle development in the embryos (Bührdel et al., 2015; Dowling et al., 2009; Bassett et al., 2003).

Endurance training can induce skeletal muscle hypertrophy and leads to strength on muscle mass in human (Sipila et al., 1995) and it likes running to exhaustion tests enhances exercise performances to 85 and 223%, respectively in mice and rats (Gilbert et al., 2014). By

applying these aerobic exercise conditions in a swimming training protocol for 20 days, a significant exercise-induced growth was demonstrated with the regulated expression of growth marker genes in fast muscle (Palstra et al., 2014). Thus, we investigated the independent and interactive effects of inflammatory myopathy and swimming behavior on commonly used fish exercise protocols. And also, I aimed to establish an TNF- $\alpha$  and H<sub>2</sub>O<sub>2</sub>-stimulated inflammatory myopathy zebrafish model and identify *Ishige okamurae*-derived Diphlorethohydroxycarmalol (DPHC) that have protective effects inflammatory myopathy through NF- $\kappa$ B and MAPKs pathways.

## **2. MATERIALS AND METODS**

### **2.1. Chemicals and reagents**

Antibodies including p-I $\kappa$ B- $\alpha$ , p-NF- $\kappa$ B, p-JNK, p-p38, MuRF-1, and MAFbx/Atrogin-1 were purchased from Santa Cruz Biotechnology, Inc. (Dallas, TX, USA).  $\beta$ -Actin, and Lamin-B antibodies were purchased from Cell Signaling Technology (Beverly, MA, USA). All the other chemicals and reagents used were analytical grade.

### **2.2. The origin and maintenance of zebrafish**

Adult zebrafish were obtained from a commercial dealer (World Fish Aquarium, Jeju, Korea) and 12 fish were kept in a 3-L acrylic tank under the following conditions: 28.5°C, in 14/10 h light/dark cycle. The fish were fed three times a day, 6 days a week, with Tetramin flake feed supplemented with live brine shrimp (*Artemia salina*). All of the experimental procedures were in accordance with the Institutional Animal Care Committee.

### **2.3. Experimental design of TNF- $\alpha$ or H<sub>2</sub>O<sub>2</sub>-induced myopathy**

The adult zebrafish ( $n=12$ ) were randomly divided in normal control group (negative control), control group (vehicle), DPHC-treated group (2 and 5  $\mu$ g/g), and octacosanol-treated group (25  $\mu$ g/g). The zebrafish were anesthetized with 0.03% ethyl 3-aminobenzoate methanesulfaonae (Sigma-Aldrich, St. Louis, MO, USA). After that, the anesthetized zebrafish were injected with DPHC (2 and 5  $\mu$ g/g) once every three days for two weeks. In the last week, the zebrafish were injected with DPHC (2 and 5  $\mu$ g/g) and TNF- $\alpha$  (200 ng/g) or

H<sub>2</sub>O<sub>2</sub> (5 μM) to induce inflammation.

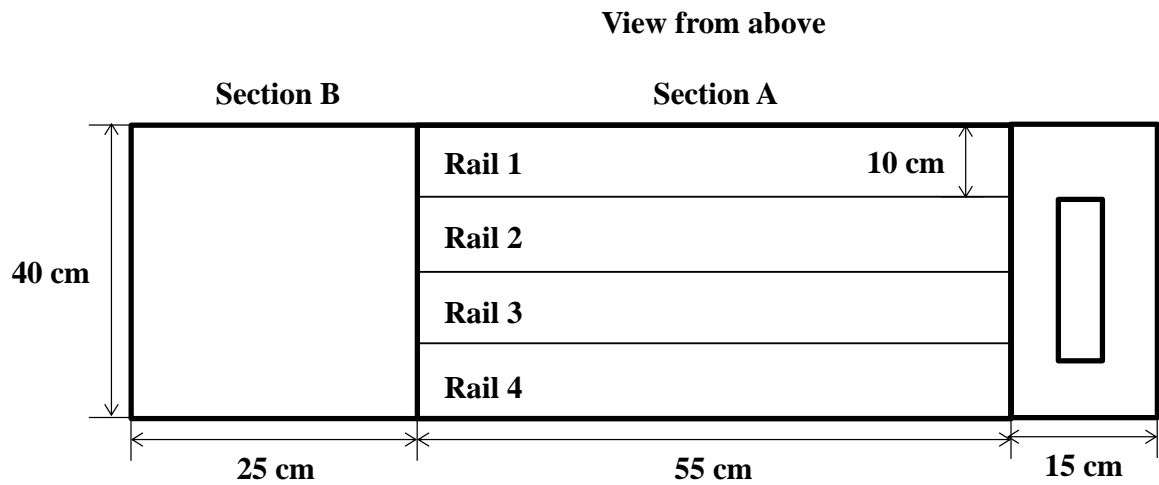
#### **2.4. Measurement of survival rates and body weights**

The survival rates and body weights were measured weekly end of experiment. The zebrafish were anesthetized 0.03% ethyl 3-aminobenzoate methanesulfaone and then drained and measured body weight.

#### **2.5. Endurance test**

The zebrafish were placed in a 30 L behavior tank with an adjustable flow and percent of slope that forced fish to swim to maintain their position. The endurance test tank has been divided into two sections, Section A is the endurance and swimming area, whereas Section B is the fall down section against water flow and gradient (Fig. 3-1). Water temperature was maintained at acclimation temperature (28.5°C). To analyze the endurance of zebrafish, after a certain time, the number of zebrafish remaining in Section A was measured. Also, the duration time, and distance moved zebrafish in Section A were analyzed with video-recorded from the top view using Loligo Systems (Viborg, Denmark).

(A)



(B)

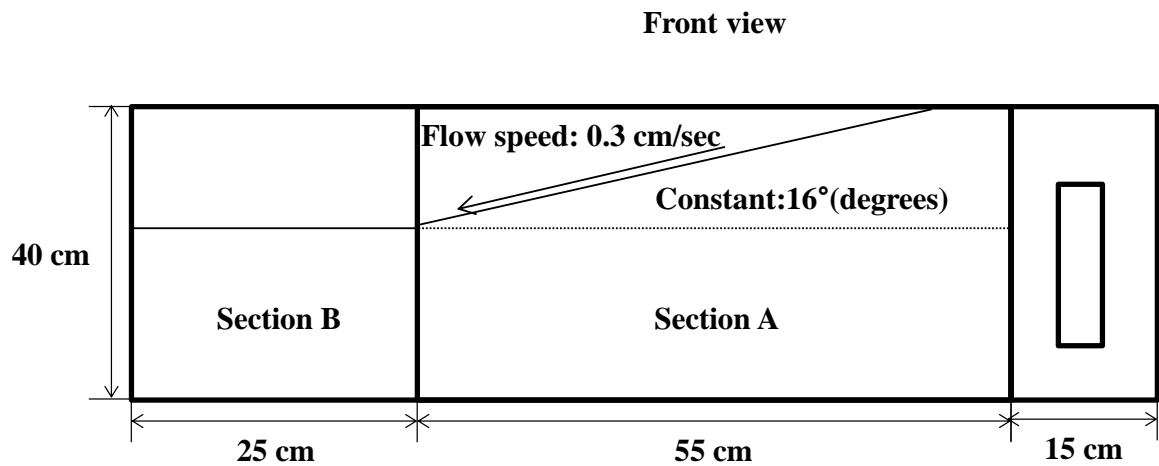


Fig. 3-1. The schematic diagram of zebrafish behavior tank for endurance test against water flow and gradient. The behavioral test Section A has a length of 55 cm and a width of 40 cm, which are divided to 4 rails (1 rail has 10 cm of width), and Section B 1 has a length of 25 cm and a width of 40 cm. A constant water flow (0.3 cm/sec) at an angle of 16° was maintained. The figure represents the tank view (A) from above and (B) the front view.

## 2.6. Western blot analysis

To determine the effects of DPHC on the protein expression levels of p-I $\kappa$ B- $\alpha$ , p-NF- $\kappa$ B, MAPKs (p-JNK, and p-p38), MuRF-1, and MAFbx/Atrogin-1 in TNF- $\alpha$  or H<sub>2</sub>O<sub>2</sub>-stimulated zebrafish muscle tissue, Western blot analysis was performed. The zebrafish muscle tissues were homogenized in lysis buffer using a homogenizer and then centrifuged at 13,000 rpm for 15 min at 4°C. The protein concentrations were determined by using Pierce<sup>TM</sup> BCA protein assay kit (Thermo Fisher Scientific, MD, USA). The lysate, containing 100  $\mu$ g of protein, was subjected to electrophoresis with a 10% SDS-polyacrylamide gel and transferred onto a nitro-cellulose (NS) membrane using a glycine transfer buffer. The membranes were blocked in a 5% blotting-grade blocker in TBST (a mixture of Tris-buffered saline and Tween 20) for 2 h. p-I $\kappa$ B- $\alpha$ , p-NF- $\kappa$ B, MAPKs (p-JNK, and p-p38), MuRF-1, and MAFbx/Atrogin-1 expression were detected using specific rabbit/mouse polyclonal antibodies and goat anti-rabbit or -mouse IgG HRP conjugated secondary antibodies. Signals were developed using an enhanced chemiluminescence (ECL) Western blotting detection kit (Amersham, Arlington Heights, IL, USA) and exposed to FusionCapt Advance FX7 program (Vilber Lourmat, Australia). The basal levels of the each protein were normalized by analyzing the level of  $\beta$ -Actin or Lamin B protein by using Image J program.

## 2.7. Histological analysis

The muscle tissues of zebrafish for histological analysis were preserved in Bioun's solution for approximately 24 h and subsequently transferred to 70% ethanol for storage. Following this, fixed zebrafish were dehydrated, embedded in paraffin, and sectioned with 6  $\mu$ m.

Standard histological slides were prepared by using hematoxylin and eosin. The muscle tissues of zebrafish were analyzed under the microscope equipped with a CoolSNAP-Pro color digital camera (Olympus, Japan).

## **2.8. Statistical analysis**

All experiments were conducted in triplicate (n=3) and an one-way analysis of variance (ANOVA) test (using SPSS 12.0 statistical software) was to analyze the data. Significant differences between the means of parameters were determined by using Tukey test to analyze the difference. P-values of less than 0.05 ( $P < 0.05$ ) and 0.01 ( $P < 0.01$ ) was considered as significant.



### **3. RESULTS AND DISCUSSION**

#### **3.1. Measurement of survival rate, and body weight**

In order to examine the potential protective effects of DPHC in TNF- $\alpha$  and H<sub>2</sub>O<sub>2</sub>-stimulated inflammatory zebrafish, survival rates were measured. Furthermore, to determine whether DPHC affect a change in weight of inflammatory zebrafish, the body weights of zebrafish were measured once a week during experimental period. The survival rate is slightly decreased in the TNF- $\alpha$ -treated zebrafish (95% of survival rates) compared to the untreated zebrafish (100% of survival rates). However, DPHC protected death of zebrafish by TNF- $\alpha$  stimulations (Fig. 3-2). The body weights of all zebrafish did not change compared to the initial body weights (Fig. 3-2). For H<sub>2</sub>O<sub>2</sub>, the survival rate is also slightly decreased (90% of survival rates) compared to the untreated zebrafish (100% of survival rates), and DPHC also showed weak toxicity (Fig. 3-3). The body weights of all zebrafish did not change compared to the initial body weights (Fig. 3-3). These results imply that DPHC, TNF- $\alpha$ /H<sub>2</sub>O<sub>2</sub>, and OCT do not affect zebrafish body weights.

#### **3.2. Effects endurance improvement in DPHC-treated inflammatory zebrafish model**

Endurance training can induce skeletal muscle hypertrophy and leads to strength on muscle mass in human (Sipila et al., 1995). Also, endurance training like running to exhaustion tests enhances exercise performances to 85 to 223%, respectively in mice and rats (Gilbert et al., 2014). In zebrafish, swimming performance improved physical ability to 25% over training period (Gilbert et al., 2014). To determine whether DPHC protects weakened muscle by TNF- $\alpha$  or H<sub>2</sub>O<sub>2</sub> and enhances the endurance in zebrafish without any training, endurance such as

number of swimming and behavior change against water flow and gradient was measured. The number of swimming zebrafish in Section A, which is remaining area in five minutes against water flow and gradient, DPHC-injected zebrafish showed a significant increase in compared to TNF- $\alpha$  or H<sub>2</sub>O<sub>2</sub>-injected inflammatory zebrafish (Fig. 3-4, and 3-5). Section A was divided into two sections to analyze the duration time, and distance moved of zebrafish. Especially, DPHC-injected zebrafish exhibited an increase in each analysis index compared to TNF- $\alpha$  or H<sub>2</sub>O<sub>2</sub>-injected inflammatory zebrafish (Fig. 3-6, and 3-7).

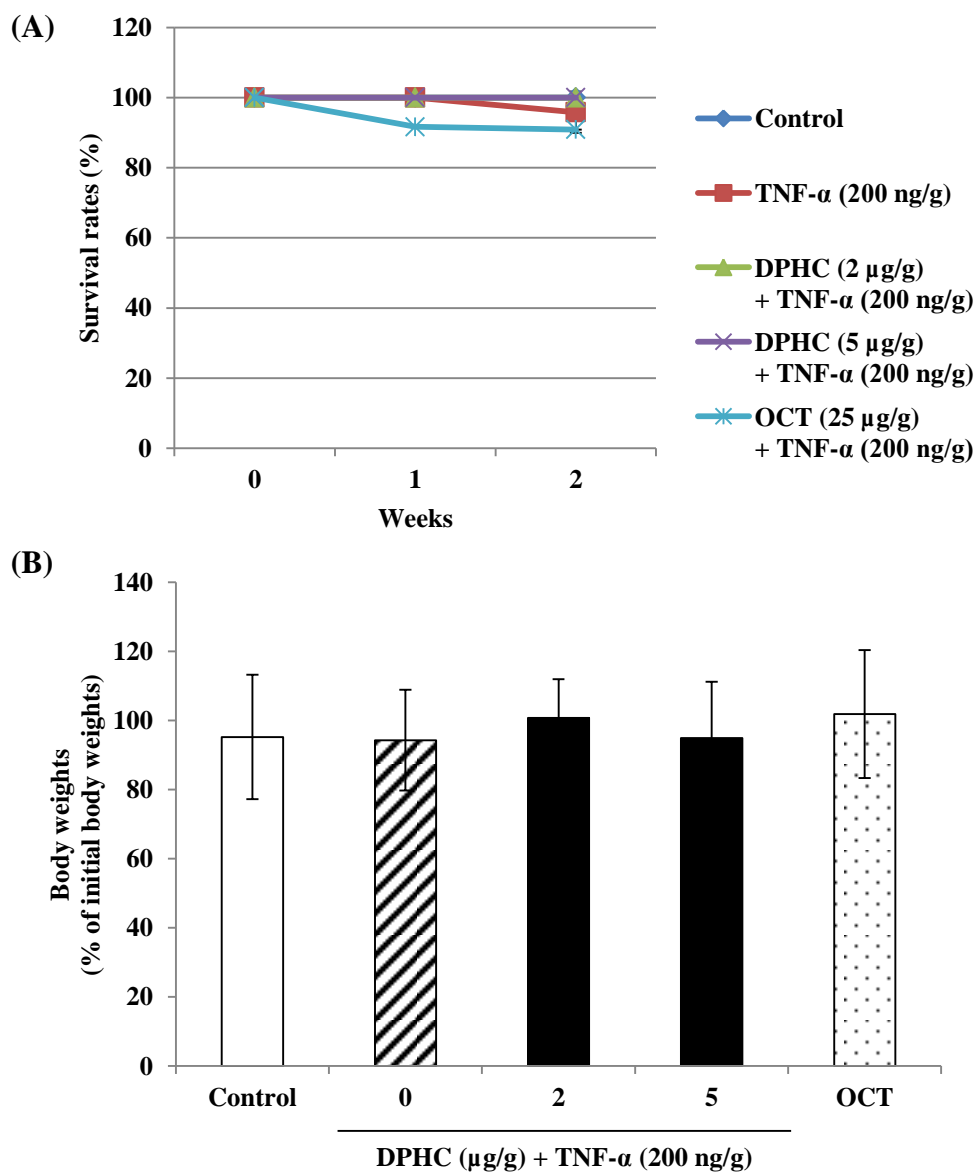


Fig. 3-2. Effect of DPHC on survival rates (A) and body weights (B) in TNF- $\alpha$ -induced myopathy zebrafish. Experiments were performed in duplicate and the data are expressed as mean  $\pm$  SE; #  $P < 0.05$ , and ##  $P < 0.01$  as compared to the untreated group. \*  $P < 0.05$ , and \*\*  $P < 0.01$  as compared to the TNF- $\alpha$ -treated group.

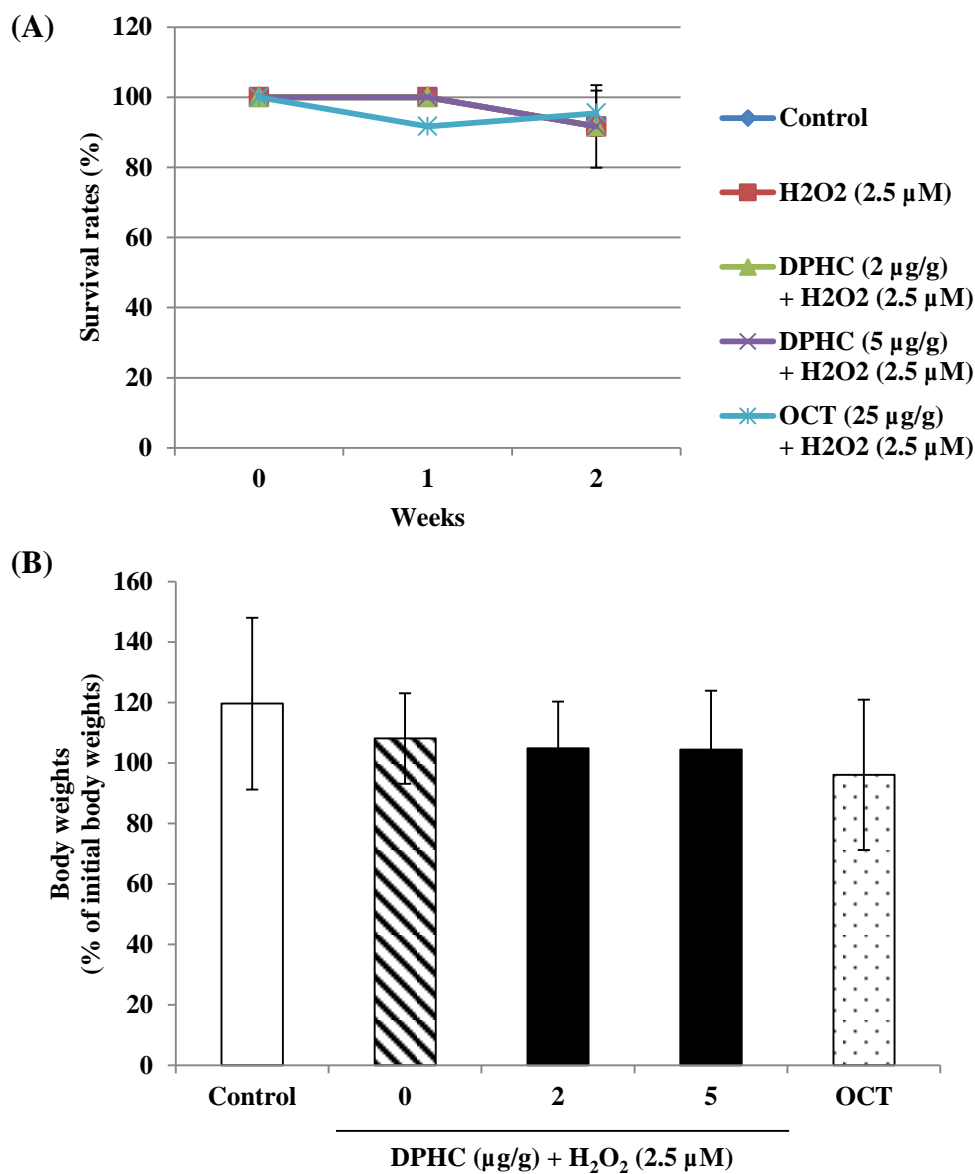


Fig. 3-3. Effect of DPHC on survival rates (A) and body weights (B) in H<sub>2</sub>O<sub>2</sub>-induced myopathy zebrafish. Experiments were performed in duplicate and the data are expressed as mean ± SE; #  $P < 0.05$ , and ##  $P < 0.01$  as compared to the untreated group. \*  $P < 0.05$ , and \*\*  $P < 0.01$  as compared to the H<sub>2</sub>O<sub>2</sub>-treated group.

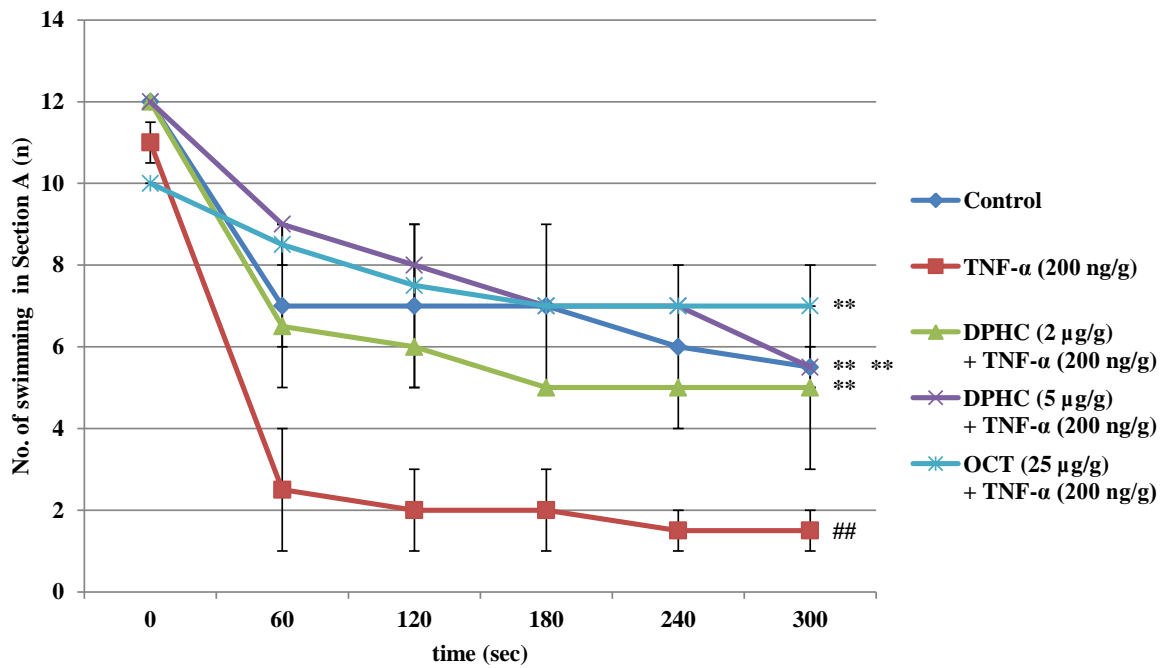


Fig. 3-4. Effect of DPHC on endurance training in TNF- $\alpha$ -induced myopathy zebrafish. Experiments were performed in duplicate and the data are expressed as mean  $\pm$  SE; #  $P < 0.05$ , and ##  $P < 0.01$  as compared to the untreated group. \*  $P < 0.05$ , and \*\*  $P < 0.01$  as compared to the TNF- $\alpha$ -treated group.

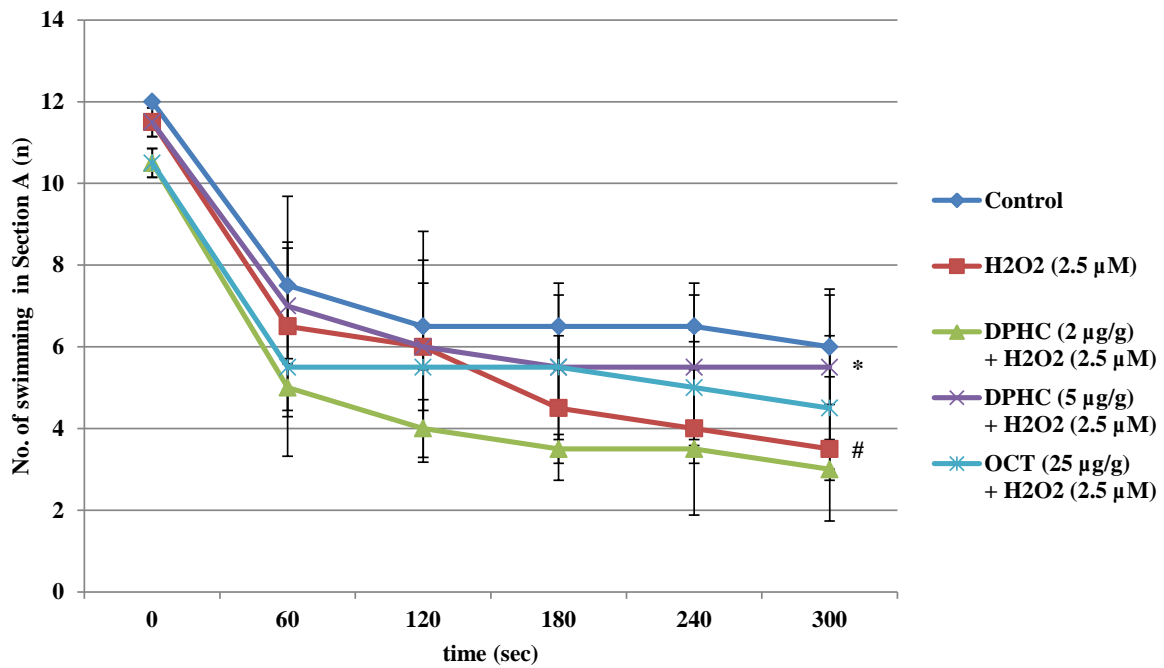


Fig. 3-5. Effect of DPHC on endurance training in H<sub>2</sub>O<sub>2</sub>-induced myopathy zebrafish. Experiments were performed in duplicate and the data are expressed as mean ± SE; # *P* < 0.05, and ## *P* < 0.01 as compared to the untreated group. \* *P* < 0.05, and \*\* *P* < 0.01 as compared to the H<sub>2</sub>O<sub>2</sub>-treated group.

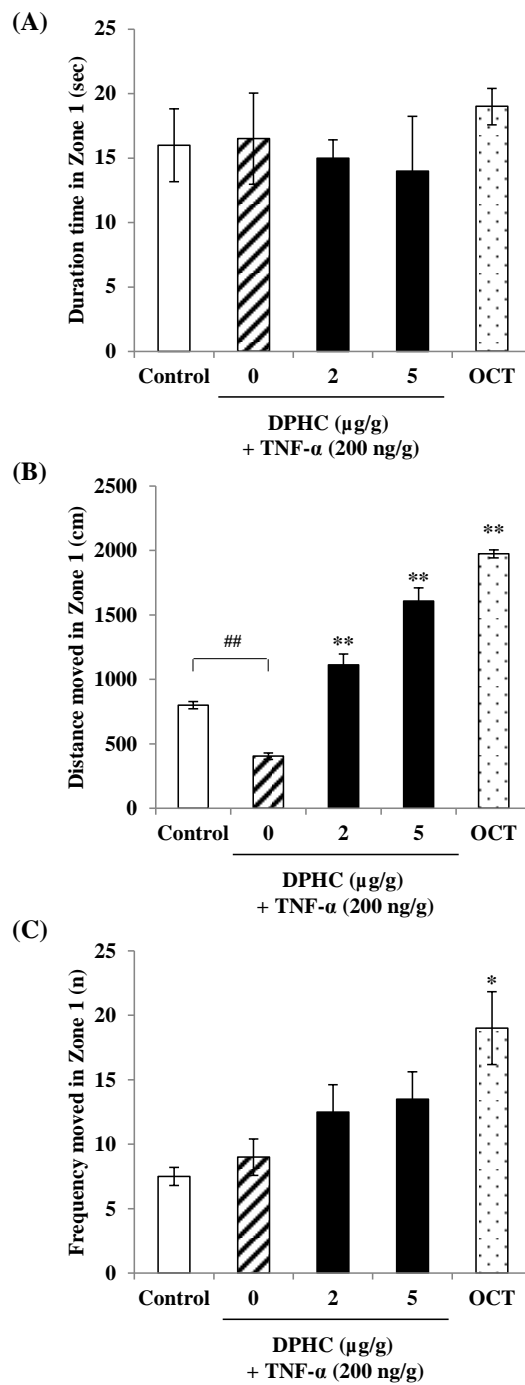


Fig. 3-6. Effect of DPHC on endurance training in TNF- $\alpha$ -induced myopathy zebrafish. Experiments were performed in duplicate and the data are expressed as mean  $\pm$  SE; #  $P < 0.05$ , and ##  $P < 0.01$  as compared to the untreated group. \*  $P < 0.05$ , and \*\*  $P < 0.01$  as compared to the TNF- $\alpha$ -treated group.

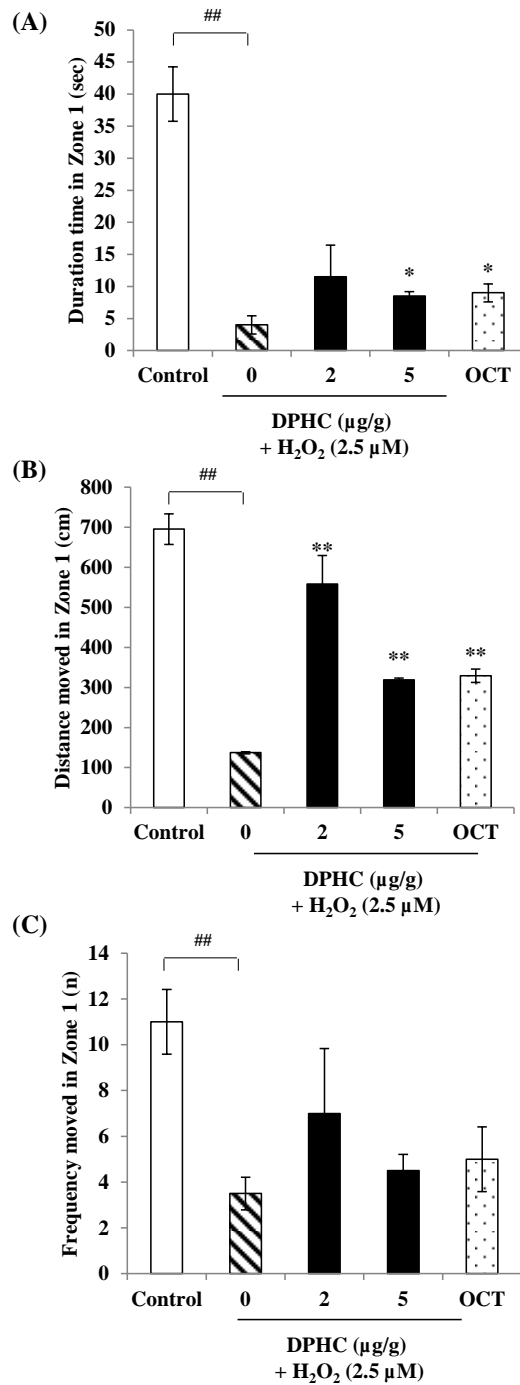


Fig. 3-7. Effect of DPHC on endurance training in  $H_2O_2$ -induced myopathy zebrafish. Experiments were performed in duplicate and the data are expressed as mean  $\pm$  SE; #  $P < 0.05$ , and ##  $P < 0.01$  as compared to the untreated group. \*  $P < 0.05$ , and \*\*  $P < 0.01$  as compared to the  $H_2O_2$ -treated group.



### **3.3. Effects of DPHC on down-regulation of inflammatory myopathy genes in zebrafish model via NF- $\kappa$ B and MAPKs signaling pathway**

Hanai et al. (2007) showed that atrophy-related genes including atrogen-1 considerably increased by muscle injury in zebrafish embryos. Although studies have been reported on muscle atrophy or injury using zebrafish model, reports are limited to using genetic loss such as knock-down or knock-out (Fu et al., 2017). Therefore, in this study, based on the results of protective effects of DPHC in inflammatory C2C12 cells that regulated the expression of MuRF-1, and MAFbx/Atrogen-1, muscle atrophy key regulators, the effectiveness of DPHC was analyzed in inflammatory zebrafish model. As shown Fig. 3-8, and 3-10, TNF- $\alpha$  or H<sub>2</sub>O<sub>2</sub> significantly promoted the phosphorylations of MAPKs (p38, and JNK) in zebrafish muscle tissues. However, DPHC significantly decreased the phosphorylations of MAPKs. In addition, p-IK-B- $\alpha$  expression increased by TNF- $\alpha$  and H<sub>2</sub>O<sub>2</sub> treatment in zebrafish muscle was significantly decreased by DPHC in a dose-dependent manner. However, NF- $\kappa$ B expression in TNF- $\alpha$ -treated zebrafish was not affected (Fig. 3-8). Furthermore, TNF- $\alpha$  or H<sub>2</sub>O<sub>2</sub> significantly promoted the MuRF-1 and MAFbx/Atrogen-1 expression, but DPHC significantly inhibited the expression of MuRF-1 and MAFbx/Atrogen-1 in zebrafish muscles (Fig. 3-9, and 3-11). These results indicated that TNF- $\alpha$  and H<sub>2</sub>O<sub>2</sub> can induce the inflammation in zebrafish muscle through MAPKs and NF- $\kappa$ B signaling pathway, and then suppressed the proteins synthesis of MuRF-1 and MAFbx/Atrogen-1. Moreover, DPHC considerably inhibits the proteins synthesis of muscle atrophy genes via MAPKs and NF- $\kappa$ B signaling pathway.

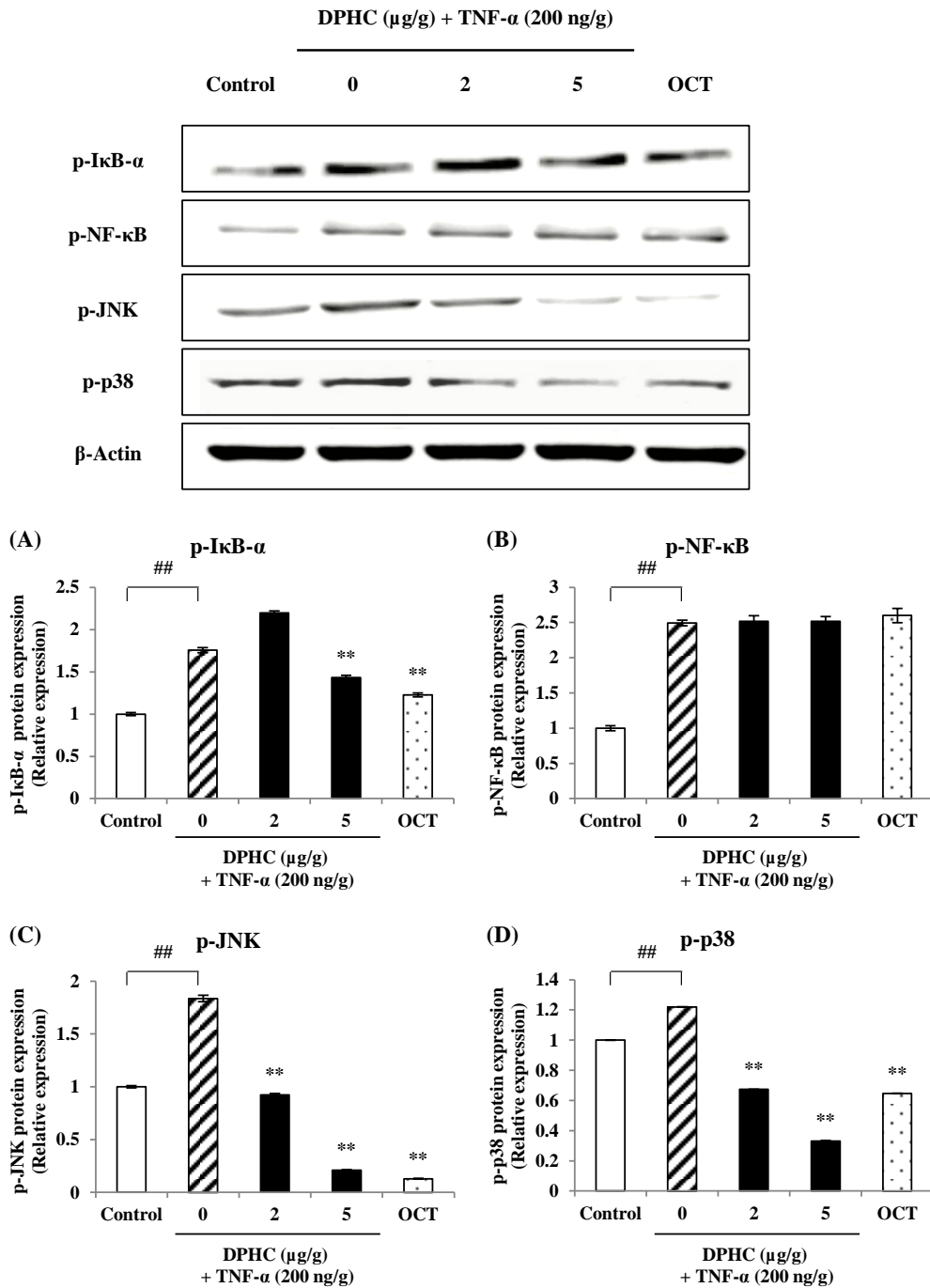


Fig. 3-8. The protein expressions of p-I $\kappa$ B- $\alpha$ , p-NF- $\kappa$ B, p-JNK, and p-p38 in TNF- $\alpha$ -induced myopathy zebrafish muscle tissues. Experiments were performed in duplicate and the data are expressed as mean  $\pm$  SE; #  $P < 0.05$ , and ##  $P < 0.01$  as compared to the untreated group. \*  $P < 0.05$ , and \*\*  $P < 0.01$  as compared to the TNF- $\alpha$ -treated group.

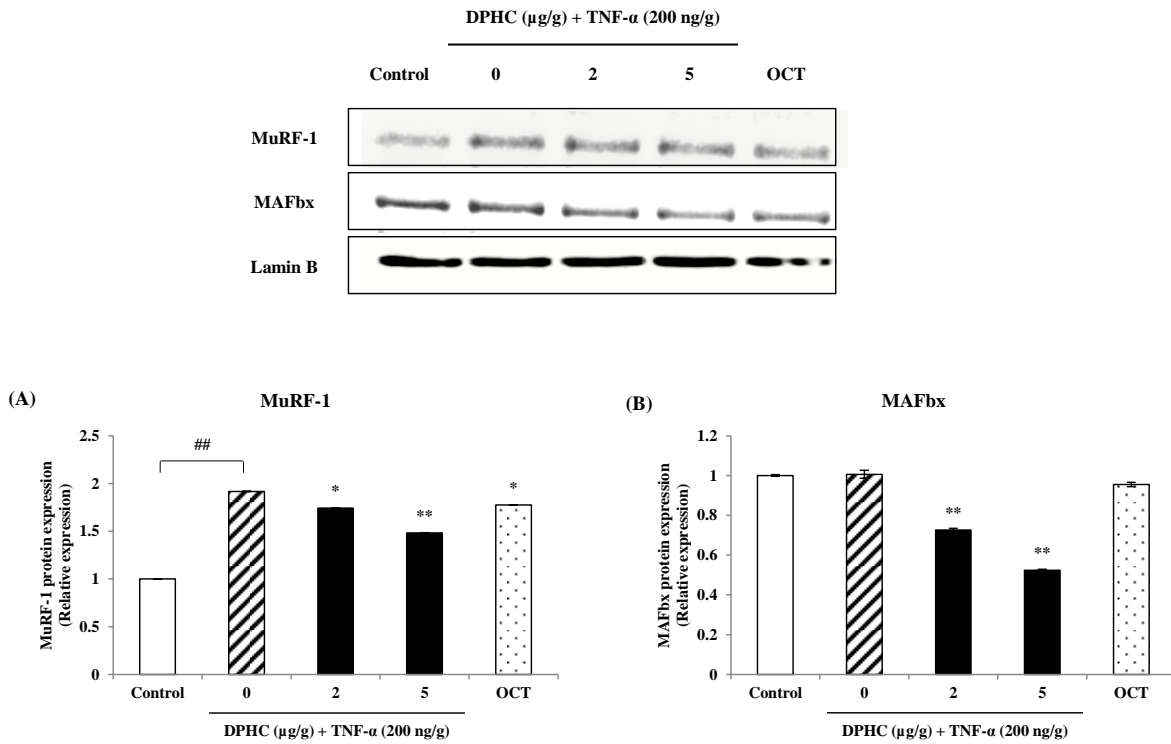


Fig. 3-9. The protein expressions of MuRF-1, and MAFbx/Atrogin-1, which are key genes in muscle atrophy in TNF- $\alpha$ -induced myopathy zebrafish muscle tissues. Experiments were performed in duplicate and the data are expressed as mean  $\pm$  SE; #  $P < 0.05$ , and ##  $P < 0.01$  as compared to the untreated group. \*  $P < 0.05$ , and \*\*  $P < 0.01$  as compared to the TNF- $\alpha$  - treated group.

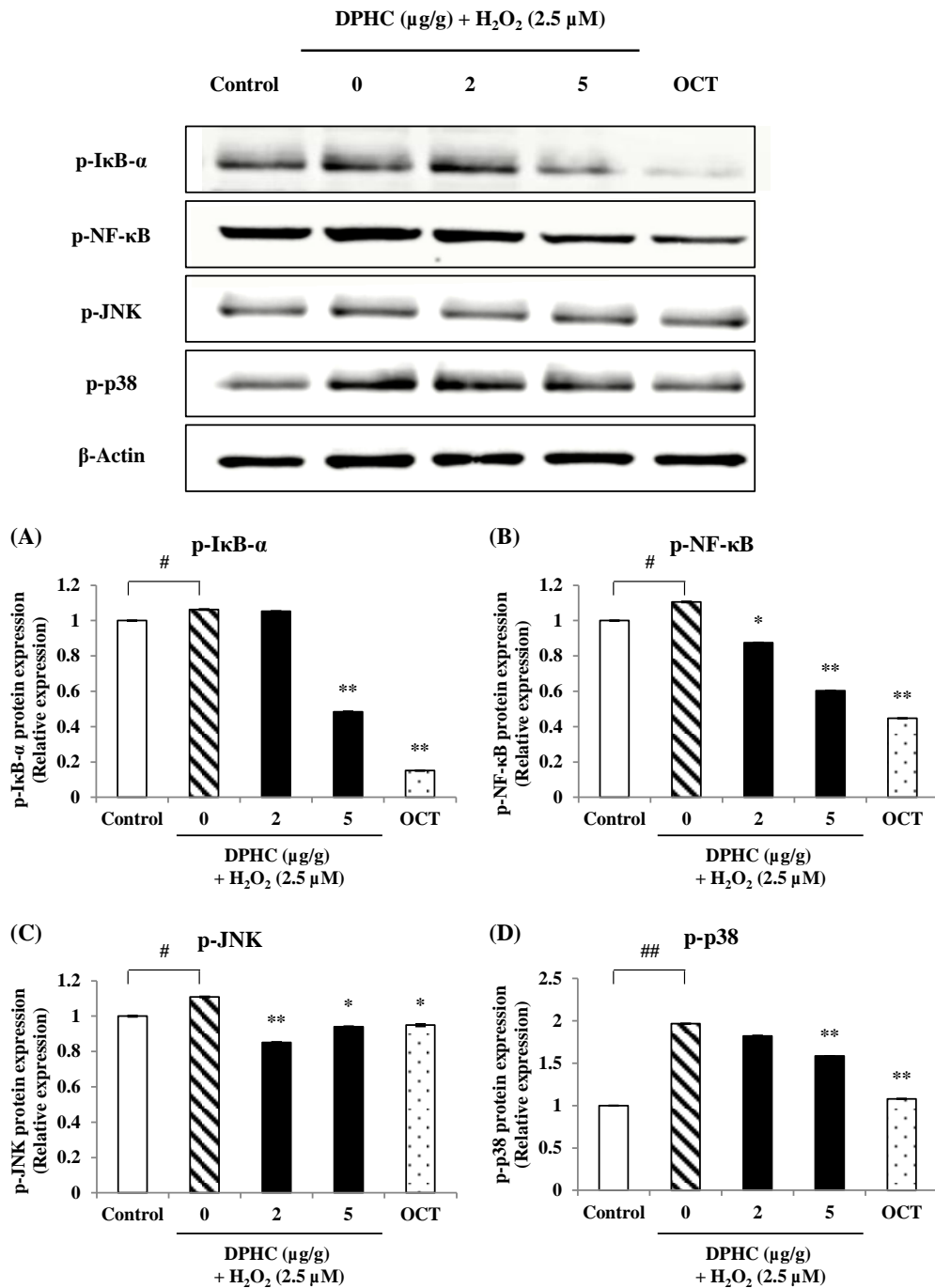


Fig. 3-10. The protein expressions of p-I $\kappa$ B- $\alpha$ , p-NF- $\kappa$ B, p-JNK, and p-p38 in  $\text{H}_2\text{O}_2$ -induced myopathy zebrafish muscle tissues. Experiments were performed in duplicate and the data are expressed as mean  $\pm$  SE; #  $P < 0.05$ , and ##  $P < 0.01$  as compared to the untreated group. \*  $P < 0.05$ , and \*\*  $P < 0.01$  as compared to the  $\text{H}_2\text{O}_2$ -treated group.

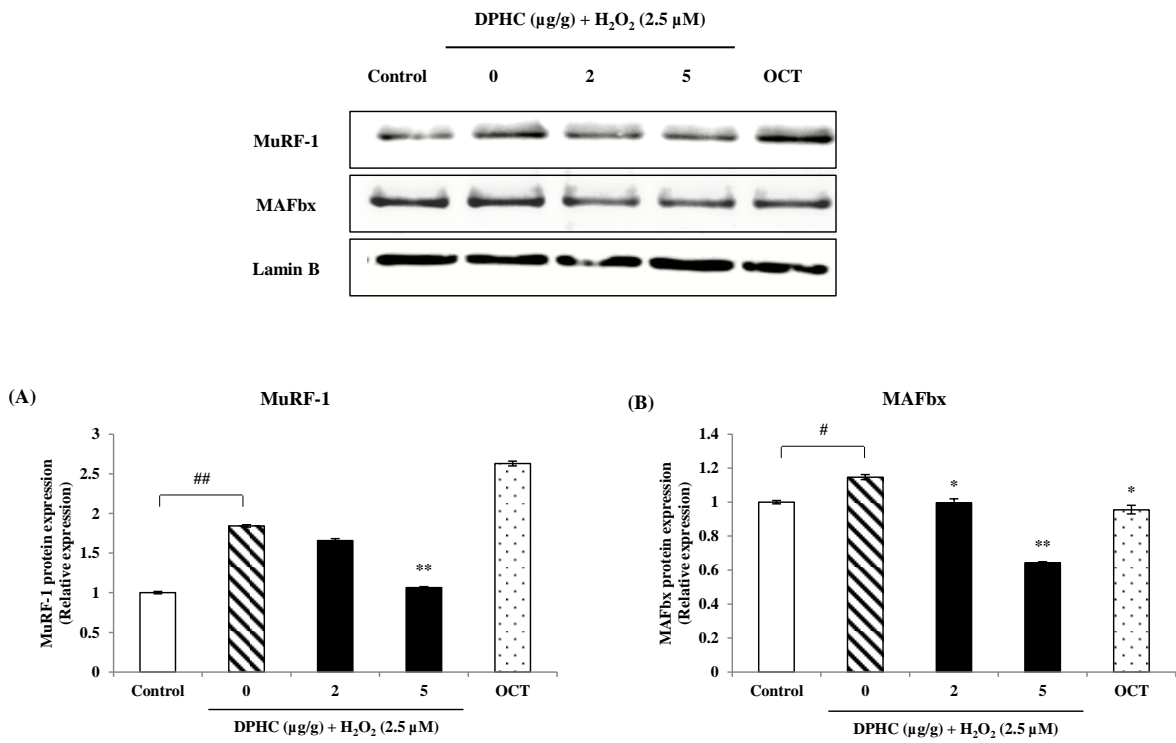


Fig. 3-11. The protein expressions of MuRF-1, and MAFbx/Atrogin-1, which are key genes in muscle atrophy H<sub>2</sub>O<sub>2</sub>-induced myopathy zebrafish muscle tissues. Experiments were performed in duplicate and the data are expressed as mean ± SE; <sup>#</sup> *P* < 0.05, and <sup>##</sup> *P* < 0.01 as compared to the untreated group. <sup>\*</sup> *P* < 0.05, and <sup>\*\*</sup> *P* < 0.01 as compared to the H<sub>2</sub>O<sub>2</sub>-treated group.

### **3.4. Histopathology in the muscle tissues of inflammatory zebrafish**

Muscle atrophy (myopathy) in muscle tissues of zebrafish was analyzed using the Hematoxylin & Eosin (H&E) staining. The morphological changes in the enucleated muscle tissues are shown in Fig. 3-12, and 3-13. The muscle tissue section of TNF- $\alpha$  or H<sub>2</sub>O<sub>2</sub>-stimulated group exhibited hisopathological changes compared to non-treated control group. The muscle tissues of TNF- $\alpha$ -stimulated inflammatory myopathy zebrafish showed increased degradation. However, degradation of muscle tissues was recovered in DPHC-treated TNF- $\alpha$ -stimulated inflammatory myopathy zebrafish group. In addition, muscle tissues of zebrafish exhibited hisopathological changes following H<sub>2</sub>O<sub>2</sub> stimulations as compared to non-treated control. However, DPHC-treated zebrafish were observed to be filled with destroyed muscle tissue.

### **4. Conclusion**

In conclusion, this zebrafish model can be used as an *in vivo* model for experiment to confirm the protective effects of inflammatory muscle atrophy. Furthermore, DPHC, a marine-derived bioactive compound, has a potential to regulate inflammatory myopathy genes through the NF- $\kappa$ B, and MAPKs signaling. Therefore, DPHC is expected to be used as possible nutraceuticals or functional food to reduce inflammation in muscle instead of the injection acting as TNF- $\alpha$  inhibitor.

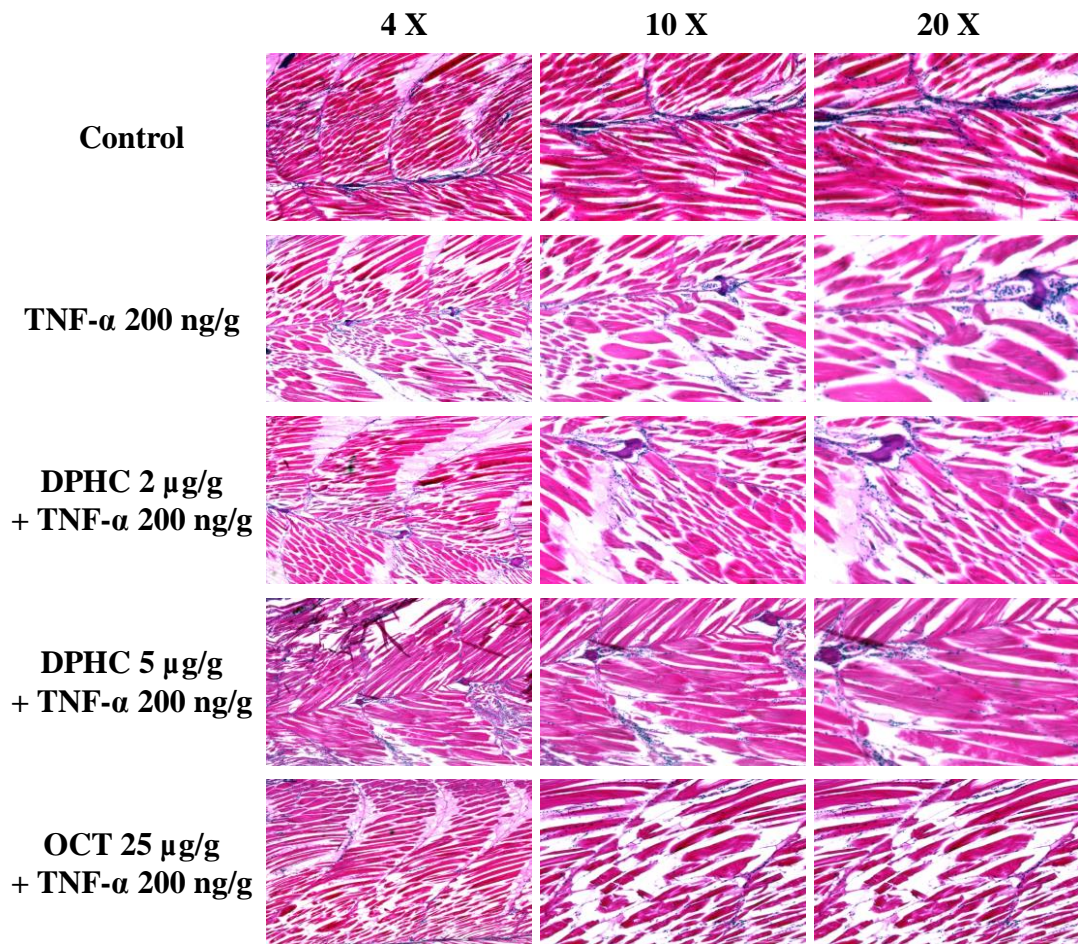


Fig. 3-12. Analysis of muscle tissues in DPHC-treated zebrafish on TNF- $\alpha$ -induced myopathy by Hematoxylin & Eosin (H&E) staining.

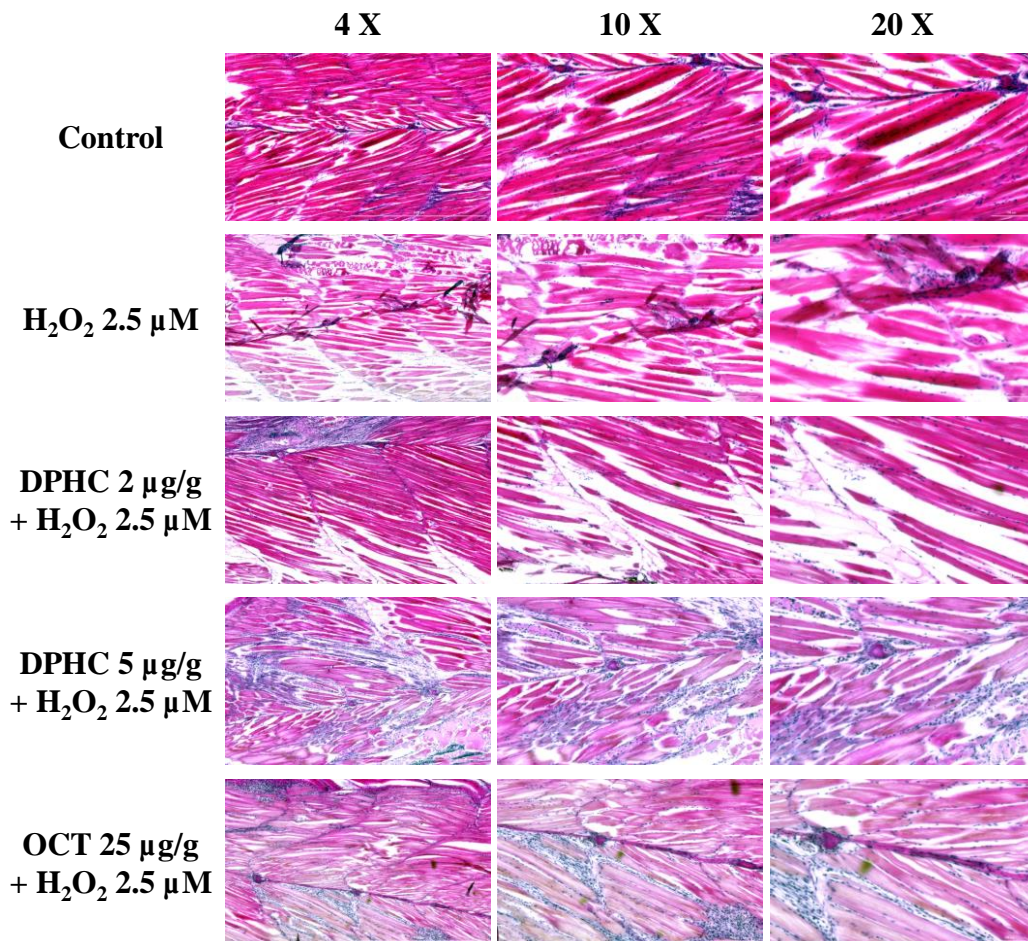


Fig. 3-13. Analysis of muscle tissues in DPHC-treated zebrafish on H<sub>2</sub>O<sub>2</sub>-induced myopathy by Hematoxylin & Eosin (H&E) staining.



## REFERENCES

Acharyya, S., Sharma, S.M., Cheng, A.S., Ladner, K.J., He, W., Kline, W. et al. (2010). TNF inhibits Notch-1 in skeletal muscle cells by Ezh2 and DNA methylation mediated repression: implications in duchenne muscular dystrophy. *PLoS One*, 5, e12479.

Arnold, L., Henry, A., Poron, F., Baba-Amer, Y., Rooijen, N., Plonquet, A., Gherardi, R.K., Chazaud, B. (2007). Inflammatory monocytes recruited after skeletal muscle injury switch into anti inflammatory macrophages to support myogenesis. *J Exp Med*, 204(5), 1057-1069.

Baek, S.H., Lee, J.H., Kim, G.T., Lee, J.W., Cho, M.R., Kim, J.I., Lee, S.H., Kim, D.S., Kim, S.I. (2008). Increased Interleukin-17 Expression in Patients with Idiopathic Inflammatory Myopathie. *Journal of Rheumatic Diseases*, 15(2), 118-122.

Bassel-Duby, R., Olson, E.N., (2006). Signaling Pathways in Skeletal Muscle Remodeling. *Annu Rev Biochem*, 75, 19-37.

Bassett, D.I., Currie, P.D. (2003). The zebrafish as a model for muscular dystrophy and congenital myopathy. *Hum Mol Genet*, 12 (Review Issue 2), R265-R270.

Bodine, S.C., Latres, E., Baumheuter, S., Lai, V.K., Nunez, L., Clarke, B.A., et al., (2001). Identification of ubiquitin ligases required for skeletal muscle atrophy. *Science*, 294, 1704-1708.

Bührdel, J.B., hirth, S., Keßler, M., Westphal, S., Forster, M., Manta, L., Wiche, G., Schoser, B., Schessl, J., Schroder, R., Clemen, C.S., Eichinger, L., Fürst, D.O., Ven, P.F.M., Rottbauer, W., Just, S. (2015). *In vivo* characterization of human myofibrillar myopathy genes in zebrafish. *Biochem Biophys Res Commun*, 461, 217-223.

Cai, D., Frantz, J.D., Tawa, N.E., Melendez, P.A., Oh, B.C., Lidov, H.G.W., Hasselgren, P.O., Frontera, W.R., Lee, J., Glass, D.J., Shoelson, S.E. (2004). IKK $\beta$ /NF- $\kappa$ B Activation Causes Severe Muscle Wasting in Mice. *Cell*, 119, 285-298.

Chico, T.J.A., Ingham, P.W., Crossman, D.C. (2008). Modeling Cardiovascular Disease in the Zebrafish. *Trends Cardiovasc Med*, 18(4), 150-155.

Dehoux, M.J., van Beneden, R.P., Fernandez-Celemin, L., Lause, P.L., Hissen, J.P. (2003). Induction of MafBx andMurf ubiquitin ligasemRNAs in rat skeletal muscle after LPS injection. *FEBS Letters*, 544, 214-217.

Dowlati, Y., Herrmann, N., Swardfager, W., Liu, H., Sham, L., Reim, E.K., Lanctôt, K.L. (2010). A meta-analysis of cytokines in major depression. *Biological Psychiatry*, 67(5), 446-457.

Duchesne, E., Dufresne, S.S., Dumont, N.A. (2017). Impact of Inflammation and Anti-inflammatory Modalities on Skeletal Muscle Healing: From Fundamental Research to the Clinic. *Phys Ther*, 97(8), 807-817.

Dowling, J.J., Vreede, A.P., Low, S.E., Gibbs, E.M., Kuwada, J.Y., Bonnemann, C.G., Feldman, E.L. (2009). Loss of Myotubularin Function Results in T-Tubule Disorganization in Zebrafish and Human Myotubular Myopathy. *PLoS Genet*, 5(2), e1000372.

Elkina, Y., Haehling, S., Anker, S.D., Springer, J. (2011). The role of myostatin in muscle wasting: an overview. *J Cachexia Sarcopenia Muscle*, 2, 143-151.

Eisen, J.S. (2006). Zebrafish Make a Big Splash. *Cell*, 87, 969-977.

Farber, M.O., Mannix, E.T. (2000). TISSUE WASTING IN PATIENTS WITH CHRONIC

OBSTRUCTIVE PULMONARY DISEASE, THE ACQUIRED IMMUNE DEFICIENCY SYNDROME, AND CONGESTIVE HEART FAILURE. *Metabolic Myopathies*, 18(1), 245-262.

Fernando, I.P.S., Nah, J.W., Jeon, Y.J. (2016). Potential anti-inflammatory natural products from marine algae. *Environ Toxicol Pharmacol*, 48, 22-30.

Fu, X.N., Xiong, H. (2017). Genetic and Clinical Advances of Congenital Muscular Dystrophy.

Gilbert, M.J.H., Zerulla, T.C., Tiemy, K.B. (2014). Zebrafish (*Danio rerio*) as a model for the study of aging and exercise: Physical ability and trainability decrease with age. *Experimental Gerontology*, 50, 106-113.

Glass, D.J. (2005). Skeletal muscle hypertrophy and atrophy signaling pathways. *Int J Biochem Cell Biol*, 37, 1974-1984.

Gomes, M.D., Lecker, S.H., Jagoe, R.T., Navon, A., Goldberg, A.L. (2001). Atrogin-1, amuscle-specific F-box protein highly expressed during muscle atrophy. *Proceedings of the National Academy of Sciences of the USA*, 98, 14440-14445.

Grivennikov, S.I., Tumanov, A.V., Liepinsh, D.J., Kruglov, A.A., Marakusha, B.I., Shakhov, A.N. et al. (2005). Distinct and nonredundant in vivo functions of TNF produced by t cells and macrophages/neutrophils: protective and deleterious effects. *Immunity*, 22, 93-104.

Guttridge, D.C., Mayo, M.W., Madrid, L.V., Wang, C.Y., Baldwin, Jr A.S. (2000). NF-kappaB-induced loss of MyoD messenger RNA: possible role in muscle decay and cachexia. *Science*, 289, 2363-2366.

Haddad, F., Roy, R.R., Zhong, H., Edgerton, V.R., Baldwin, K.M. (2003). Atrophy responses to muscle inactivity. II. Molecular markers of protein deficits. *Journal of Applied Physiology*, 95, 791-802.

Hanai, J., Cao, P., Tanksale, P., Imamura, S., Koshimizu, E., Zhao, J., Kishi, S., Yamashita, M., Phillips, P.S., Sukhatme, V.P., Lecker, S.H. (2007). The muscle-specific ubiquitin ligase atrogin-1/MAFbx mediates statin-induced muscle toxicity. *The Journal of Clinical Investigation*, 117(12), 3940-3951.

Howe, K., Clark, M.D., Torroja, C.F., Torrance, J., Berthelot, C., Muffato, M., et al., (2013). The zebrafish reference genome sequence and its relationship to the human genome. *Nature*, 496, 498-503.

Jagoe, R.T., Lecker, S.H., Gomes, M., Goldberg, A.L. (2002). Patterns of gene expression in atrophying skeletal muscles: response to food deprivation. *The FASEB Journal*, 16, 1697-1712.

Jiang, X.H., Wong, B.C., Lin, M.C., Zhu, G.H., Kung, H.F., Jiang, S.H., Yang, D., Lam, S.K. (2001). Functional p53 is required for triptolide-induced apoptosis and AP-1 and nuclear factor- $\kappa$ B activation in gastric cancer cells. *Oncogene*, 20, 8009-8018.

Jing, L., Zon, L.I. (2011). Zebrafish as a model for normal and malignant hematopoiesis. *Dis Model Mech*, 4, 433-438.

Kang, M.C., Kang, N., Kim, S.Y., Kima, I.S., Ko, S.C., Kim, Y.T., Kim, Y.B., Jeung, H.D., Choi, K.S., Jeon, Y.J. (2016). Popular edible seaweed, *Gelidium amansii* prevents against diet-induced obesity. *Food and Chemical Toxicology*, 90, 181-187.

Kawahara, G., Karpf, J.A., Myers, J.A., Alexander, M.S., Guyon, J.R., Kunkel, L.M. (2011). Drug screening in a zebrafish model of Duchenne muscular dystrophy. *Proc Natl Acad Sci USA*, 108(13), 5331-5336.

Kim, E.A., Lee, S.H., Lee, J.H., Kang, N., Oh, J.Y., Ahn, G., Ko, S.C. Fernando, S.P., Kim, S.Y., Park, S.J., Kim, Y.T., Jeon, Y.J. (2016a). A marine algal polyphenol, dieckol, attenuates blood glucose levels by Akt pathway in alloxan induced hyperglycemia zebrafish model. *RSC Advances*, 6, 78570-78575.

Kim, H.H., Kim, H.S., Ko, J.Y., Kim, C.Y., Lee, J.H., Jeon, Y.J. (2016b). A single-step isolation of useful antioxidant compounds from *Ishige okamurae* by using centrifugal partition chromatography. *Fisheries and Aquatic Sciences*, 19, 22-28.

Kim, K.N., Yang, H.M., Kang, S.M., Ahn, G., Roh, S.W. Lee, W.W., Kim, D., Jeon, Y.J. (2015). Whitening Effect of Octaphlorethol A Isolated from *Ishige foliacea* in an *In Vivo* Zebrafish Model. *J Microbio Biotechnol*, 25(4), 448-451.

Kim, S.Y., Kim, E.A., Kang, M.C., Lee, J.H., Yang, H.W., Lee, J.S., Lim, T.I., Jeon, Y.J. (2014). Polyphenol-rich fraction from *Ecklonia cava* (a brown alga) processing by-product reduces LPS-induced inflammation *in vitro* and *in vivo* in a zebrafish model. *Algae*, 29(2), 165-174.

Ko, E.Y., Cho, S.H., Kwon, S.H., Eom, C.Y., Jeong, M.S., Lee, W.W., Kim, S.Y., Heo, S.J., Ahn, G., Lee, K.P., Jeon, Y.J., Kim, K.N. (2017). The roles of NF- $\kappa$ B and ROS in regulation of pro-inflammatory mediators of inflammation induction in LPS-stimulated zebrafish embryos, *Fish & Shellfish Immunology*, 68, 525-529.

Ko, S.C., Jeon, Y.J. (2015). Anti-inflammatory effect of enzymatic hydrolysates from *Styela clava* flesh tissue in lipopolysaccharide-stimulated RAW 264.7 macrophages and *in vivo* zebrafish model. *Nutr Res Pract*, 9(3), 219-226.

Kuru, S. Inukai, A., Kato, T., Liang, Y., Kimura, S., Sobue, G. (2003). Expression of tumor necrosis factor- $\alpha$  in regenerating muscle fibers in inflammatory and non-inflammatory myopathies. *Acta Neuropathol*, 105, 217-224.

Lai, K.M.V., Gonzalez, M., Poueymirou, W.T., Kline, W.O., Na, E., Zlotchenko, E., Stitt, T.N., Economides, A.N., Yancopoulos, G.D., Glass, D.J. (2004). Conditional Activation of Akt in Adult Skeletal Muscle Induces Rapid Hypertrophy. *Mol Cell Biol*, 24(21), 9295-9304.



Lawrence, T., Willoughby, D.A., Gilroy, D.W. (2002). ANTI-INFLAMMATORY LIPID MEDIATORS AND INSIGHTS INTO THE RESOLUTION OF INFLAMMATION. *Nat Rev Immunol*, 2, 787-795.

Lecker, S.H., Jagoe, R.T., Gilbert, A., Gomes, M., Baracos, V., Bailey, J., Price, S.R., Mitch, W.E., Goldberg, A.L. (2004). Multiple types of skeletal muscle atrophy involve a common program of changes in gene expression. *The FASEB Journal*, 18, 39-51.

Lee, J.H., Zhang, C., Ko, J.Y., Lee, J.S., Jeon, Y.J. (2015). Evaluation on Anticancer Effect Against HL-60 Cells and Toxicity *in vitro* and *in vivo* of the Phenethyl Acetate Isolated from a Marine Bacterium *Streptomyces griseus*. *Fisheries and Aquatic Sciences*. 18, 35-44.

Lemos, D.R., Babaeijandaghi, F., Low, M., Chang, C.K., Lee, S.T., Fiore, D., Zhang, R.H., Natarajan, A., Nedospasov, S.A., Rossi, F.M.V. (2015). Nilotinib reduces muscle fibrosis in chronic muscle injury by promoting TNF-mediated apoptosis of fibro/adipogenic progenitors. *Nat Med*, 21, 786-794.

Li, Y.P., Reid, M.B. (2000). NF- $\kappa$ B mediates the protein loss induced by TNF- $\alpha$  in differentiated skeletal muscle myotubes. *Am J Physiol Regulatory Integrative Comp Physiol*, 279, R1165-R1170.

Li, H.H., Kedar, V., Zhang, C., McDonough, H., Arya, R., Wnag, D.Z., et al. (2004). Atrogin-1/muscle atrophy F-box inhibits calcineurin-dependent cardiac hypertrophy by participating in an SCF ubiquitin ligase complex. *Journal of Clinical Investigation*, 114, 1058-1071.

Li, Y.P. (2003). TNF-alpha is a mitogen in skeletal muscle. *American Journal of Physiology-Cell Physiology*, 285, C370-C376.

Li, Y.P., Chen, Y., John, J., Moylan, J., Jin, B., Mann, D.L., Reid, M.B. (2005). TNF- $\alpha$  acts via p38 MAPK to stimulate expression of the ubiquitin ligase atrogin1/MAFbx in skeletal muscle. *The FASEB Journal*, 19(3), 362-370.

Locksley, R.M., Killeen, N., Lenardo, M.J. (2001). The TNF and TNF receptor superfamilies: integrating mammalian biology. *Cell*, 104(4), 487-501.

Londhe, P., Guttridge, D.C. (2015). Inflammation induced loss of skeletal muscle. *Bone*, 80, 131-142.

Mann, C.J., Perdiguero, E., Kharraz, Y., Aguilar, S., Pessina, P., Serrano, A.L., Muñoz-Cánoves, P. (2011). Aberrant repair and fibrosis development in skeletal muscle. *Skeletal Muscle*, 2011, 1-21.

Mourkioti, F., Kratsios, P., Luedde, T., Song, Y.H., Delafontaine, p., Adamio, R., Parente, V., Bottinelli, R., Pasparakis, M., Rosenthal, N. (2006). Targeted ablation of IKK2 improves skeletal muscle strength, maintains mass, and promotes regeneration. *J Clin Invest*, 116(11), 2945-2954.

Musarò, A., McCullagh, K. Pau, A., Houghton, L., Dobrowolny, G. Molinaro, M., Barton, E.R., Lee Sweeney, H., Rosenthal, N. (2001). *Nat Genet*, 27, 195-200.

Palstra, A.P., Rovira, M., Rizo-Roca, D., Torrella, J.R., Spaink, h.P., Planas, J.V. (2014). *BMC Genomics*, 15, 1136.

Salomonsson, S., Lundberg, I.E. (2006). Cytokines in idiopathic inflammatory myopathies. *Autoimmunity*, 39(3), 177-190.

Sanjewa, K.K.A., Fernando, I.P.S., Kim, E.A., Ahn, G., Jee, Y., Jeon, Y.J. (2017). Anti-inflammatory activity of a sulfated polysaccharide isolated from an enzymatic digest of

brown seaweed *Sargassum horneri* in RAW 264.7 cells. *Nutrition Research and Practice*, 11, 3-10.

Sipila, S., Suominen, H. (1995). Effects of strength and endurance training on thigh and leg muscle mass and composition in elderly women. *Journal of Applied Physiology*, 78(1), 334-340

Smith, C., Kruger, M.J., Smith, R.M., Myburgh, K.H. (2008). The Inflammatory Response to Skeletal Muscle Injury Illuminating Complexities. *Sports Med*, 38(11), 947-969.

Staudt, D., Stainier, D. (2012). Uncovering the Molecular and Cellular Mechanisms of Heart Development Using the Zebrafish. *Annu Rev Genet*, 46, 395-416.

Steffen, B.T., Lees, S.J., Booth, F.W. (2008). Anti-TNF treatment reduces rat skeletal muscle wasting in monocrotaline-induced cardiac cachexia. *J Appl Physiol*, 105, 1950-1958.

Stewart, A.M., Braubach, O., Spitsbergen, J., Gerlai, R., Kalueff, A.V. (2014). Zebrafish models for translational neuroscience research: from tank to bedside. *Trends Neurosci*, 37(5), 264-278.

Swardfager, W., Lanctot, K., Rothenburg, L., Wong, A., Cappell, J., Herrmann, N. (2010). A Meta-Analysis of Cytokines in Alzheimer's Disease. *Biological Psychiatry*, 68(10), 930-941.

Tidball, J.G. (2005). Inflammatory processes in muscle injury and repair. *Am J Physiol Regul Integr Comp Physiol*, 288, R345-R353. *FEBS J*, 278, 862-876.

Vogel, B., Meder, B., Just, S., Laufer, C., Berger, I., Weber, S., Katus, H.A., Rottbauer, W. (2009). *In-vivo* characterization of human dilated cardiomyopathy genes in zebrafish. *Biochem Biophys Res Commun*, 390, 516-522.

Wajant, H., Scheurich, P. (2011). TNFR1-induced activation of the classical NF- $\kappa$ B pathway. *FEBS J*, 278, 862-876.

Wijesinghe, W.A.J.P., Ko, S.C., Jeon, Y.J. (2011). Effect of phlorotannins isolated from *Ecklonia cava* on angiotensin I-converting enzyme (ACE) inhibitory activity. *Nutrition Research and Practice*, 5, 93-100.

Yoon, M.S., Chen, J. (2008). PLD regulates myoblast differentiation through the mTOR-IGF2 pathway. *J Cell Sci*, 121, 282-289.

Zaho, Q., Yang, S.T., Wnag, J.J., Zhou, J. Xing, S.S., Shen, C.C., Wang, X.X., Yue, Y.X., Song, J., Chen, M., Wei, Y.Y., Zhou, Q.P., Dai, T., Song, Y.H. (2015). TNF alpha inhibits myogenic differentiation of C2C12 cells through NF-kB activation and impairment of IGF-1 signaling pathway. *Biochem Biophys Res Commun*, 458, 790-795.

Zhou, J., Liu, B., Liang, C., Li, Y., Song, Y.H. (2016). Cytokine Signaling in Skeletal Muscle Wasting. *Trends Endocrinol Metab*, 27(5), 335-347.

## ACKNOWLEDGEMENT

부족한 제가 제주에 와서 연구의 길을 걸을 수 있도록 이끌어주신 덕분에 석사를 마치고 박사과정을 거쳐 본 논문이 있기까지 세심한 가르침과 사랑과 격려를 아끼시지 않은 전유진 교수님께 진심으로 감사 드립니다. 또한, 바쁘신 와중에도 이 논문이 좀 더 나은 방향으로 나아 갈 수 있게 심사해 주시고 관심을 보여주신 송춘복 교수님, 최광식 교수님, 이제희 교수님, 허문수 교수님, 이경준 교수님, 여인규 교수님, 김기영 교수님, 정준범 교수님, 이승헌 교수님께 감사 드립니다.

제주에 어떤 연고도 없는 제가 제주에 내려와 연구실 생활을 잘 해나갈 수 있도록 이끌어주시고 응원해주신 우리 해양생물자원이용공학 연구실원들에게 감사의 표현을 하려고 합니다. 연구자의 길을 가기 위해서 아낌없이 조언해 주시는 허수진 선배님, 좋은 연구 결과를 얻을 수 있도록 조언과 응원해주시는 김길남 선배님, 언제나 많은 도움 주시고 마음 써 주시는 안긴내 선배님, 무심한 듯 하지만 아낌없는 응원을 주시는 저의 파트너 이승홍 선배님, 조용히 잘 챙겨주시고 조언 해주시는 고석천 선배님, 계속 옆 짝꿍일 것 만 같았던 제가 많이 의지했던 이원우 선배님, 연구실에 처음 들어왔을 때부터 많은 실험과 조언 및 도움을 주셔서 잘 적응할 수 있게 해 주신 강민철 선배님, 여러 분야에서 도움을 주시는 이지혁 선배님, 고주영 선배님, 무심한 듯 하지만 잘 챙겨주는 오재영 선배님, 연구실 생활뿐만 아니라 사소한 것도 많이 챙겨주시고, 실험에 대한 고민도 같이 해 준 김은아 선배님, 강나래 선배님, 그리고 나의 단짝 혜원이와 실험 방향에 대해서 같

이 고민해주고 많은 조언을 해 주시는 류보미 박사님, 그리고 함께 즐겁게 연구실 생활을 했던 준성오빠, 은이언니, 윤택이와 사랑하는 후배인 효근, 완택, 준건, 지민, 외국에서 와서 연구실 생활 잘 하고 있는 페르난도, 왕퇴, 아산카, 위린, 윤페이, 티리나, 히루니, 시닝과 석사와 박사과정 모든 시간 동안 함께 연구하고, 뜻깊은 시간 보낸 동기 현수오빠까지 해양생물자원이용공학 연구실 식구들께 감사드립니다.

멀리서 공부하고 있는 저에게 아낌없는 사랑과 믿음을 주시고, 또 저의 연구의 길을 자랑스러워하시는 우리 아빠 김경일, 엄마 이미형님 사랑합니다. 그리고, 동생 의현이도 집에서 큰 힘이 되어줘서 너무 고맙고, 너의 꿈도 이뤄지길 기도할게. 그리고, 저의 대학원 생활을 언제나 응원해주시고 기도해주는 할머니 박복수 권사님, 김성실 큰고모와 김성은 작은고모, 외할아버지, 그리고 하늘 나라에서 지켜보고 있을 외할머니 모두 저를 위한 배려와 사랑에 감사 드립니다.

다시 한번 더 저를 지금까지 응원해주시고 기도해주신 모든 분들께 감사의 마음을 전합니다. 앞으로도 즐겁게 열심히 연구하도록 하겠습니다. 여러 가지 모습으로 도움을 주신 분들에게 모두 감사 드리며 항상 건강하고 좋은 일만 있기를 바랍니다.